

Topological spin liquids in honeycomb iridates and RuCl_3 ?

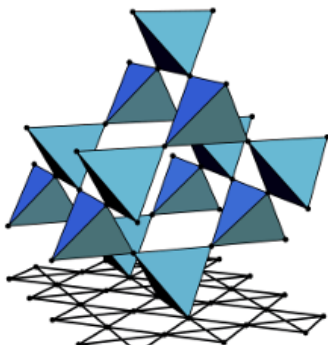
Jeroen van den Brink



Leibniz Institute
for Solid State and
Materials Research
Dresden



TECHNISCHE
UNIVERSITÄT
DRESDEN



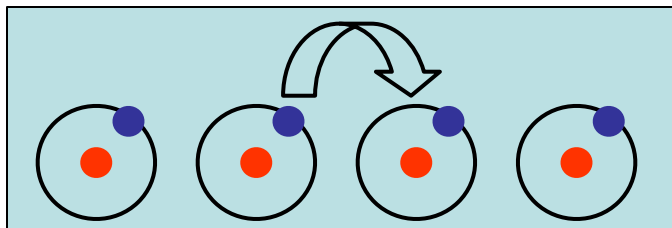
SFB 1143



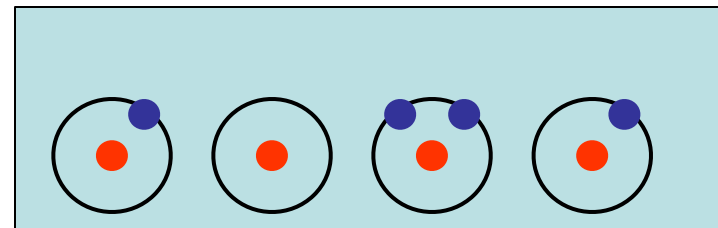
Ravi Yadav
Mohamed Eldeeb
Raajyavardhan Ray
Satoshi Nishimoto
Liviu Hozoi

Topoquant19
KITP
Santa Barbara
28.08.2019

Chain of hydrogen atoms



Hopping amplitude: t



Coulomb interaction: U

$$U = 0$$

Bands: Metallic behaviour

$$U \gg t$$

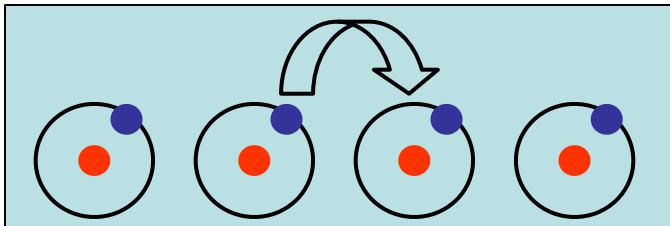
Mott-Hubbard Insulator



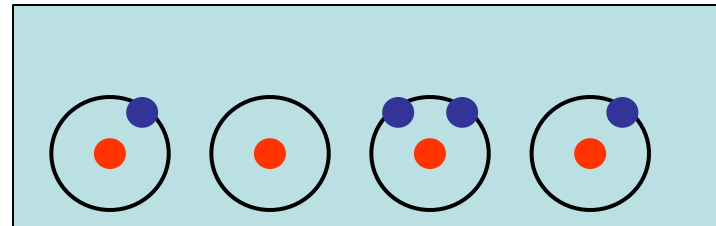
Antiferromagnetism

Hubbard Hamiltonian

$$H_{Hub} = t \sum_{\langle ij \rangle, \sigma} (c_{i\sigma}^\dagger c_{j\sigma} + h.c) + U \sum_i n_{i\uparrow} n_{i\downarrow}$$



Hopping amplitude: t



Coulomb interaction: U

$$U = 0$$

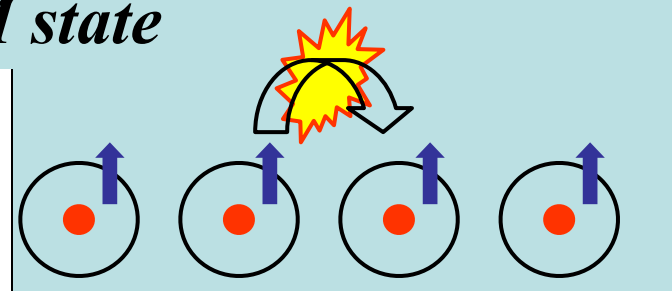
Bands: Metallic behaviour

$$U \gg t$$

Mott-Hubbard Insulator

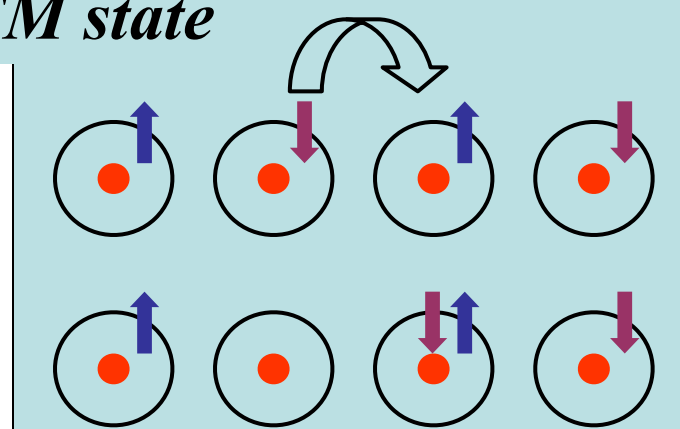
Antiferromagnetism

FM state



$$E = 0$$

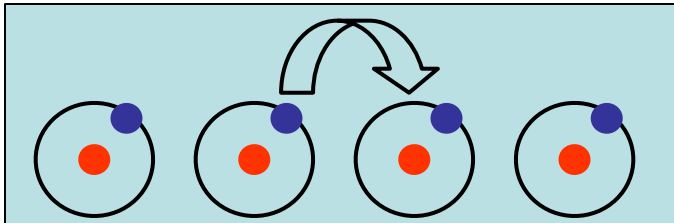
AFM state



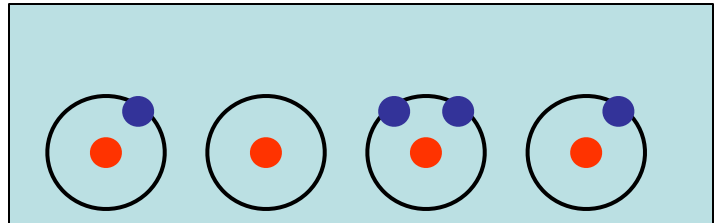
$$E = -t^2/U$$

Hubbard Hamiltonian

$$H_{Hub} = t \sum_{\langle ij \rangle, \sigma} (c_{i\sigma}^\dagger c_{j\sigma} + h.c) + U \sum_i n_{i\uparrow} n_{i\downarrow}$$



Hopping amplitude: t



Coulomb interaction: U

$U \gg t$

Mott-Hubbard Insulator



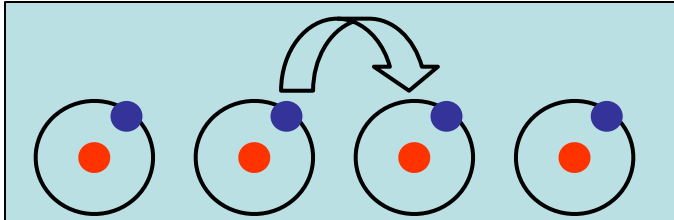
Antiferromagnetism

Heisenberg Hamiltonian

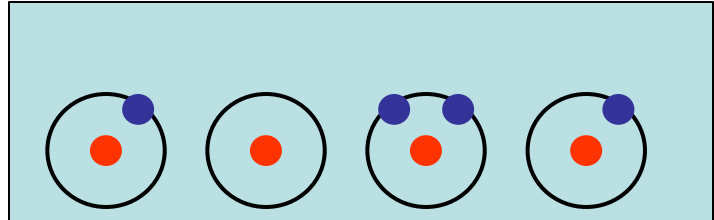
$$H_{Heis} = J \sum_{\langle ij \rangle} \vec{S}_i \cdot \vec{S}_j \quad [S^x, S^y] = i S^z$$

Hubbard Hamiltonian

$$H_{Hub} = t \sum_{\langle ij \rangle, \sigma} (c_{i\sigma}^\dagger c_{j\sigma} + h.c) + U \sum_i n_{i\uparrow} n_{i\downarrow}$$



Hopping amplitude: t



Coulomb interaction: U

$U \gg t$

Mott-Hubbard Insulator



Antiferromagnetism

Heisenberg Hamiltonian

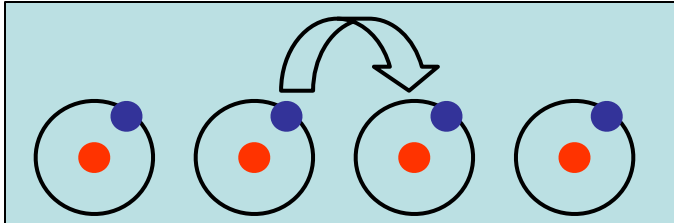
$$H_{Heis} = J \sum_{\langle ij \rangle} \vec{S}_i \cdot \vec{S}_j \quad [S^x, S^y] = i S^z$$



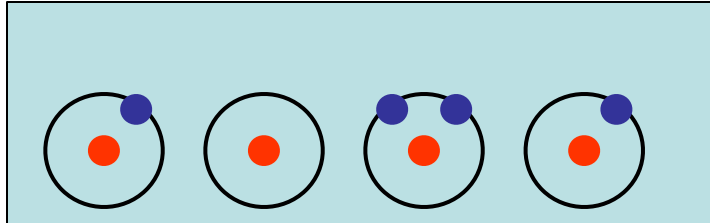
Rotational invariant

Hubbard Hamiltonian

$$H_{Hub} = t \sum_{\langle ij \rangle, \sigma} (c_{i\sigma}^\dagger c_{j\sigma} + h.c) + U \sum_i n_{i\uparrow} n_{i\downarrow}$$



Hopping amplitude: t



Coulomb interaction: U

$U \gg t$

Mott-Hubbard Insulator



Antiferromagnetism

Heisenberg Hamiltonian

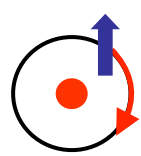
$$H_{Heis} = J \sum_{\langle ij \rangle} \vec{S}_i \cdot \vec{S}_j \quad [S^x, S^y] = i S^z$$



Rotational invariant

In real materials: (easy axis) exchange anisotropy

Magnetic anisotropy

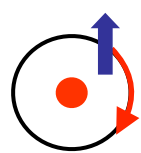


$$\vec{B} = \frac{\vec{v} \times \vec{E}}{c^2}, \quad \vec{E} = -\nabla V$$

Zeeman : $\vec{B} \cdot \vec{S} \sim \vec{L} \cdot \vec{S}$

spin-orbit coupling

Magnetic anisotropy



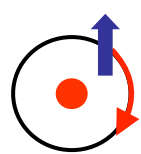
$$\vec{B} = \frac{\vec{v} \times \vec{E}}{c^2}, \quad \vec{E} = -\nabla V$$

Zeeman : $\vec{B} \cdot \vec{S} \sim \vec{L} \cdot \vec{S}$

spin-orbit coupling

1. When $c \rightarrow \infty$ anisotropy $\rightarrow 0$

Magnetic anisotropy



$$\vec{B} = \frac{\vec{v} \times \vec{E}}{c^2}, \quad \vec{E} = -\nabla V$$

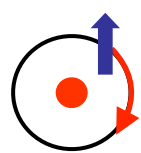
Zeeman : $\vec{B} \cdot \vec{S} \sim \vec{L} \cdot \vec{S}$

spin-orbit coupling

1. When $c \rightarrow \infty$ anisotropy $\rightarrow 0$

2. Total angular momentum $\vec{J} = \vec{L} + \vec{S}$

Magnetic anisotropy



$$\vec{B} = \frac{\vec{v} \times \vec{E}}{c^2}, \quad \vec{E} = -\nabla V$$

Zeeman : $\vec{B} \cdot \vec{S} \sim \vec{L} \cdot \vec{S}$

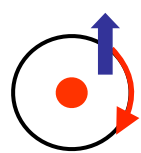
spin-orbit coupling

1. When $c \rightarrow \infty$ anisotropy $\rightarrow 0$

2. Total angular momentum $\vec{J} = \vec{L} + \vec{S}$

3. ∇V large when Z large \rightarrow heavy elements \rightarrow 4d, 5d

Magnetic anisotropy



$$\vec{B} = \frac{\vec{v} \times \vec{E}}{c^2}, \quad \vec{E} = -\nabla V$$

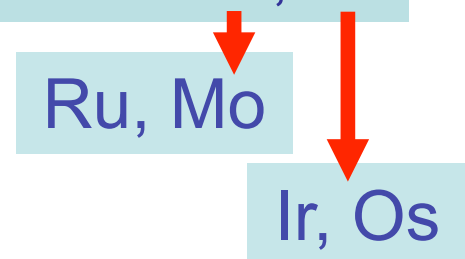
$$Zeeman : \vec{B} \cdot \vec{S} \sim \vec{L} \cdot \vec{S}$$

spin-orbit coupling

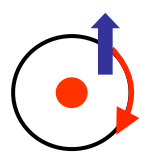
1. When $c \rightarrow \infty$ anisotropy $\rightarrow 0$

2. Total angular momentum $\vec{J} = \vec{L} + \vec{S}$

3. ∇V large when Z large \rightarrow heavy elements \rightarrow 4d, 5d



Magnetic anisotropy



$$\vec{B} = \frac{\vec{v} \times \vec{E}}{c^2}, \quad \vec{E} = -\nabla V$$

$$Zeeman : \vec{B} \cdot \vec{S} \sim \vec{L} \cdot \vec{S}$$

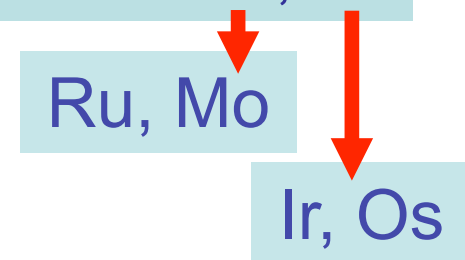
spin-orbit coupling

1. When $c \rightarrow \infty$ anisotropy $\rightarrow 0$

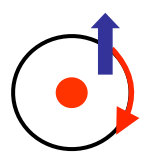
2. Total angular momentum $\vec{J} = \vec{L} + \vec{S}$

3. ∇V large when Z large \rightarrow heavy elements \rightarrow 4d, 5d

4. \vec{J} has direction & breaks rotational invariance of H



Magnetic anisotropy



$$\vec{B} = \frac{\vec{v} \times \vec{E}}{c^2}, \quad \vec{E} = -\nabla V$$

$$Zeeman : \vec{B} \cdot \vec{S} \sim \vec{L} \cdot \vec{S}$$

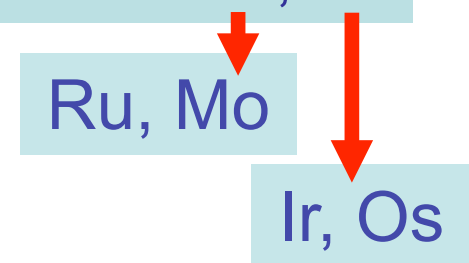
spin-orbit coupling

1. When $c \rightarrow \infty$ anisotropy $\rightarrow 0$

2. Total angular momentum $\vec{J} = \vec{L} + \vec{S}$

3. ∇V large when Z large \rightarrow heavy elements \rightarrow 4d, 5d

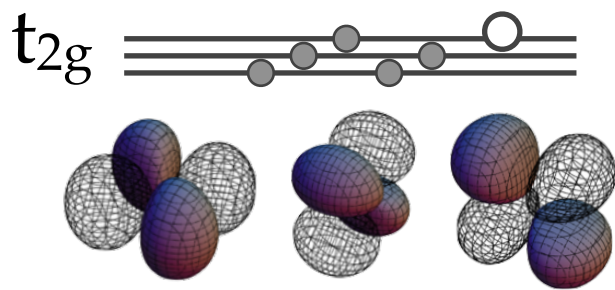
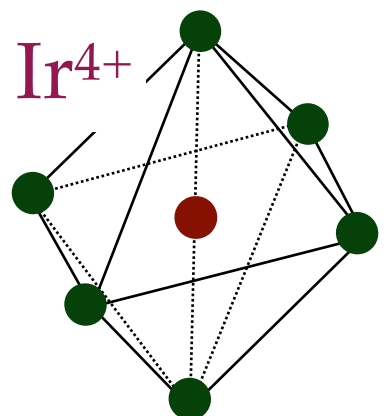
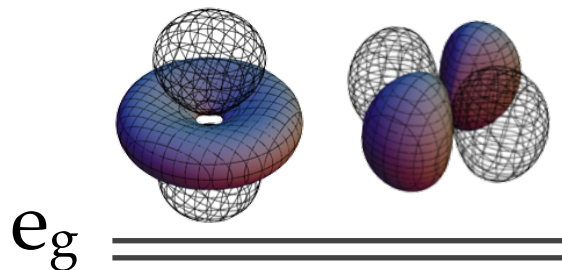
4. \vec{J} has direction & breaks rotational invariance of H



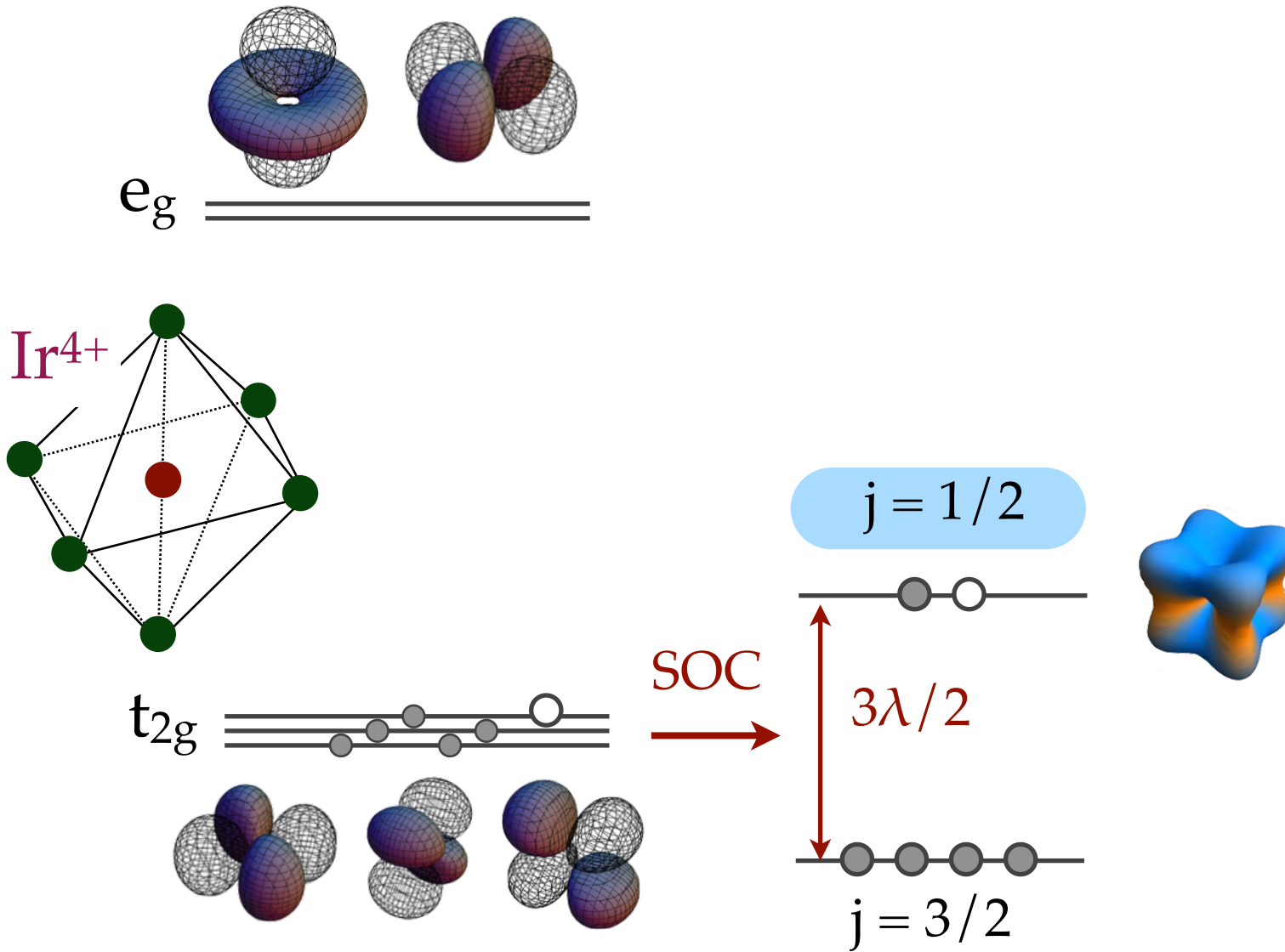
$S_i^z S_j^z$ instead of $\vec{S}_i \cdot \vec{S}_j$

(for $S = 1/2$ we have $(S_i^z)^2 = 1/4$)

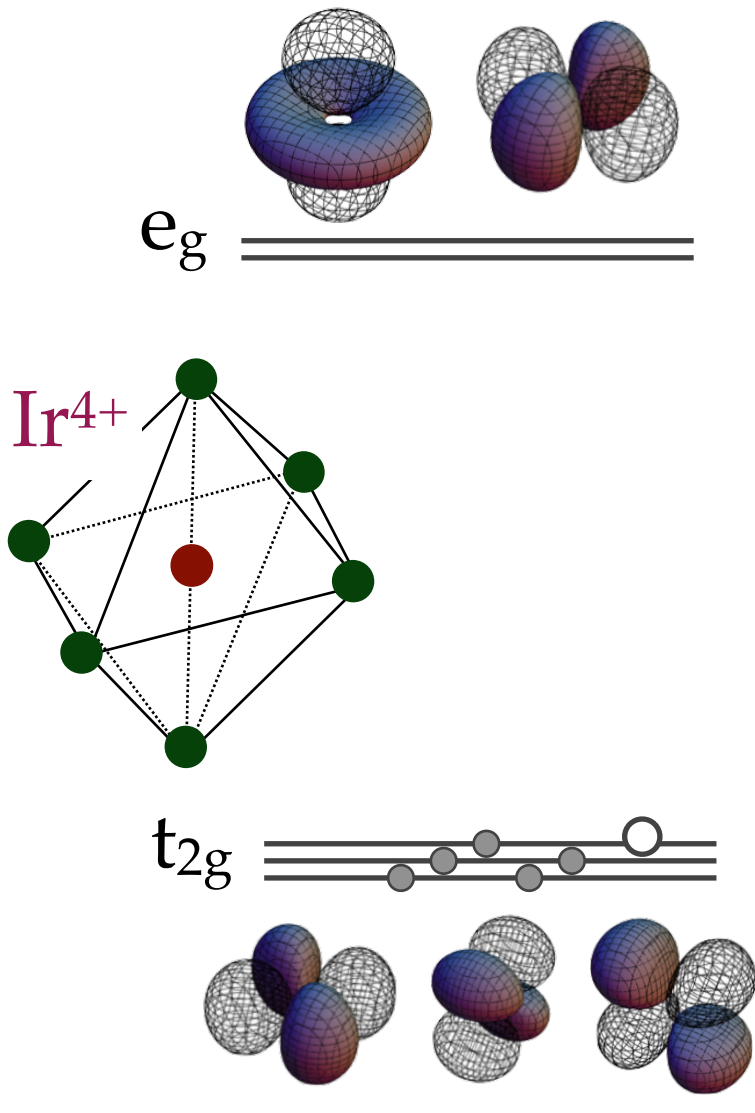
Magnetic Iridium Oxides: Ir⁴⁺



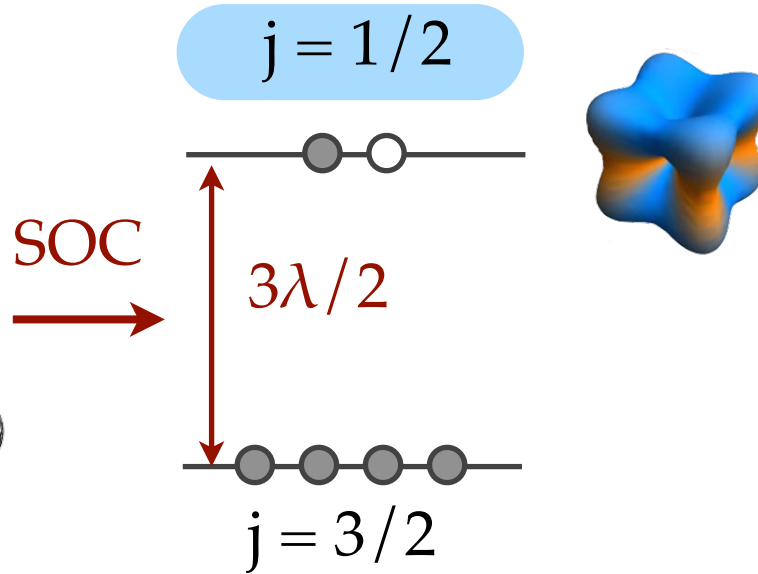
Magnetic Iridium Oxides: Ir⁴⁺



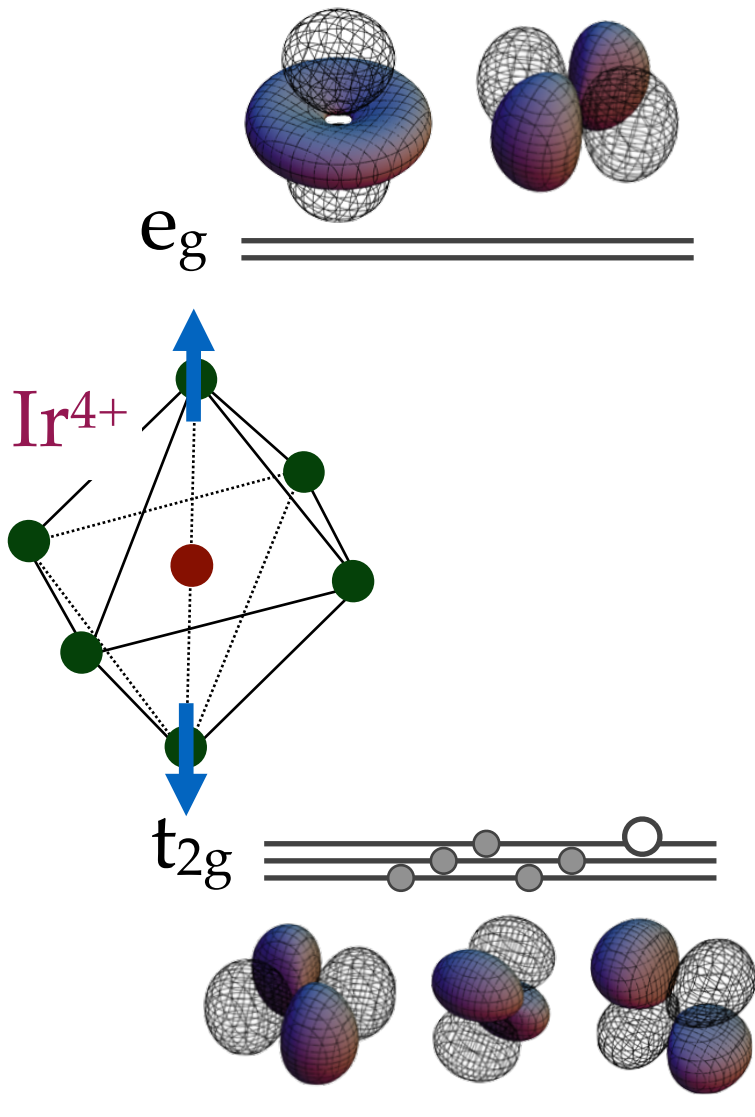
Magnetic Iridium Oxides: Ir⁴⁺



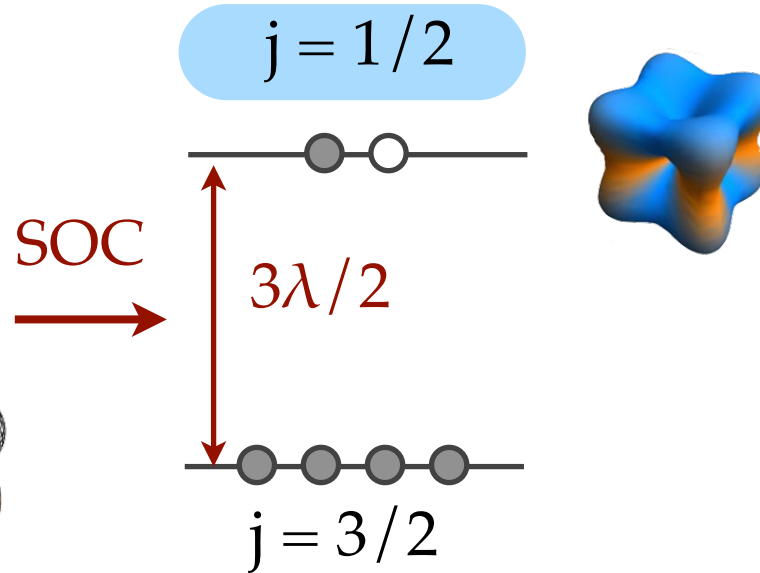
$$|j^z = +\frac{1}{2}\rangle = \frac{|yz\uparrow\rangle - i|zx\uparrow\rangle - |xy\downarrow\rangle}{\sqrt{3}}$$
$$|j^z = -\frac{1}{2}\rangle = \frac{|yz\downarrow\rangle + i|zx\downarrow\rangle - |xy\uparrow\rangle}{\sqrt{3}}$$



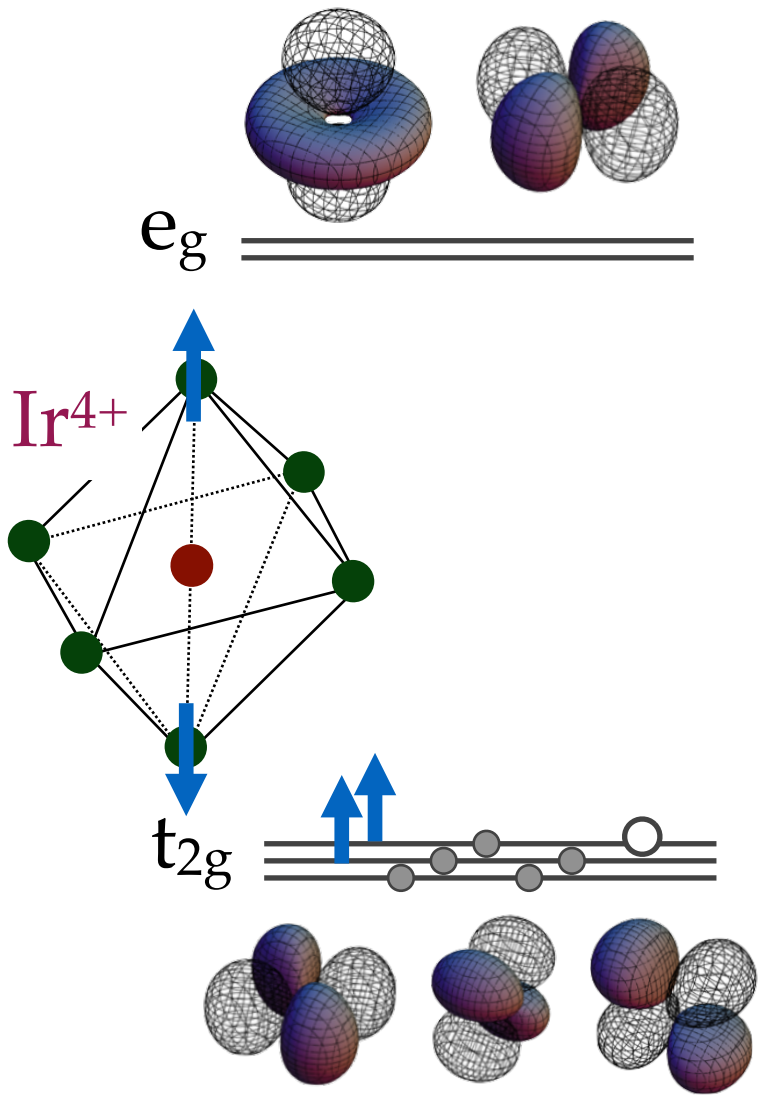
Magnetic Iridium Oxides: Ir⁴⁺



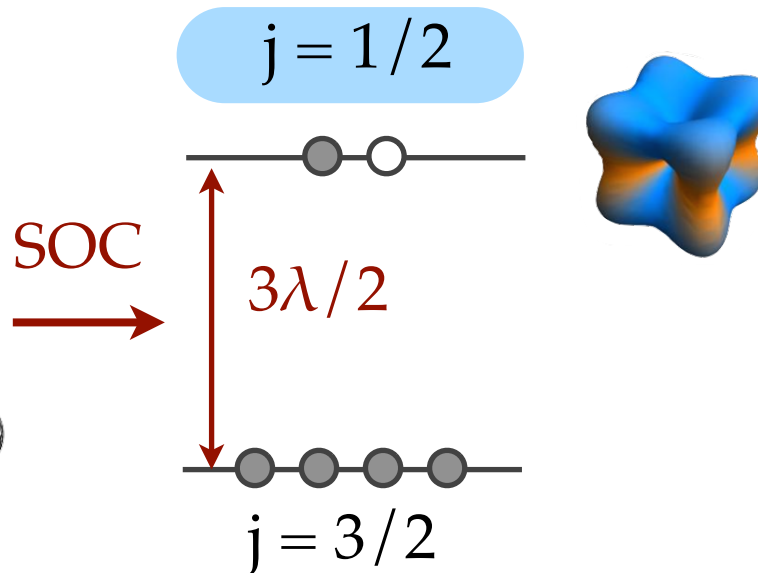
$$|j^z = +\frac{1}{2}\rangle = \frac{|yz\uparrow\rangle - i|zx\uparrow\rangle - |xy\downarrow\rangle}{\sqrt{3}}$$
$$|j^z = -\frac{1}{2}\rangle = \frac{|yz\downarrow\rangle + i|zx\downarrow\rangle - |xy\uparrow\rangle}{\sqrt{3}}$$



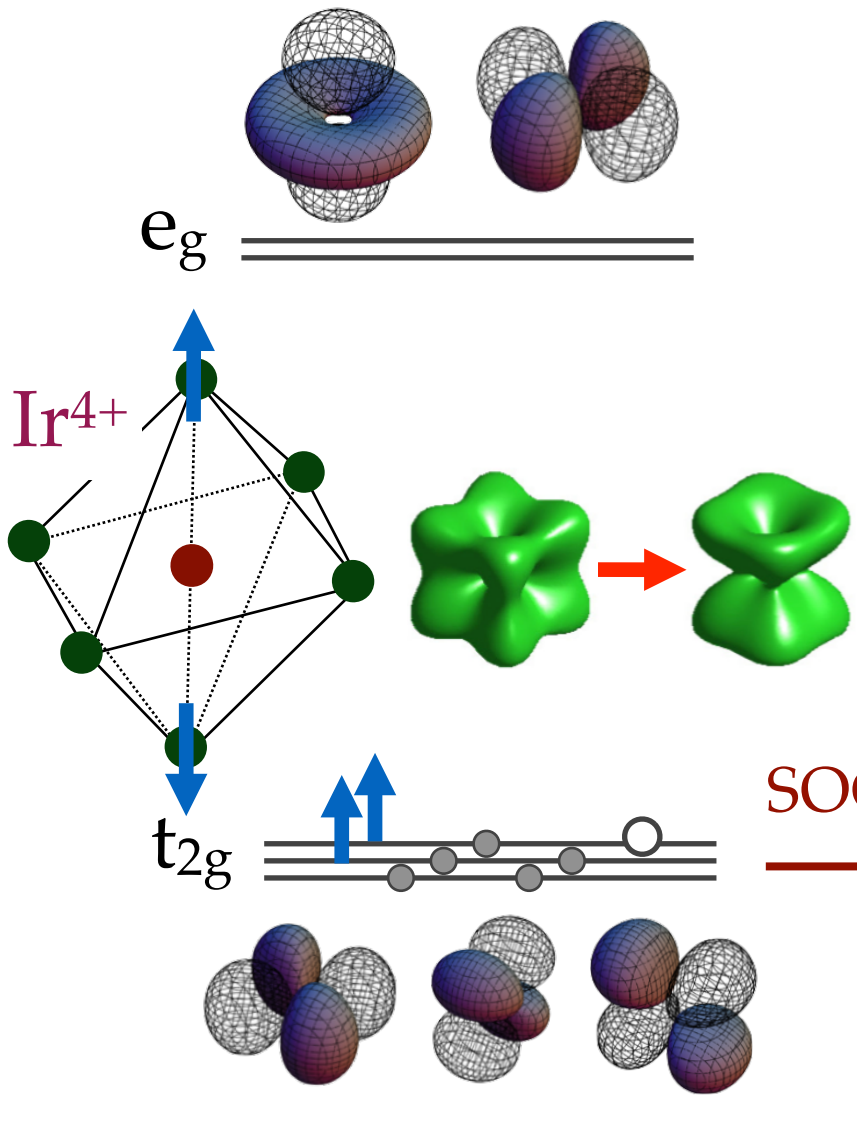
Magnetic Iridium Oxides: Ir⁴⁺



$$|j^z = +\frac{1}{2}\rangle = \frac{|yz\uparrow\rangle - i|zx\uparrow\rangle - |xy\downarrow\rangle}{\sqrt{3}}$$
$$|j^z = -\frac{1}{2}\rangle = \frac{|yz\downarrow\rangle + i|zx\downarrow\rangle - |xy\uparrow\rangle}{\sqrt{3}}$$

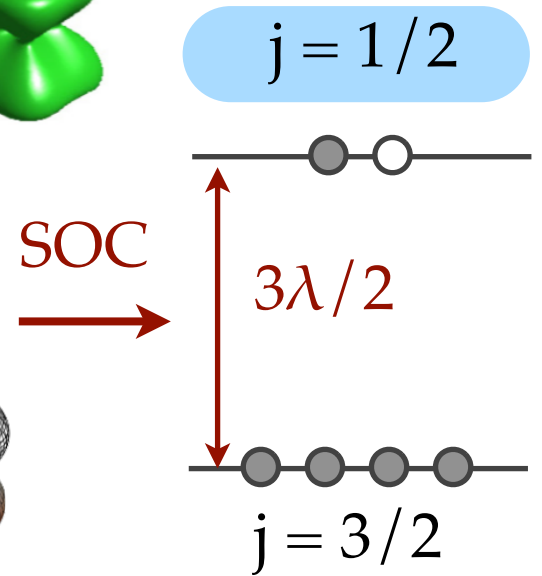


Magnetic Iridium Oxides: Ir⁴⁺



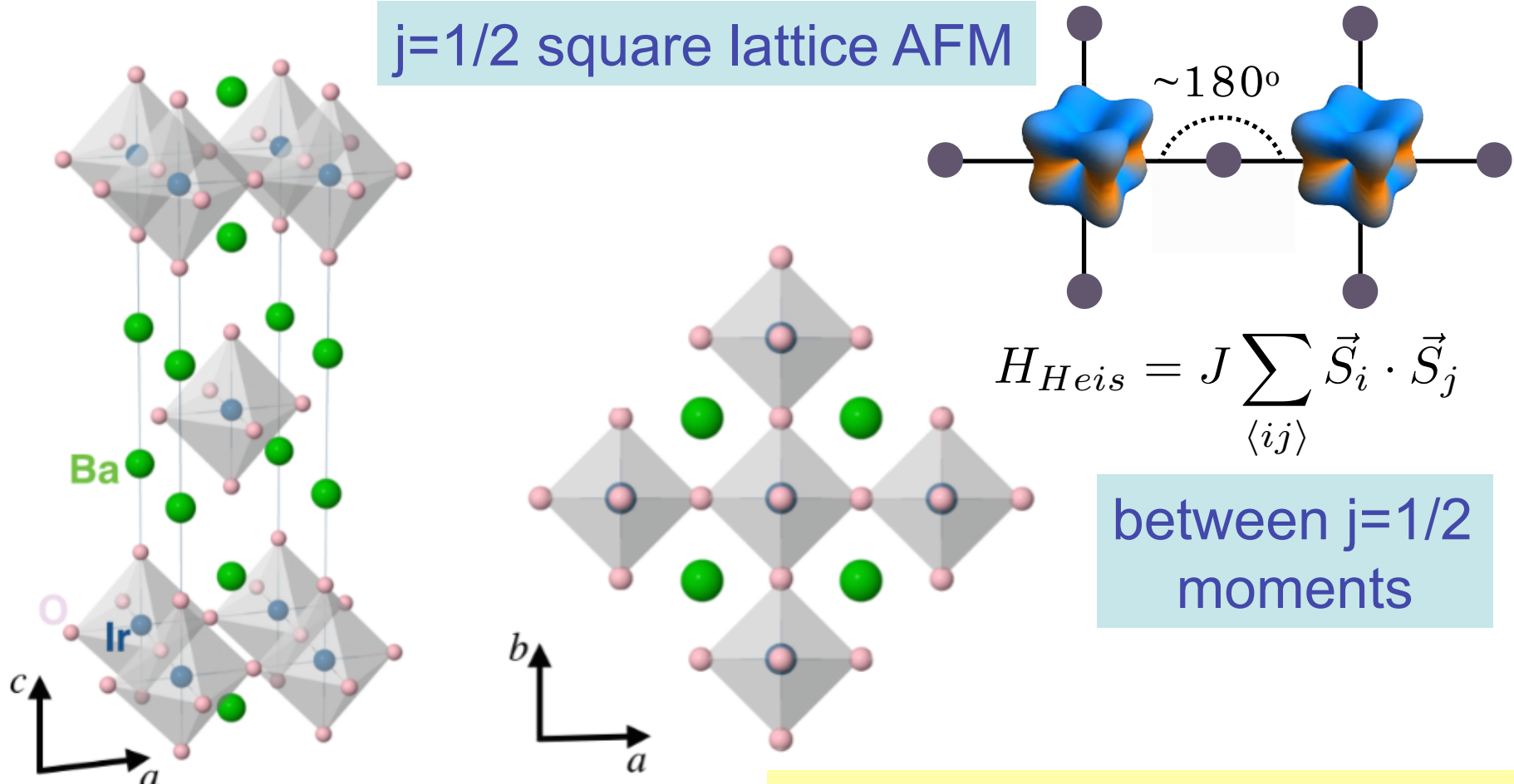
$$|j^z = +\frac{1}{2}\rangle = \frac{|yz \uparrow\rangle - i|zx \uparrow\rangle - |xy \downarrow\rangle}{\sqrt{3}}$$

$$|j^z = -\frac{1}{2}\rangle = \frac{|yz \downarrow\rangle + i|zx \downarrow\rangle - |xy \uparrow\rangle}{\sqrt{3}}$$



214 Magnetic Iridium Oxides

Sr_2IrO_4 : equivalent of cuprate La_2CuO_4

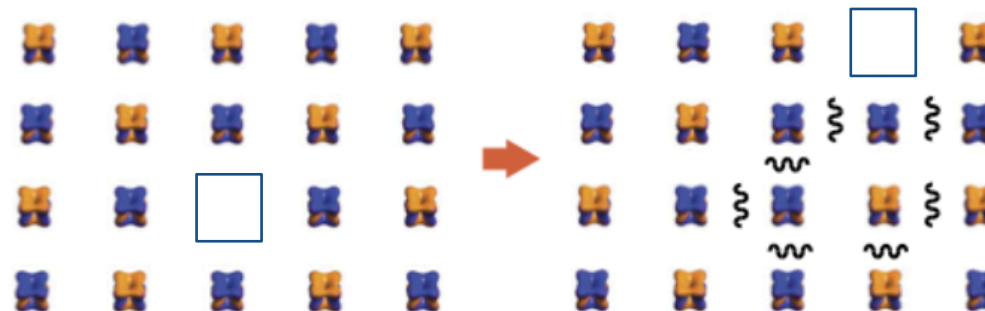


Electron/hole propagation in Sr₂IrO₄

hole hopping in s=1/2 AFM creates string of spin flips

d^5

$$\left. \begin{array}{l} s=\frac{1}{2} \\ l=1 \end{array} \right\} j = \begin{array}{l} \frac{1}{2} \\ \frac{3}{2} \end{array}$$

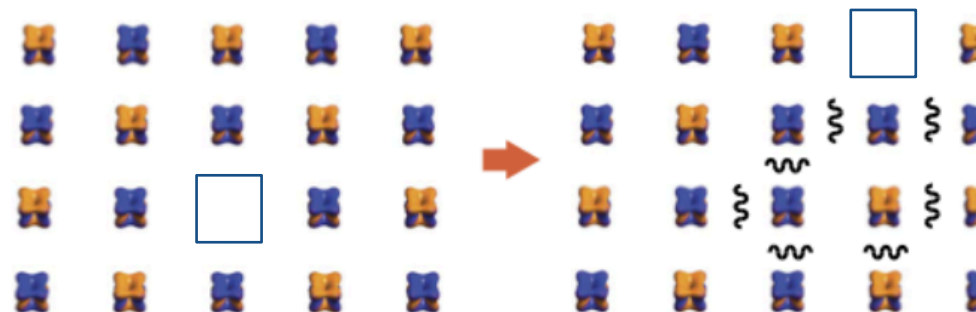


Pärschke, Wohlfeld, Foyevtsova & JvdB,
Nature Comm. 8, 686 (2017)

Electron/hole propagation in Sr₂IrO₄

hole hopping in s=1/2 AFM creates string of spin flips

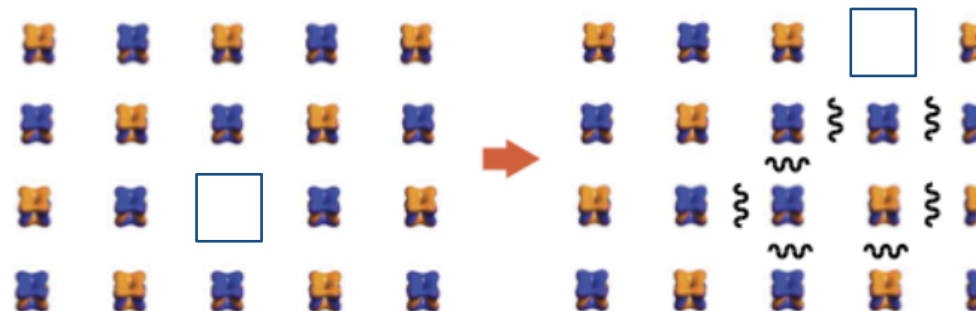
$$\begin{array}{ccc} & \xrightarrow{\hspace{2cm}} & \\ d^5 & & d^6 \\ \\ \left. \begin{array}{c} s = \frac{1}{2} \\ l = 1 \end{array} \right\} j = \frac{1}{2} & & \left. \begin{array}{c} S = 0 \\ L = 0 \end{array} \right\} J = 0 \end{array}$$



Electron/hole propagation in Sr_2IrO_4

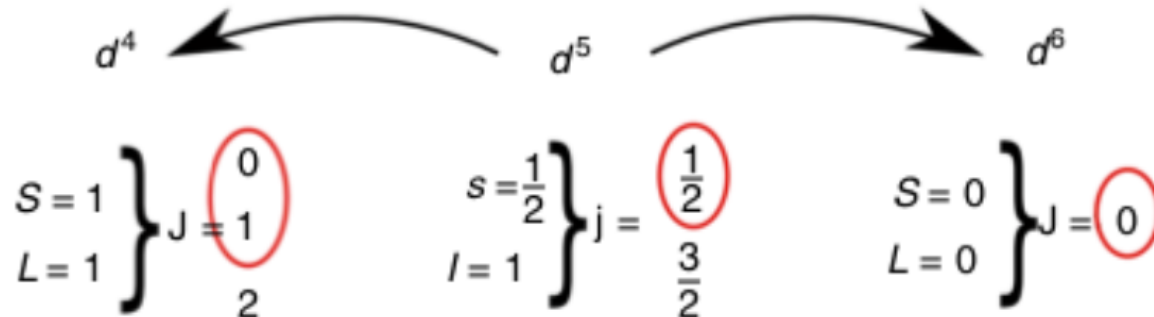
hole hopping in $s=1/2$ AFM creates string of spin flips

$$\begin{array}{ccc} d^4 & \xleftarrow{\quad} & d^5 & \xrightarrow{\quad} & d^6 \\ S = 1 & \left\{ \begin{matrix} J = 1 \\ l = 1 \end{matrix} \right. & \left. \begin{matrix} s = \frac{1}{2} \\ j = \frac{3}{2} \end{matrix} \right. & & S = 0 & \left\{ \begin{matrix} J = 0 \\ L = 0 \end{matrix} \right. \end{array}$$



Electron/hole propagation in Sr₂IrO₄

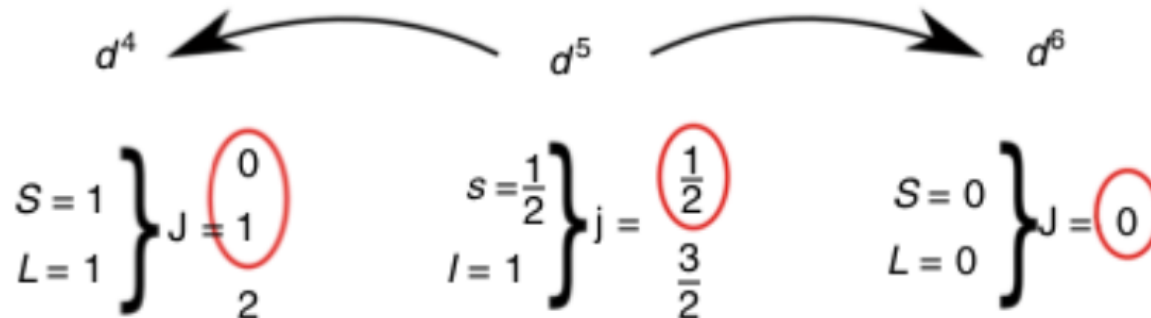
hole hopping in s=1/2 AFM creates string of spin flips



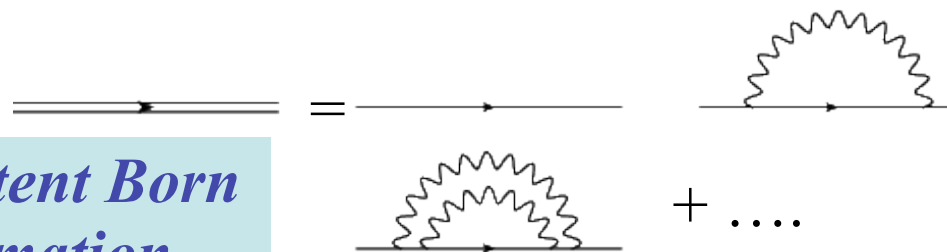
$$\begin{aligned}\mathcal{H}_t^d &= \sum_k V_k^0 (d_{kA}^\dagger d_{kA} + d_{kB}^\dagger d_{kB}) \\ &\quad + \sum_{k,q} V_{k,q} \left(d_{k-qB}^\dagger d_{kA} \alpha_q^\dagger + d_{k-qA}^\dagger d_{kB} \beta_q^\dagger + h.c. \right)\end{aligned}$$

Electron/hole propagation in Sr_2IrO_4

hole hopping in $s=1/2$ AFM creates string of spin flips



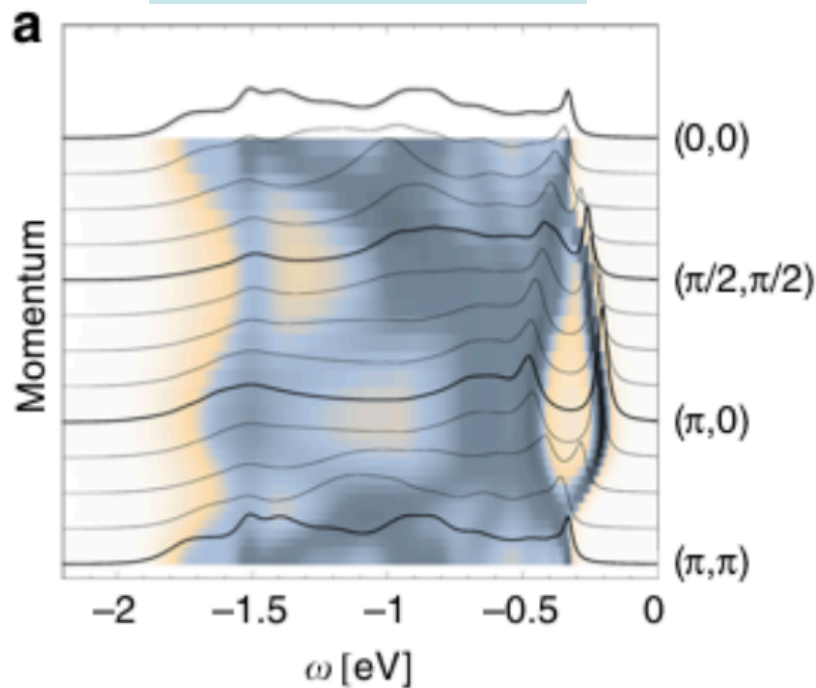
$$\begin{aligned} \mathcal{H}_t^d &= \sum_k V_k^0 (d_{kA}^\dagger d_{kA} + d_{kB}^\dagger d_{kB}) \\ &+ \sum_{k,q} V_{k,q} \left(d_{k-qB}^\dagger d_{kA} \alpha_q^\dagger + d_{k-qA}^\dagger d_{kB} \beta_q^\dagger + h.c. \right) \end{aligned}$$



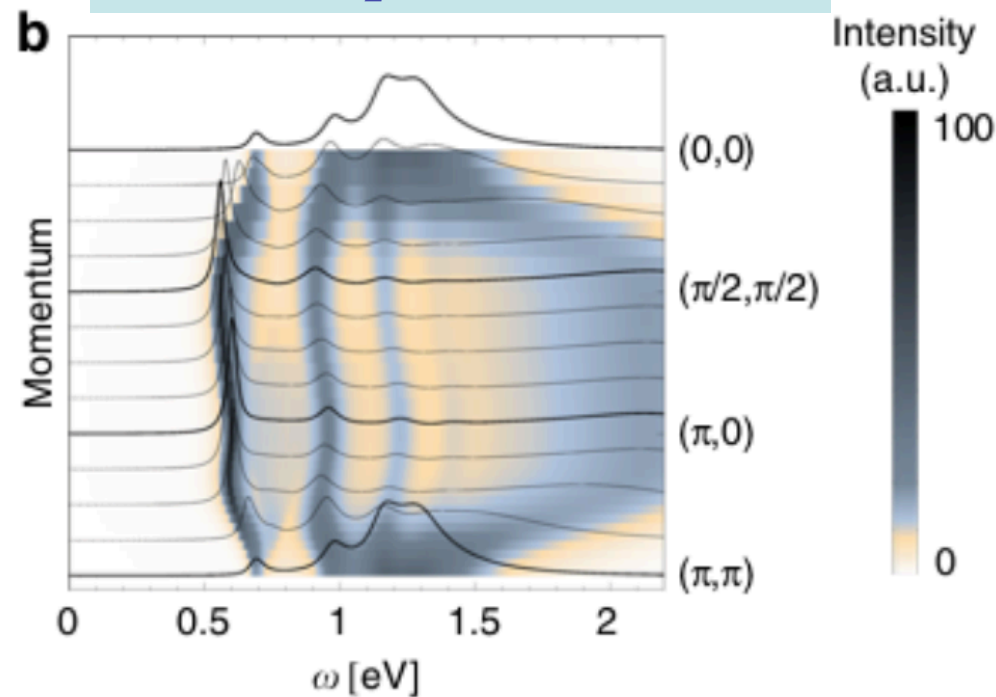
Pärschke, Wohlfeld, Foyevtsova & JvdB,
Nature Comm. 8, 686 (2017)

Electron/hole propagation in Sr₂IrO₄

photoemission



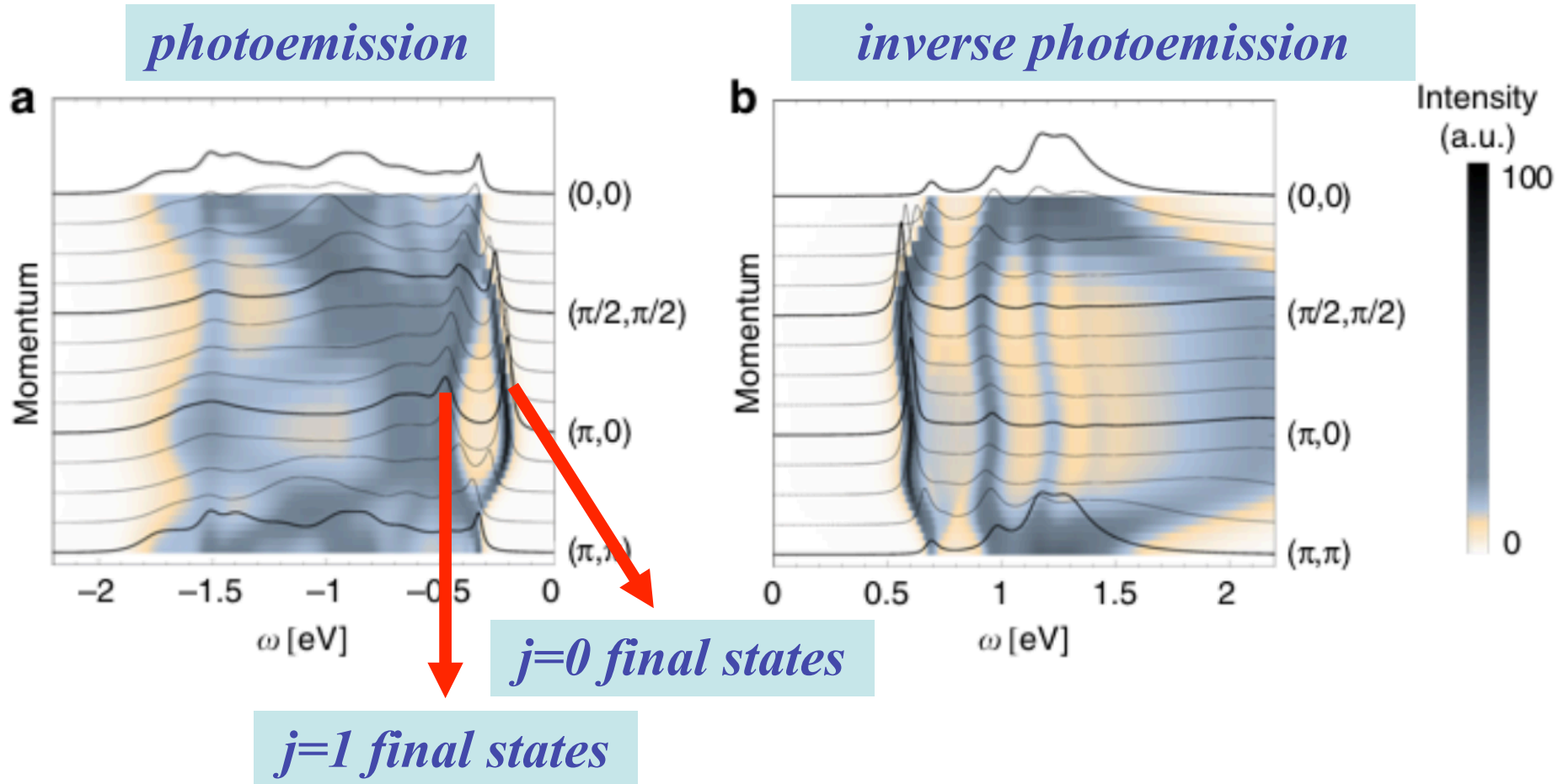
inverse photoemission



Strong electron-hole asymmetry

Pärschke, Wohlfeld, Foyevtsova & JvdB,
Nature Comm. 8, 686 (2017)
see also PRB 99, 121114(R)

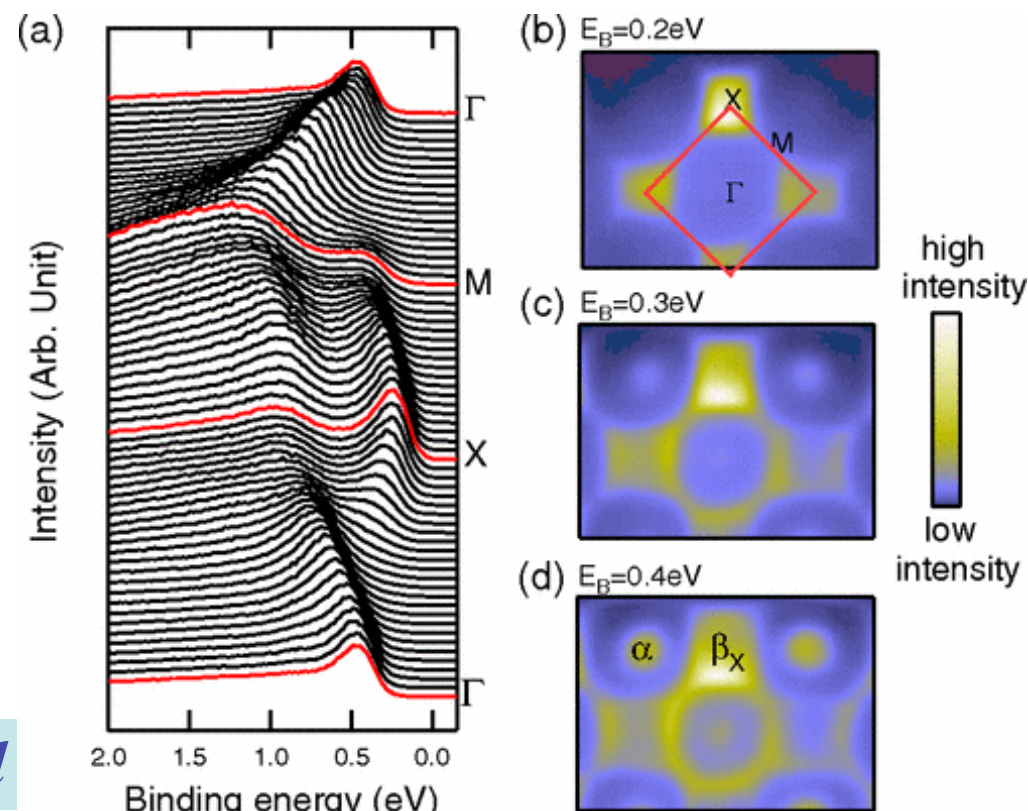
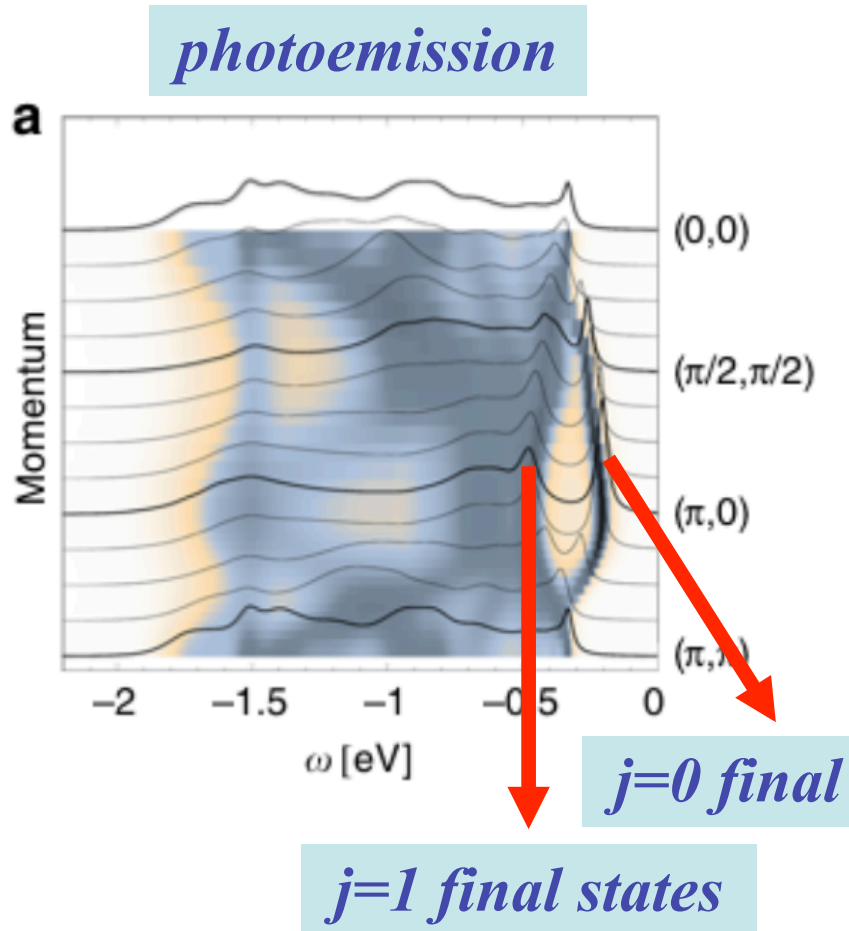
Electron/hole propagation in Sr_2IrO_4



Strong electron-hole asymmetry

Pärschke, Wohlfeld, Foyevtsova & JvdB,
Nature Comm. 8, 686 (2017)
see also PRB 99, 121114(R)

Electron/hole propagation in Sr_2IrO_4



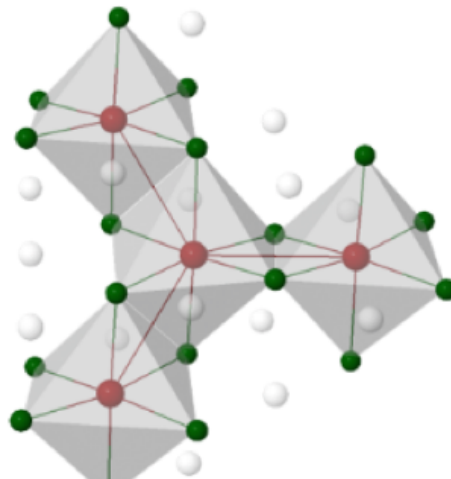
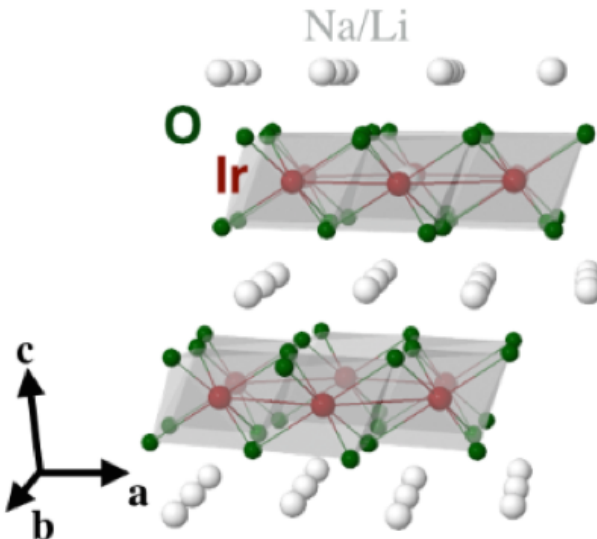
B. J. Kim et al., PRL 101, 076402 (2008)

Strong electron-hole asymmetry

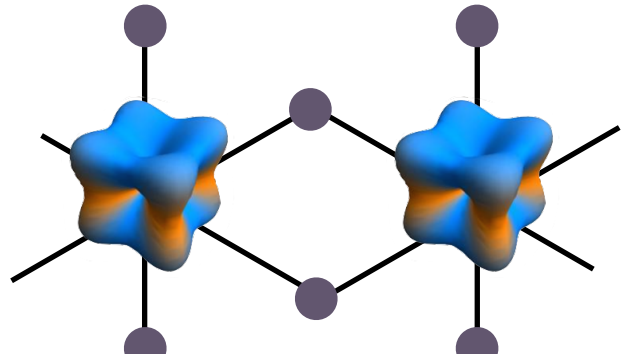
Pärschke, Wohlfeld, Foyevtsova & JvdB,
Nature Comm. 8, 686 (2017)
see also PRB 99, 121114(R)

Exchange between edge-sharing $j=1/2$ moments

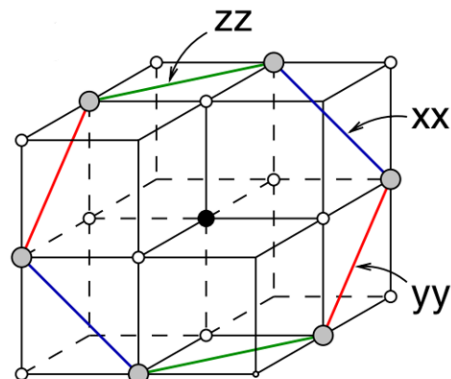
Na_2IrO_3 : honeycomb structure



$$\angle \text{Ir} - \text{O} - \text{Ir} \sim 90^\circ$$



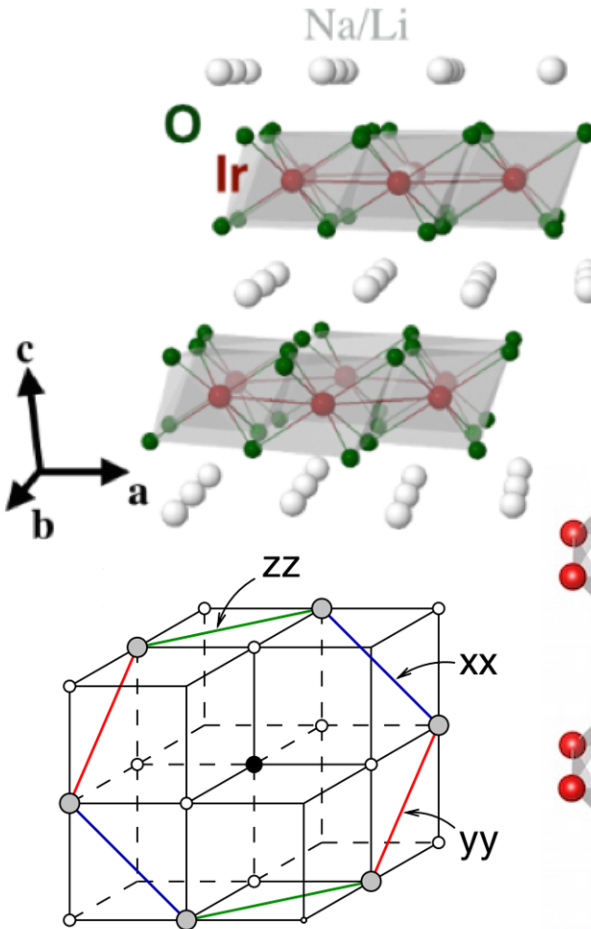
$$H_{ij}^{(1)} = K S_i^z S_j^z$$



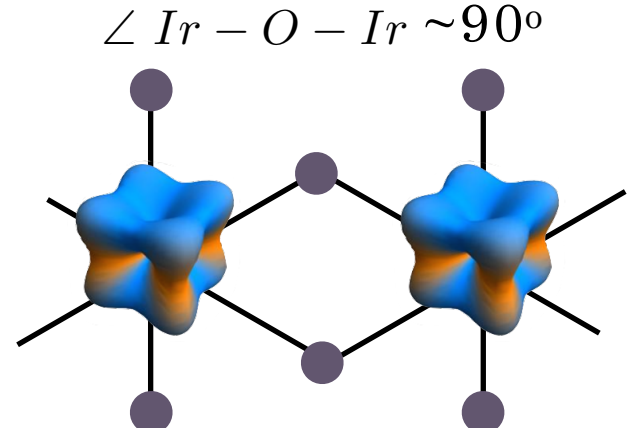
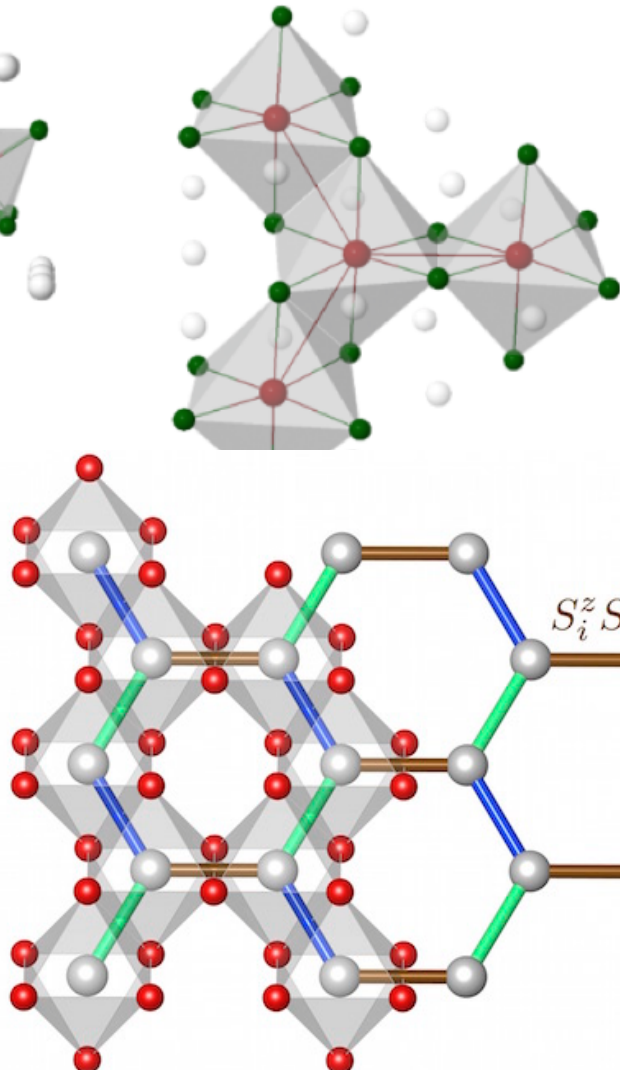
Jackeli & Khaliullin,
PRL 102, 017205 (2009)

Exchange between edge-sharing $j=1/2$ moments

Na_2IrO_3 : honeycomb structure



Jackeli & Khaliullin,
PRL 102, 017205 (2009)



$$H_{ij}^{(1)} = K S_i^z S_j^z$$

$$H_{ij}^{(2)} = K S_i^y S_j^y$$

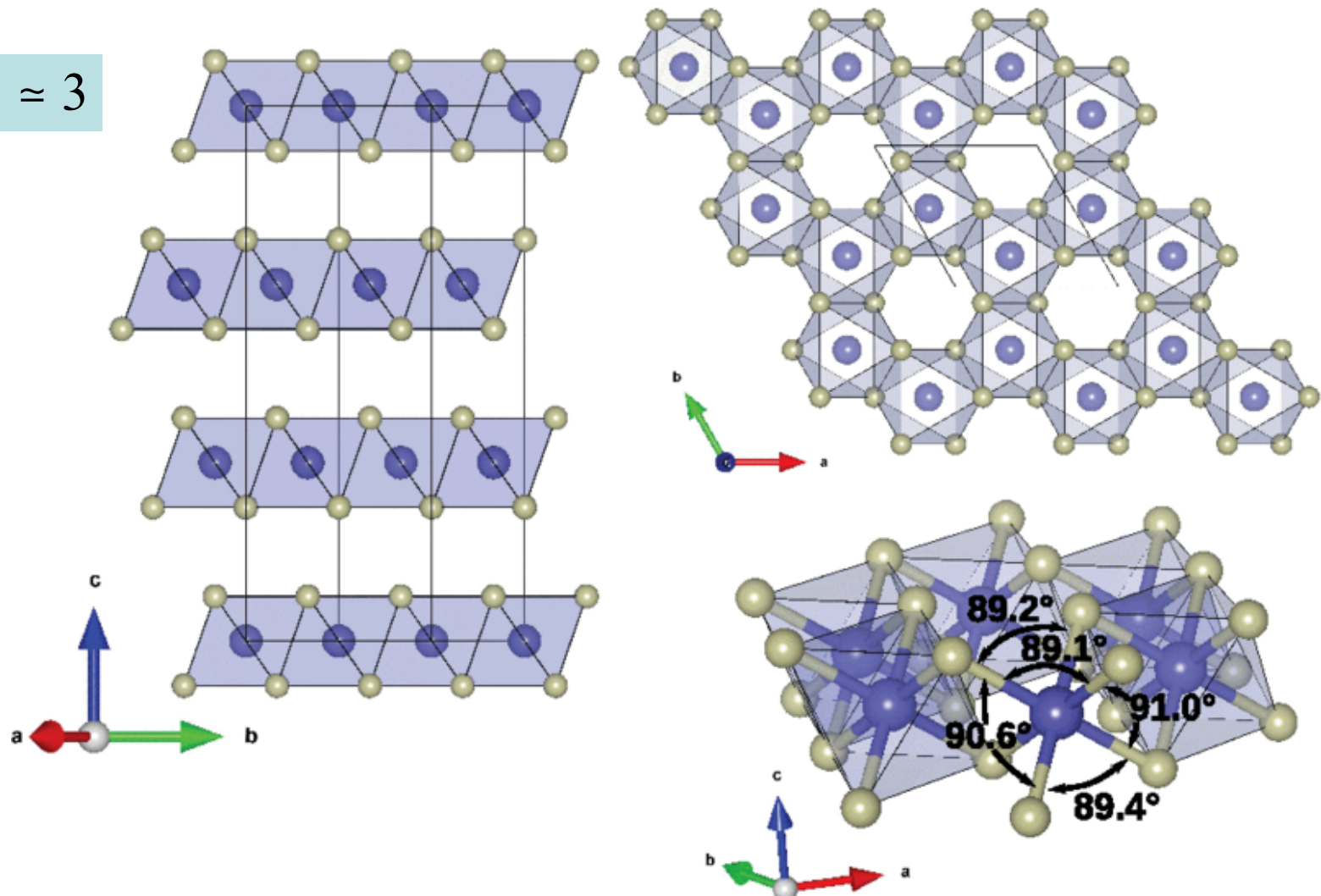
$$H_{ij}^{(3)} = K S_i^x S_j^x$$

$$H_{\text{Kitaev}} = \sum_{\langle ij \rangle_\gamma} K_\gamma S_i^\gamma S_j^\gamma$$

Kitaev, Ann. Phys. 321, 2 (2006)

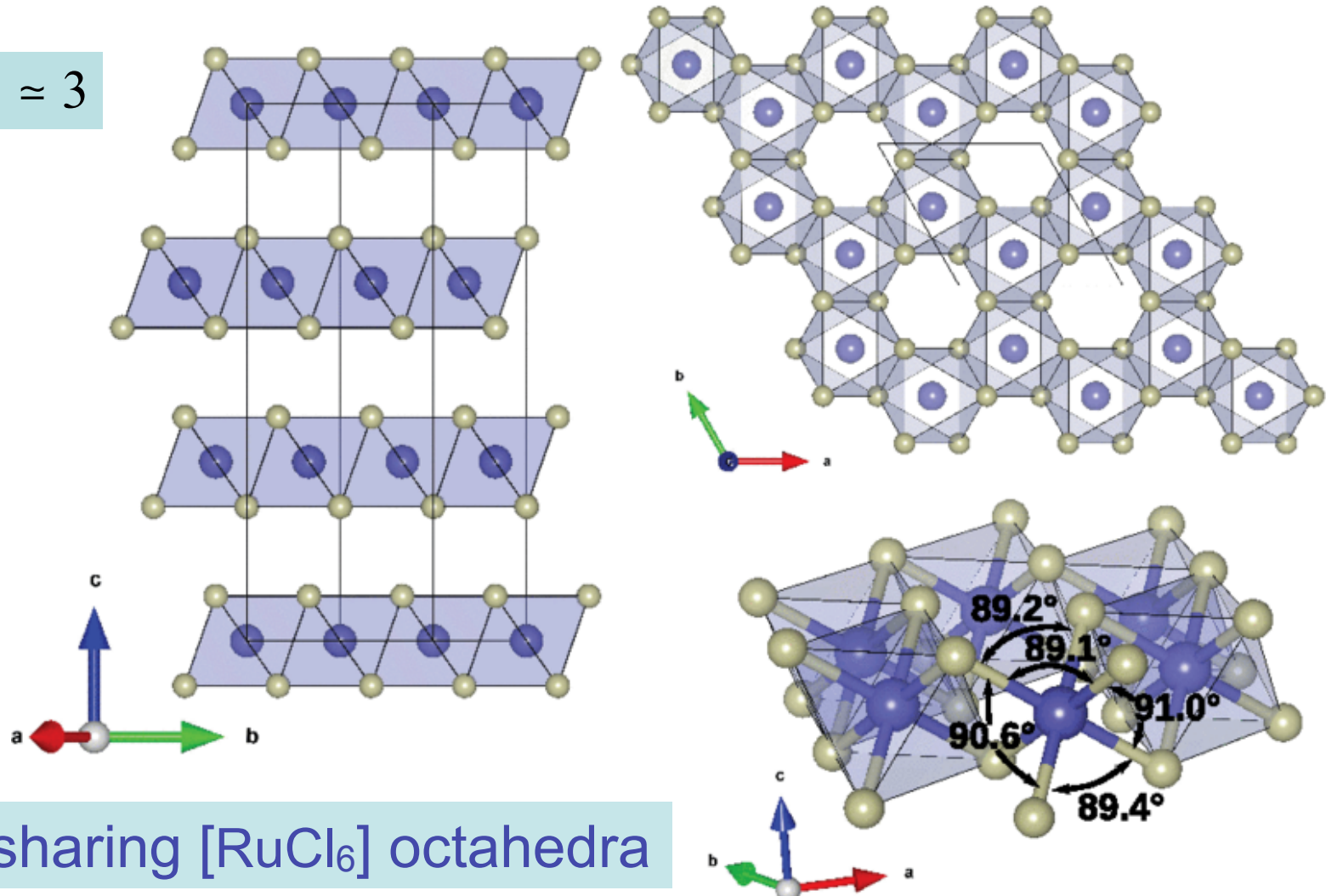
Honeycomb $\alpha\text{-RuCl}_3$

$$\lambda_{\text{Ir}}/\lambda_{\text{Ru}} \simeq 3$$



Honeycomb α -RuCl₃

$$\lambda_{\text{Ir}}/\lambda_{\text{Ru}} \approx 3$$

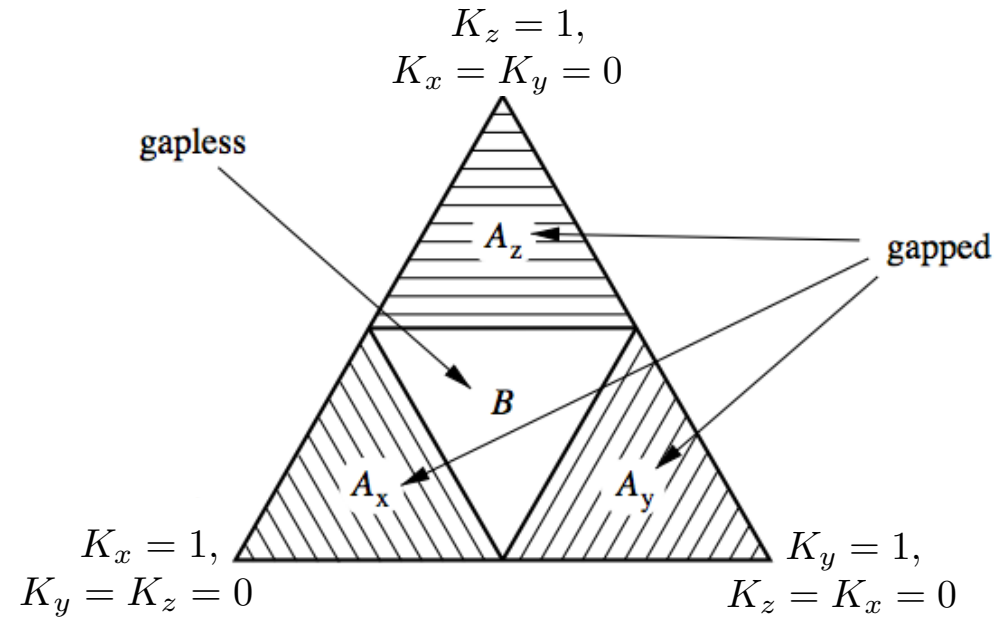


edge sharing [RuCl₆] octahedra

Honeycomb Kitaev model

$$H_{Kitaev} = \sum_{\langle ij \rangle_\gamma} K_\gamma S_i^\gamma S_j^\gamma$$

- phase diagram

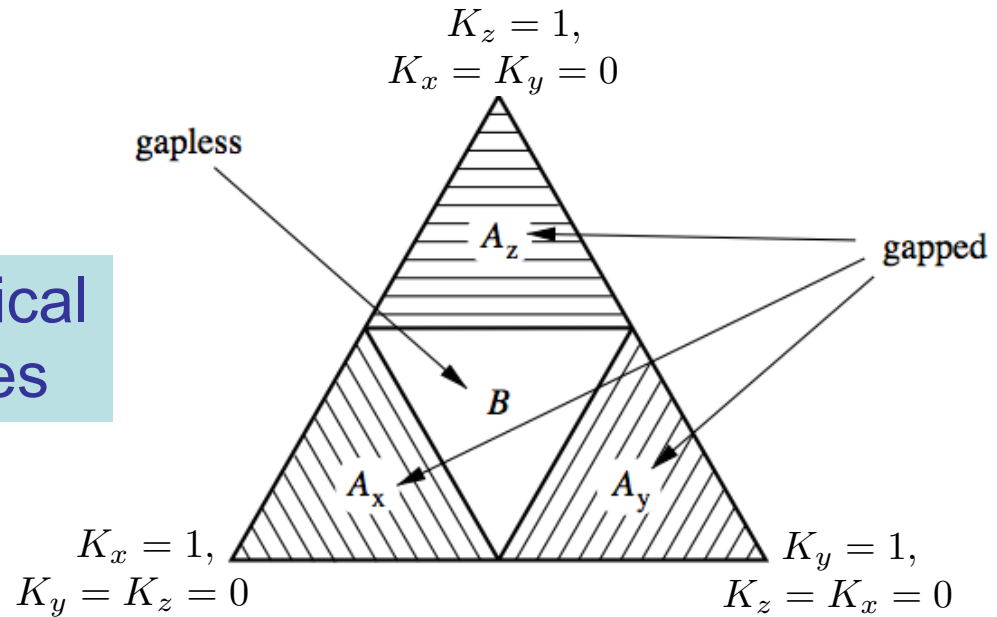


Honeycomb Kitaev model

$$H_{Kitaev} = \sum_{\langle ij \rangle_\gamma} K_\gamma S_i^\gamma S_j^\gamma$$

- phase diagram

Abelian topological
spin-liquid phases

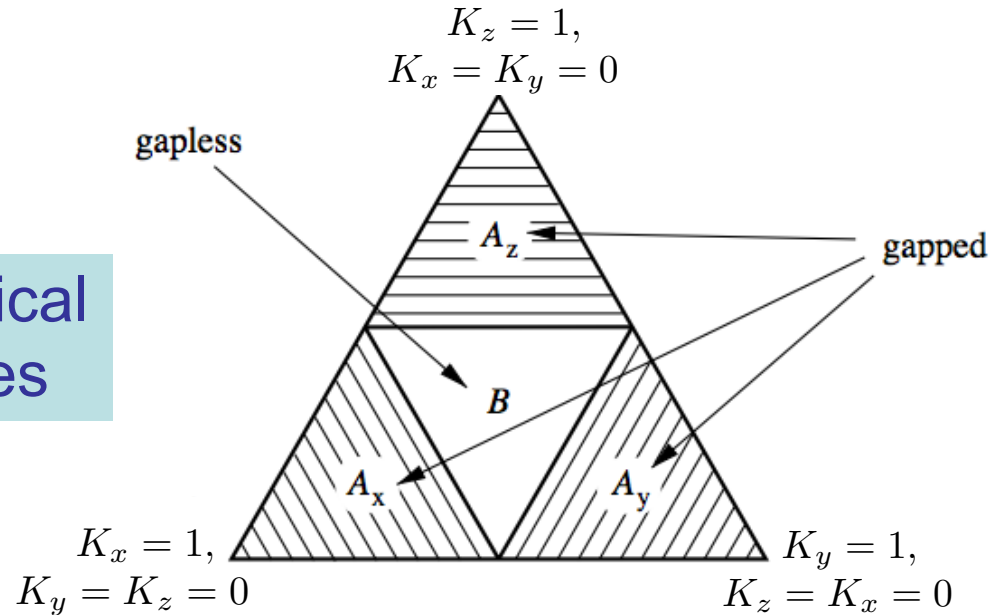


Honeycomb Kitaev model

$$H_{Kitaev} = \sum_{\langle ij \rangle_\gamma} K_\gamma S_i^\gamma S_j^\gamma$$

- phase diagram

Abelian topological
spin-liquid phases



- in magnetic field

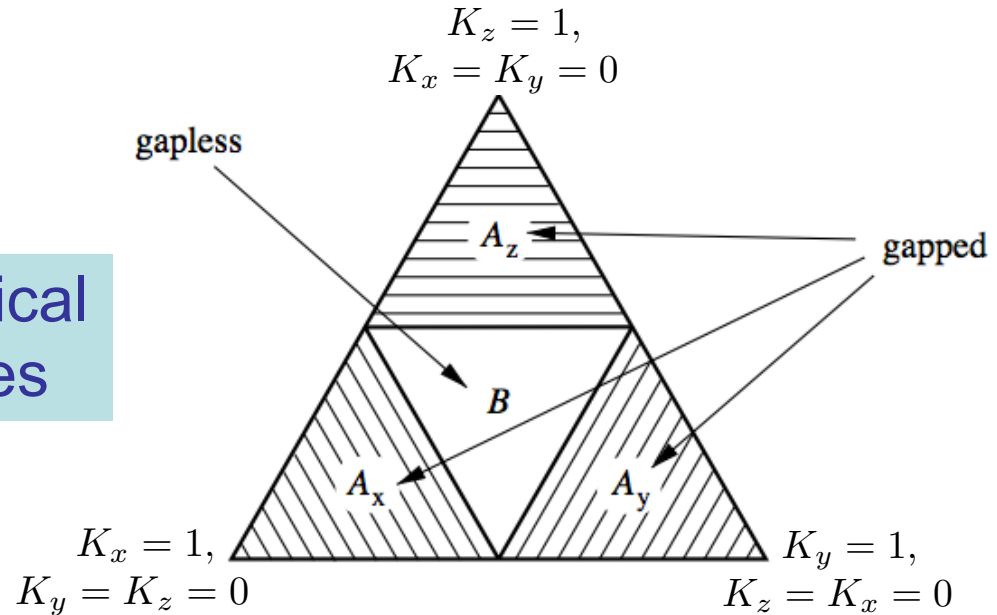
$$H_{K-B} = K \sum_{\langle ij \rangle_\gamma} S_i^\gamma S_j^\gamma + B \sum_{i\gamma} S_i^\gamma$$

Honeycomb Kitaev model

$$H_{Kitaev} = \sum_{\langle ij \rangle_\gamma} K_\gamma S_i^\gamma S_j^\gamma$$

- phase diagram

Abelian topological
spin-liquid phases



- in magnetic field

$$H_{K-B} = K \sum_{\langle ij \rangle_\gamma} S_i^\gamma S_j^\gamma + B \sum_{i\gamma} S_i^\gamma$$

gapped non-Abelian topological spin-liquid phase

(perturbative in B/K)

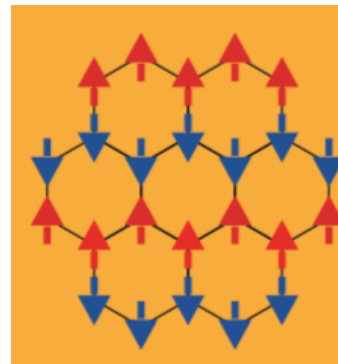
magnetic interactions in 213 iridates and α -RuCl₃

$$H_{Kitaev} = \sum_{\langle ij \rangle_\gamma} K_\gamma S_i^\gamma S_j^\gamma$$

magnetic interactions in 213 iridates and α -RuCl₃

$$H_{Kitaev} = \sum_{\langle ij \rangle_\gamma} K_\gamma S_i^\gamma S_j^\gamma$$

Experimentally: zig-zag order at low T

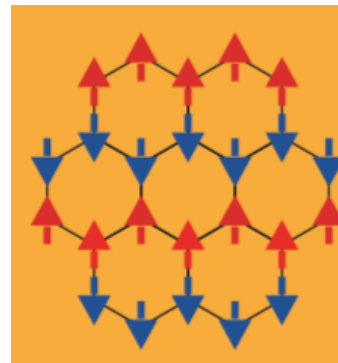


magnetic interactions in 213 iridates and α -RuCl₃

$$H_{Kitaev} = \sum_{\langle ij \rangle_\gamma} K_\gamma S_i^\gamma S_j^\gamma$$

$$H = K \sum_{\langle ij \rangle_\gamma} S_i^\gamma S_j^\gamma + J \sum_{\langle ij \rangle} \vec{S}_i \cdot \vec{S}_j + \dots$$

Experimentally: zig-zag order at low T



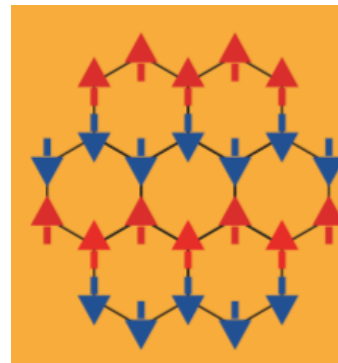
magnetic interactions in 213 iridates and α -RuCl₃

$$H_{Kitaev} = \sum_{\langle ij \rangle_\gamma} K_\gamma S_i^\gamma S_j^\gamma$$

$$H = K \sum_{\langle ij \rangle_\gamma} S_i^\gamma S_j^\gamma + J \sum_{\langle ij \rangle} \vec{S}_i \cdot \vec{S}_j + \dots$$

$$\mathcal{H}_{i,j} = J \tilde{\mathbf{S}}_i \cdot \tilde{\mathbf{S}}_j + K \tilde{S}_i^z \tilde{S}_j^z + \sum_{\alpha \neq \beta} \Gamma_{\alpha\beta} (\tilde{S}_i^\alpha \tilde{S}_j^\beta + \tilde{S}_i^\beta \tilde{S}_j^\alpha)$$

Experimentally: zig-zag order at low T



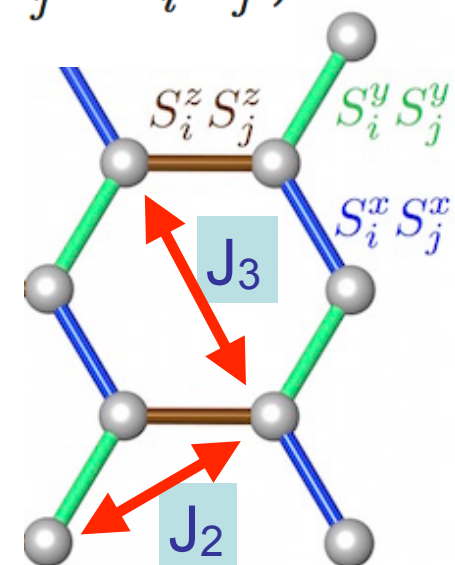
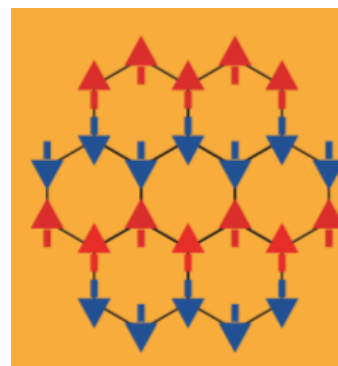
magnetic interactions in 213 iridates and α -RuCl₃

$$H_{Kitaev} = \sum_{\langle ij \rangle_\gamma} K_\gamma S_i^\gamma S_j^\gamma$$

$$H = K \sum_{\langle ij \rangle_\gamma} S_i^\gamma S_j^\gamma + J \sum_{\langle ij \rangle} \vec{S}_i \cdot \vec{S}_j + \dots$$

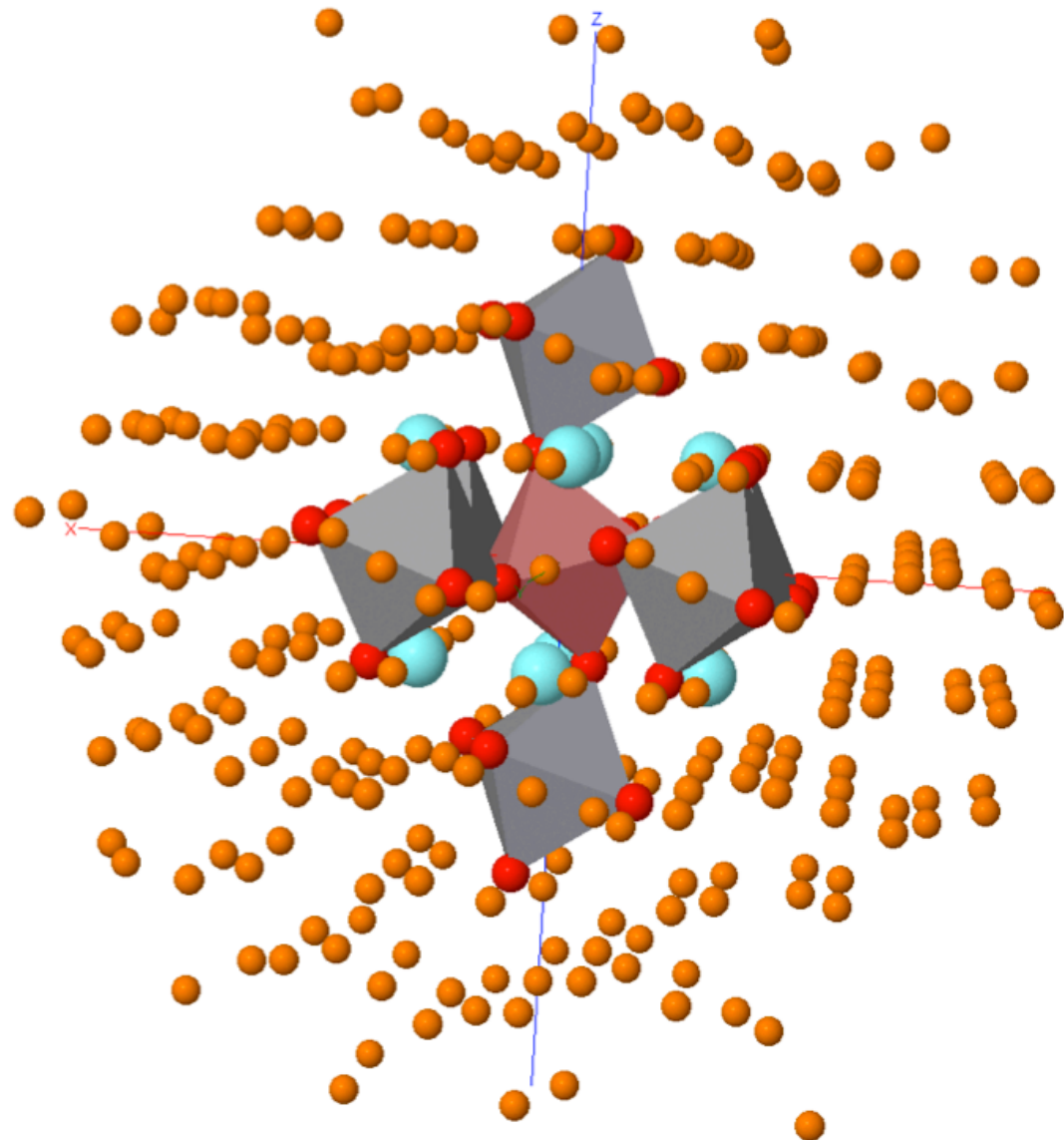
$$\mathcal{H}_{i,j} = J \tilde{\mathbf{S}}_i \cdot \tilde{\mathbf{S}}_j + K \tilde{S}_i^z \tilde{S}_j^z + \sum_{\alpha \neq \beta} \Gamma_{\alpha\beta} (\tilde{S}_i^\alpha \tilde{S}_j^\beta + \tilde{S}_i^\beta \tilde{S}_j^\alpha)$$

Experimentally: zig-zag order at low T



QC: wavefunction-based correlation methods

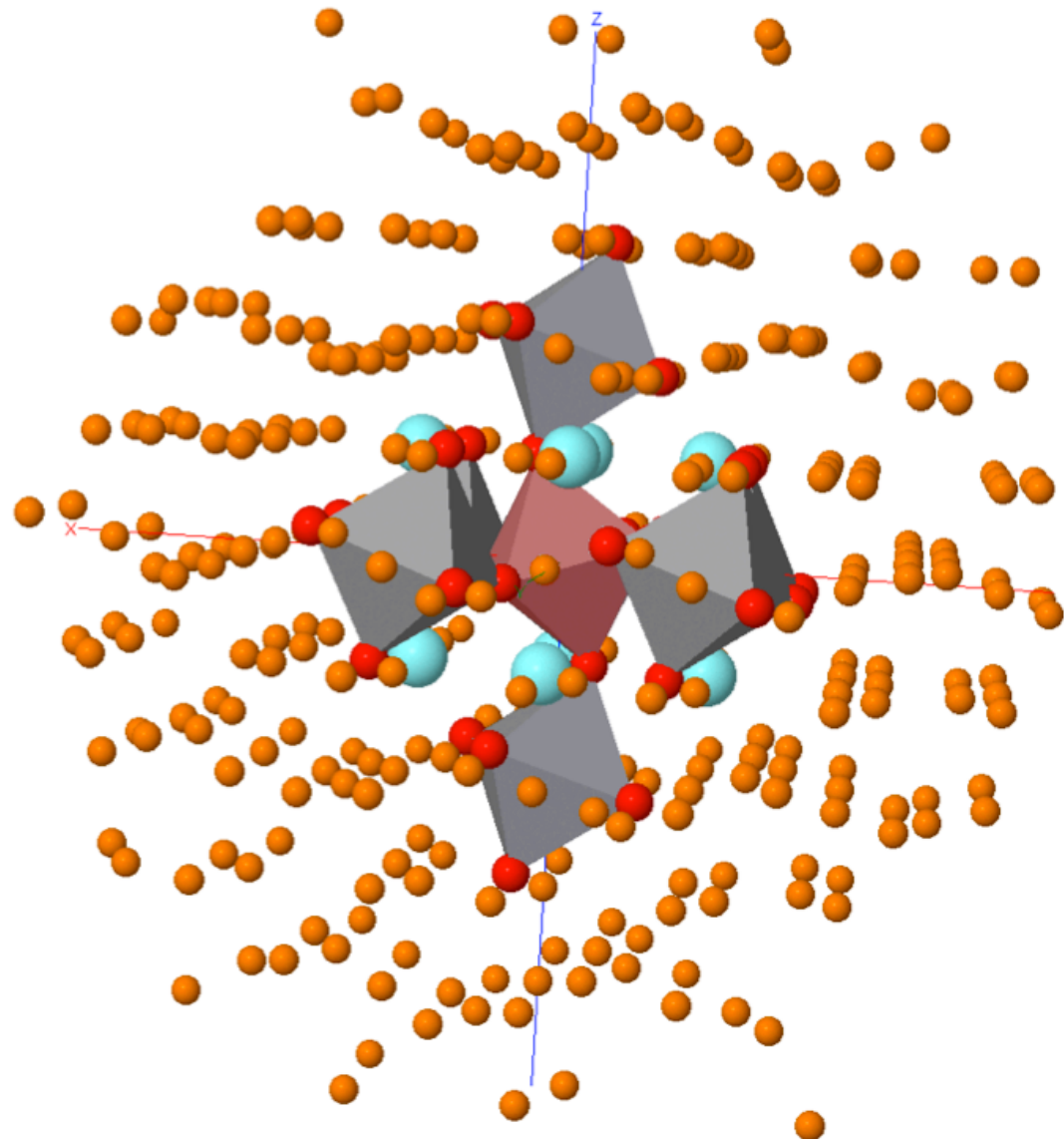
Finite embedded clusters



QC: wavefunction-based correlation methods

*Fully ab initio for ground
and excited states*

Finite embedded clusters

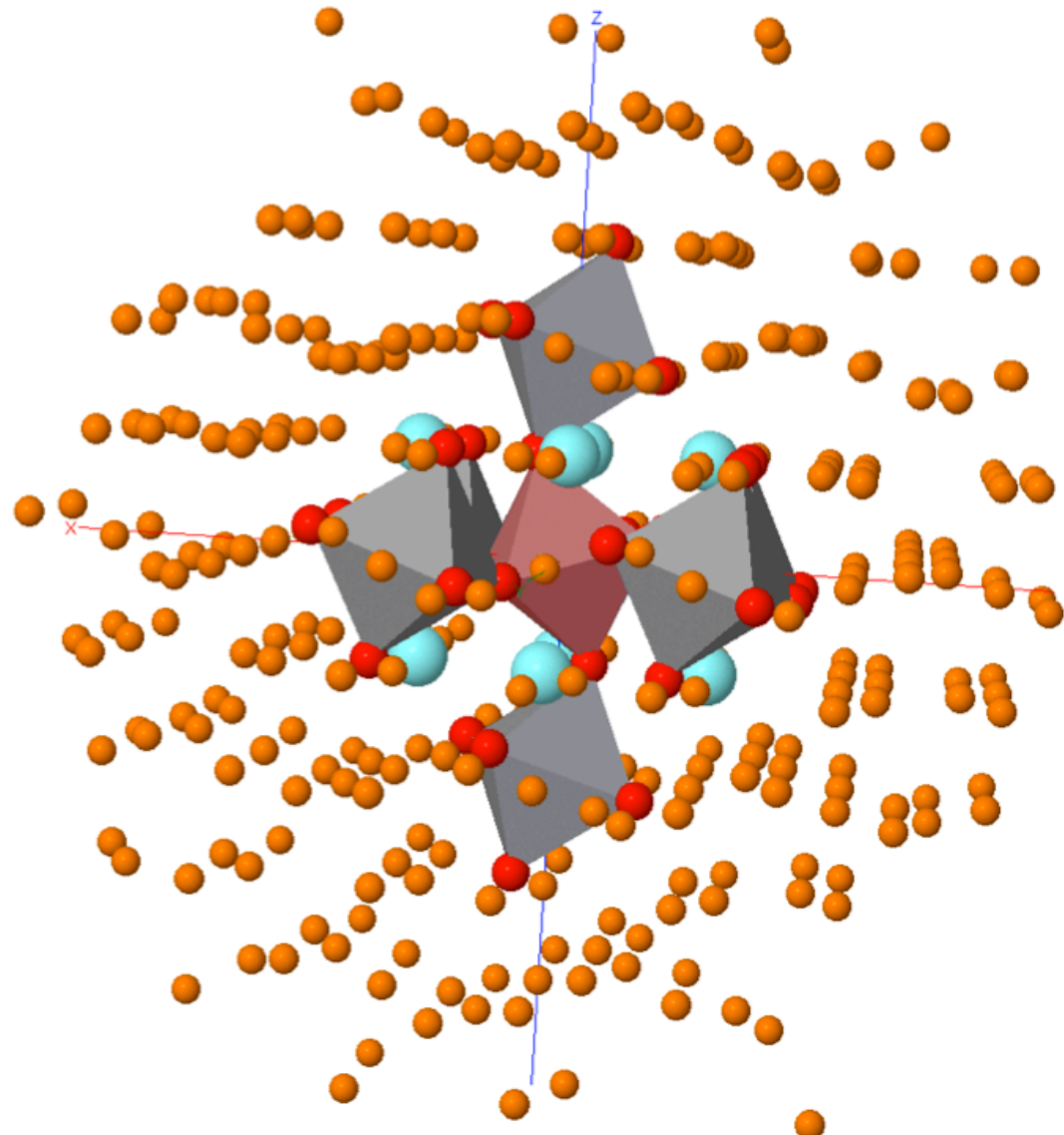


QC: wavefunction-based correlation methods

*Fully ab initio for ground
and excited states*

*Fully correlated:
multi-configuration
wave-functions*

Finite embedded clusters



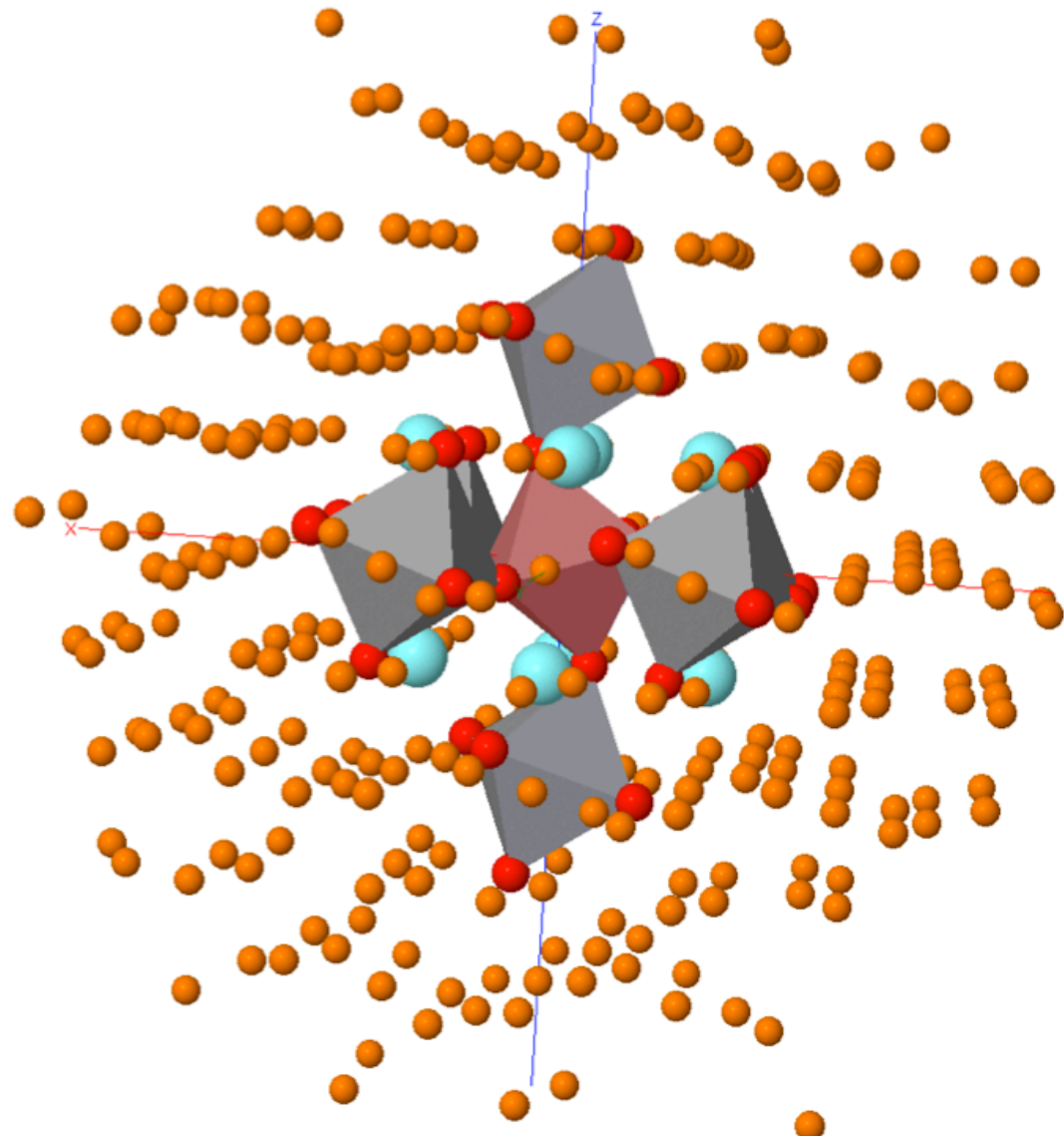
QC: wavefunction-based correlation methods

*Fully ab initio for ground
and excited states*

*Fully correlated:
multi-configuration
wave-functions*

Heavy machinery

Finite embedded clusters



QC: wavefunction-based correlation methods

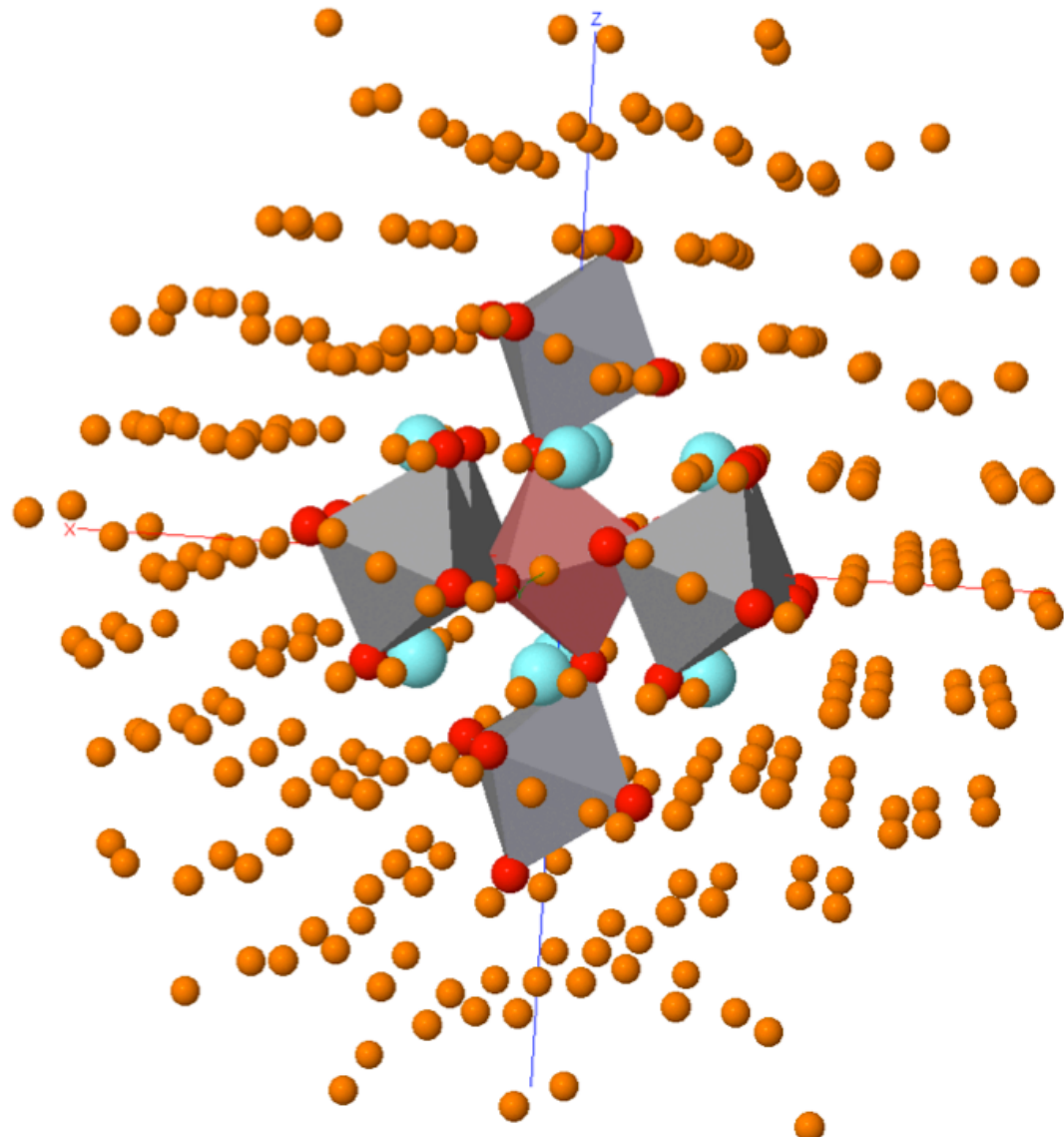
*Fully ab initio for ground
and excited states*

*Fully correlated:
multi-configuration
wave-functions*

Heavy machinery

*Excellent for systems
with localized electrons*

Finite embedded clusters



QC: wavefunction-based correlation methods

*Fully ab initio for ground
and excited states*

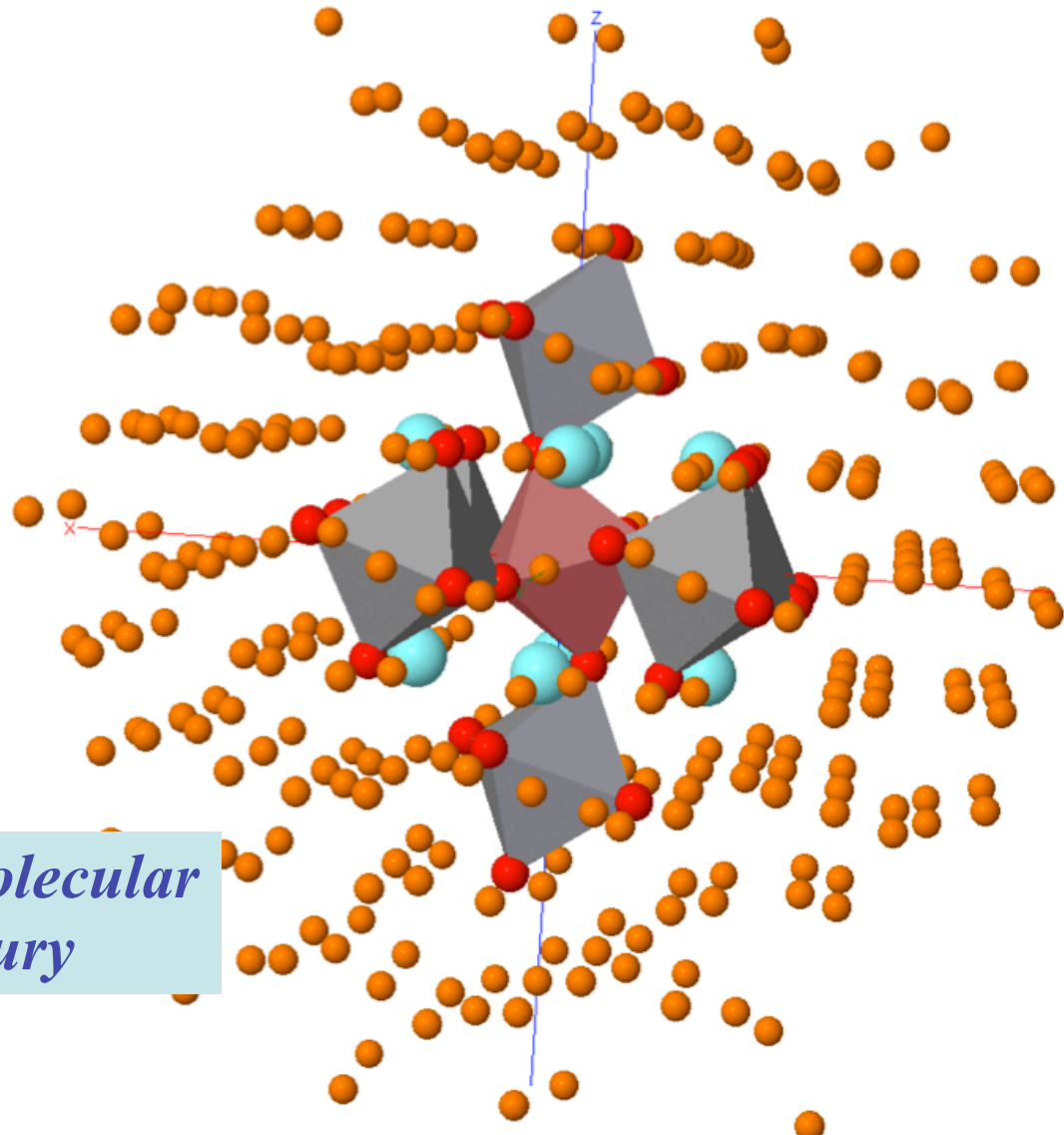
*Fully correlated:
multi-configuration
wave-functions*

Heavy machinery

*Excellent for systems
with localized electrons*

*Approximations tested in molecular
systems since half century*

Finite embedded clusters



QC: wavefunction-based correlation methods

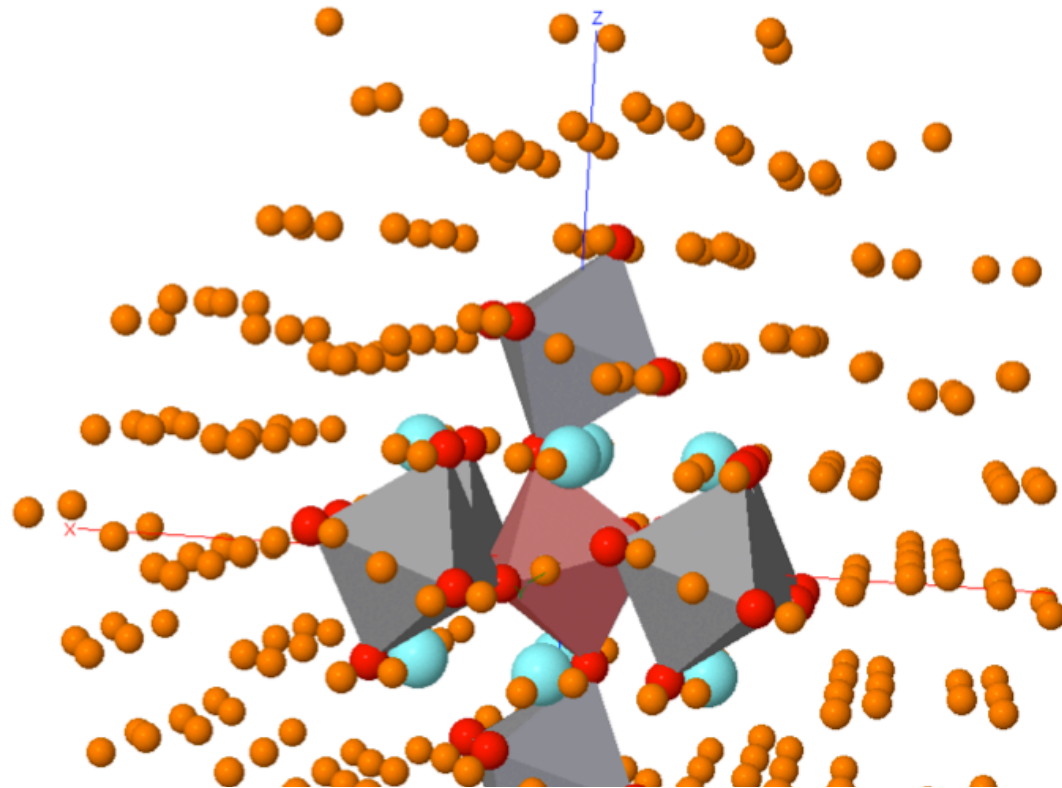
*Fully ab initio for ground
and excited states*

*Fully correlated:
multi-configuration
wave-functions*

Heavy machinery

*Excellent for systems
with localized electrons*

Finite embedded clusters



Our scheme: direct-space multireference CI, finite embedded clusters

The infinite solid-state environment: one-electron embedding potential

- simplest: point-charge array
- more advanced: based on prior periodic Hartree-Fock

honeycomb Kitaev materials to consider

Na_2IrO_3

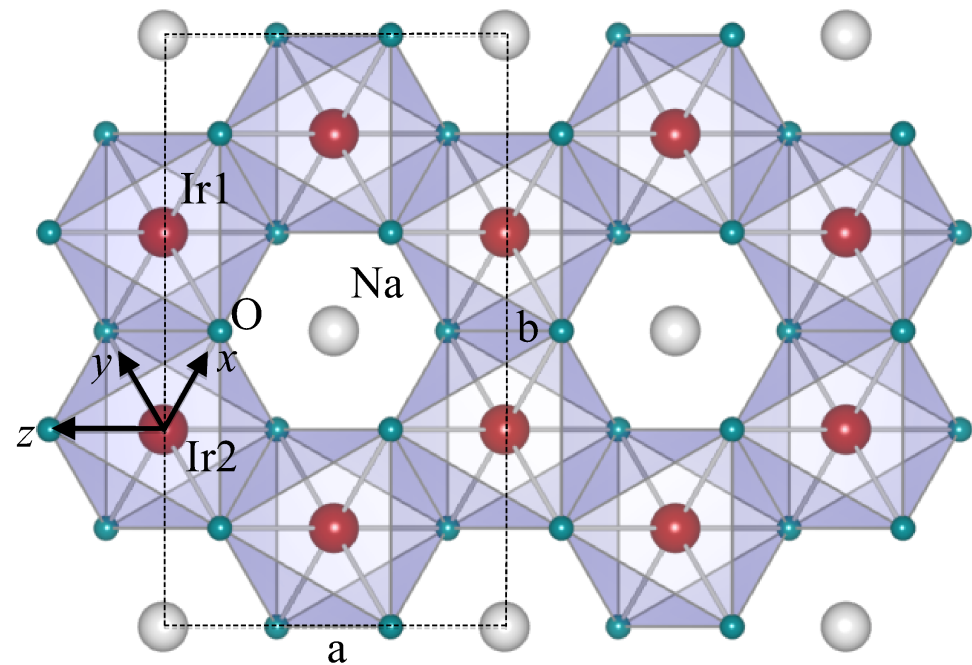
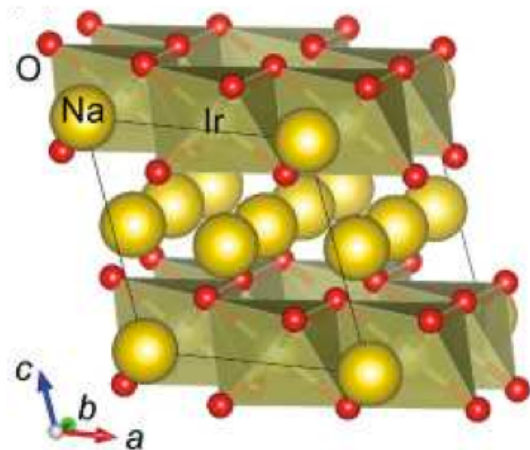
Li_2IrO_3

$H_3LiIr_2O_6$

K_2IrO_3

$RuCl_3$

honeycomb Na_2IrO_3



$$\mathcal{H}_{ij}^{\text{D}_{2\text{h}}} = J \tilde{\mathbf{S}}_i \cdot \tilde{\mathbf{S}}_j + K \tilde{S}_i^z \tilde{S}_j^z + J_{xy} \left(\tilde{S}_i^x \tilde{S}_j^y + \tilde{S}_i^y \tilde{S}_j^x \right)$$

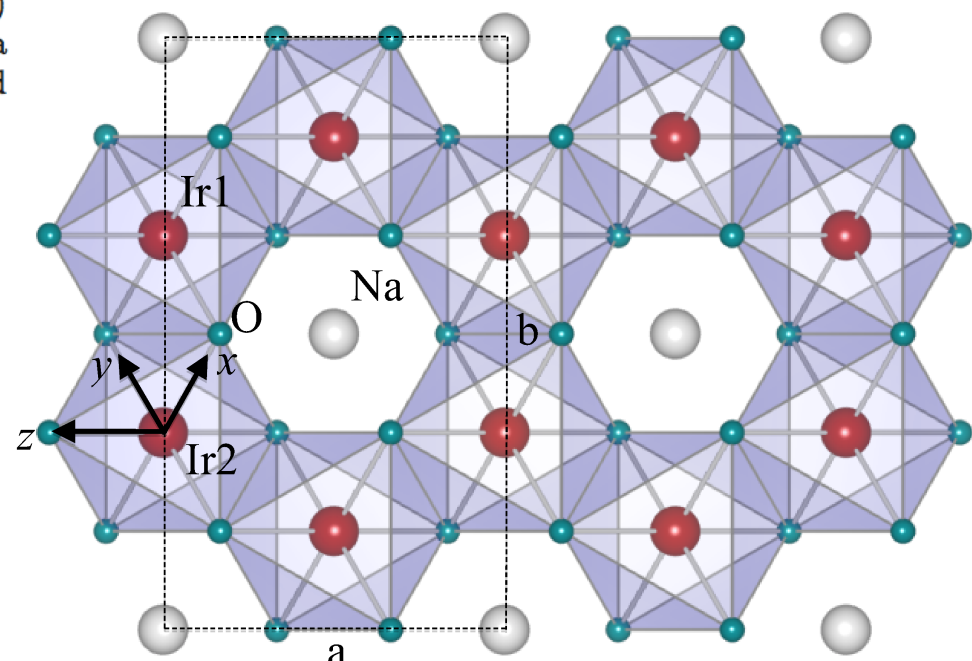
Katakuri, Nishimoto, Yushankhai, Stoyanova, Kandpal, Choi, Coldea, Rousouchatzakis, Hozoi & JvdB, NJP 16, 013056 (2014)

TABLE II. Energy splittings and effective parameters (meV) for the four lowest magnetic states of two NN IrO₆ octahedra in the *C2/m* structure of **4**. The weight of $(\uparrow\downarrow + \downarrow\uparrow)/\sqrt{2}$ and $(\uparrow\uparrow + \downarrow\downarrow)/\sqrt{2}$ in Ψ'_1 and Ψ'_2 , respectively, is $\approx 98\%$, see text.

Method	CAS+SOC	MRCI+SOC
$\angle(\text{Ir-O-Ir})=99.45^\circ$, $d(\text{Ir}_1-\text{Ir}_2)=3.138 \text{ \AA}$ ($\times 1$) ^a :		
Ψ'_2	0.0	0.0
$\Psi_3 = (\uparrow\uparrow - \downarrow\downarrow)/\sqrt{2}$	0.2	0.5
$\Psi_S = (\uparrow\downarrow - \downarrow\uparrow)/\sqrt{2}$	4.4	5.5
Ψ'_1	6.3	10.5
(J, K, J_{xy})	$(1.9, -12.4, 0.2)$	$(5.0, -20.5, 0.5)$
$\angle(\text{Ir-O-Ir})=97.97^\circ$, $d(\text{Ir}_2-\text{Ir}_3)=3.130 \text{ \AA}$ ($\times 2$) ^b :		
Ψ'_2	0.0	0.0
$\Psi_3 = (\uparrow\uparrow - \downarrow\downarrow)/\sqrt{2}$	0.3	1.2
$\Psi_S = (\uparrow\downarrow - \downarrow\uparrow)/\sqrt{2}$	4.6	6.7
Ψ'_1	5.8	8.2
(J, K, J_{xy})	$(1.2, -11.3, 0.3)$	$(1.5, -15.2, 1.2)$

^a $d(\text{Ir-O}_{1,2})=2.056 \text{ \AA}$.

^b $d(\text{Ir-O}_1)=2.065 \text{ \AA}$, $d(\text{Ir-O}_2)=2.083 \text{ \AA}$.



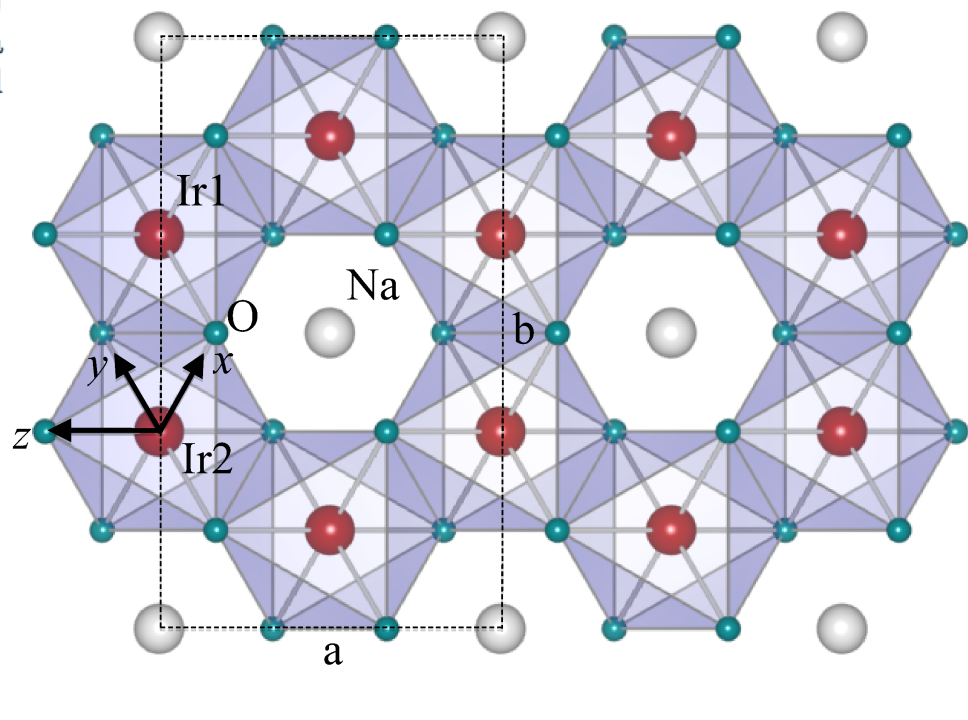
$$\mathcal{H}_{ij}^{\text{D}_{2\text{h}}} = J \tilde{\mathbf{S}}_i \cdot \tilde{\mathbf{S}}_j + K \tilde{S}_i^z \tilde{S}_j^z + J_{xy} \left(\tilde{S}_i^x \tilde{S}_j^y + \tilde{S}_i^y \tilde{S}_j^x \right)$$

TABLE II. Energy splittings and effective parameters (meV) for the four lowest magnetic states of two NN IrO₆ octahedra in the *C2/m* structure of **4**. The weight of $(\uparrow\downarrow + \downarrow\uparrow)/\sqrt{2}$ and $(\uparrow\uparrow + \downarrow\downarrow)/\sqrt{2}$ in Ψ'_1 and Ψ'_2 , respectively, is $\approx 98\%$, see text.

Method	CAS+SOC	MRCI+SOC
$\angle(\text{Ir-O-Ir})=99.45^\circ$, $d(\text{Ir}_1-\text{Ir}_2)=3.138 \text{ \AA}$ ($\times 1$) ^a :		
Ψ'_2	0.0	0.0
$\Psi_3 = (\uparrow\uparrow - \downarrow\downarrow)/\sqrt{2}$	0.2	0.5
$\Psi_S = (\uparrow\downarrow - \downarrow\uparrow)/\sqrt{2}$	4.4	5.5
Ψ'_1	6.3	10.5
(J, K, J_{xy})	$(1.9, -12.4, 0.2)$	$(5.0, -20.5, 0.5)$
$\angle(\text{Ir-O-Ir})=97.97^\circ$, $d(\text{Ir}_2-\text{Ir}_3)=3.130 \text{ \AA}$ ($\times 2$) ^b :		
Ψ'_2	0.0	0.0
$\Psi_3 = (\uparrow\uparrow - \downarrow\downarrow)/\sqrt{2}$	0.3	1.2
$\Psi_S = (\uparrow\downarrow - \downarrow\uparrow)/\sqrt{2}$	4.6	6.7
Ψ'_1	5.8	8.2
(J, K, J_{xy})	$(1.2, -11.3, 0.3)$	$(1.5, -15.2, 1.2)$

^a $d(\text{Ir-O}_{1,2})=2.056 \text{ \AA}$.

^b $d(\text{Ir-O}_1)=2.065 \text{ \AA}$, $d(\text{Ir-O}_2)=2.083 \text{ \AA}$.



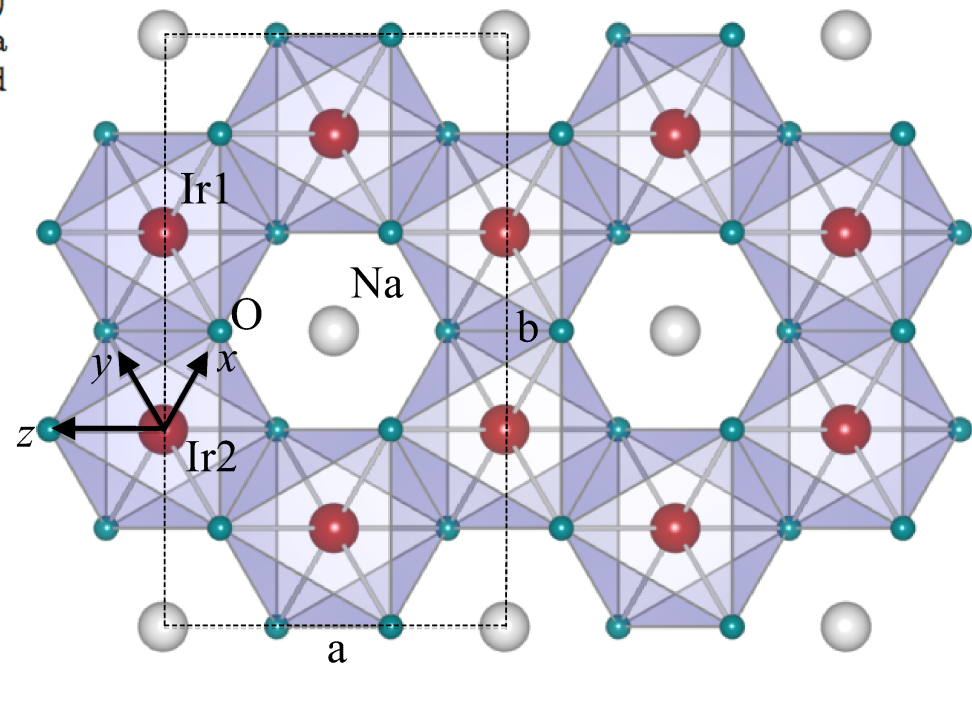
$$\mathcal{H}_{ij}^{\text{D}_{2\text{h}}} = J \tilde{\mathbf{S}}_i \cdot \tilde{\mathbf{S}}_j + K \tilde{S}_i^z \tilde{S}_j^z + J_{xy} \left(\tilde{S}_i^x \tilde{S}_j^y + \tilde{S}_i^y \tilde{S}_j^x \right)$$

TABLE II. Energy splittings and effective parameters (meV) for the four lowest magnetic states of two NN IrO₆ octahedra in the *C2/m* structure of **4**. The weight of $(\uparrow\downarrow + \downarrow\uparrow)/\sqrt{2}$ and $(\uparrow\uparrow + \downarrow\downarrow)/\sqrt{2}$ in Ψ'_1 and Ψ'_2 , respectively, is $\approx 98\%$, see text.

Method	CAS+SOC	MRCI+SOC
$\angle(\text{Ir-O-Ir})=99.45^\circ$, $d(\text{Ir}_1-\text{Ir}_2)=3.138 \text{ \AA}$ ($\times 1$) ^a :		
Ψ'_2	0.0	0.0
$\Psi_3 = (\uparrow\uparrow - \downarrow\downarrow)/\sqrt{2}$	0.2	0.5
$\Psi_S = (\uparrow\downarrow - \downarrow\uparrow)/\sqrt{2}$	4.4	5.5
Ψ'_1	6.3	10.5
(J, K, J_{xy})	$(1.9, -12.4, 0.2)$	$(5.0, -20.5, 0.5)$
$\angle(\text{Ir-O-Ir})=97.97^\circ$, $d(\text{Ir}_2-\text{Ir}_3)=3.130 \text{ \AA}$ ($\times 2$) ^b :		
Ψ'_2	0.0	0.0
$\Psi_3 = (\uparrow\uparrow - \downarrow\downarrow)/\sqrt{2}$	0.3	1.2
$\Psi_S = (\uparrow\downarrow - \downarrow\uparrow)/\sqrt{2}$	4.6	6.7
Ψ'_1	5.8	8.2
(J, K, J_{xy})	$(1.2, -11.3, 0.3)$	$(1.5, -15.2, 1.2)$

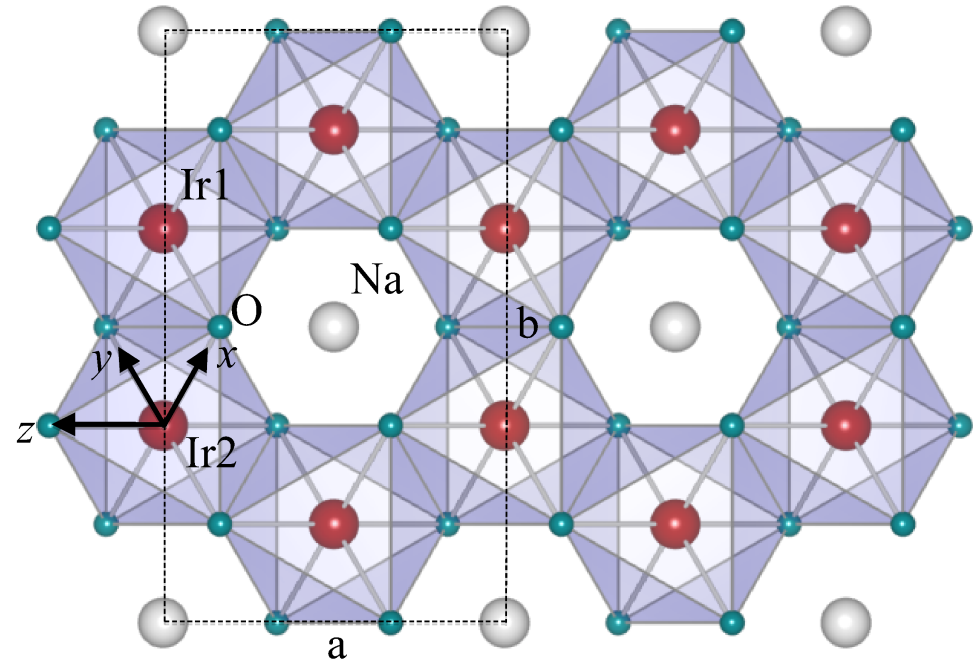
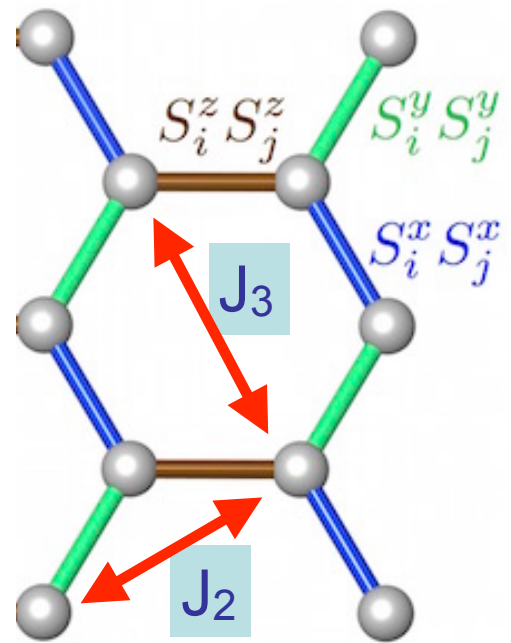
^a $d(\text{Ir-O}_{1,2})=2.056 \text{ \AA}$.

^b $d(\text{Ir-O}_1)=2.065 \text{ \AA}$, $d(\text{Ir-O}_2)=2.083 \text{ \AA}$.



$$\mathcal{H}_{ij}^{\text{D}_{2\text{h}}} = J \tilde{\mathbf{S}}_i \cdot \tilde{\mathbf{S}}_j + K \tilde{S}_i^z \tilde{S}_j^z + J_{xy} \left(\tilde{S}_i^x \tilde{S}_j^y + \tilde{S}_i^y \tilde{S}_j^x \right)$$

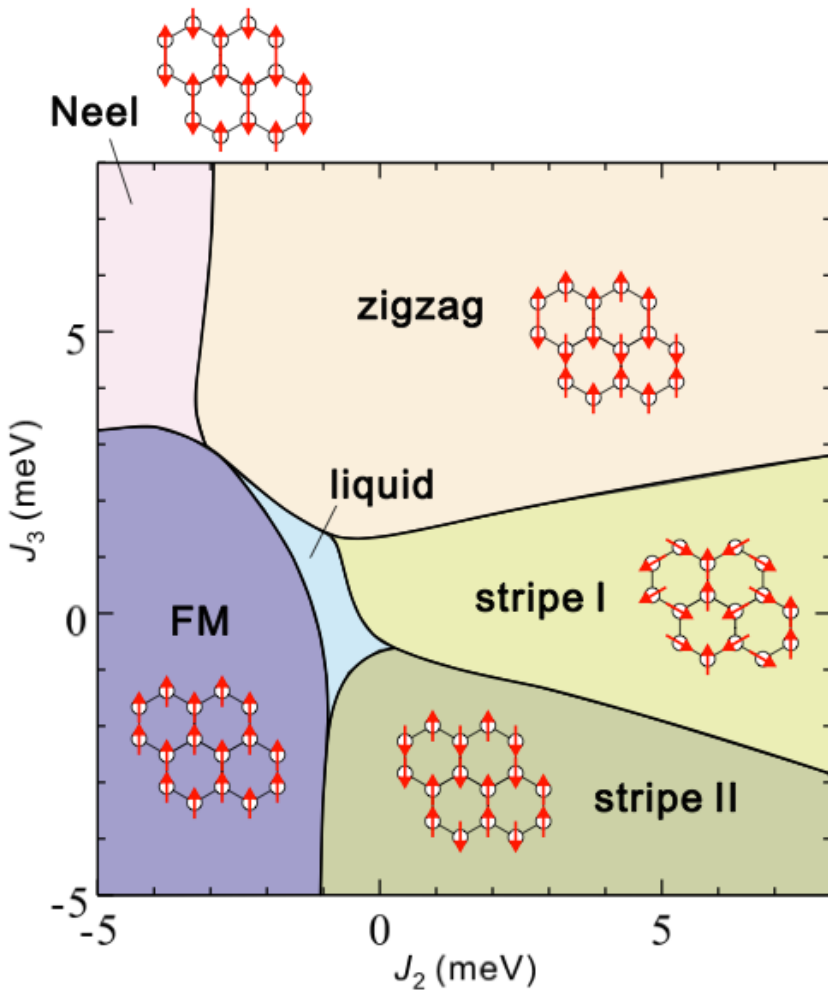
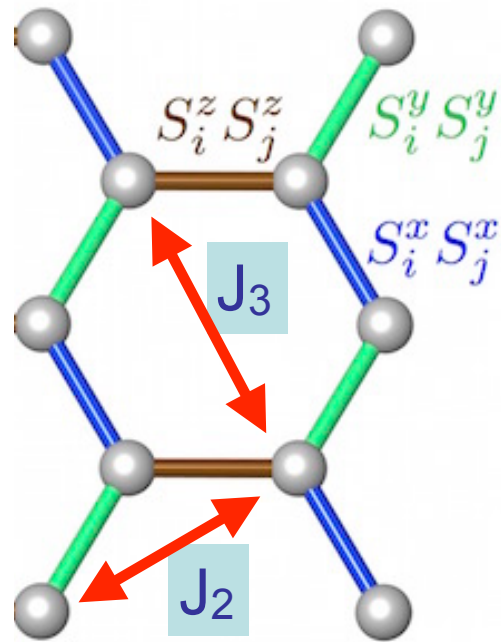
K large and FM, J small and AFM substantial anisotropy between links



$$\mathcal{H}_{ij}^{\text{D}_{2\text{h}}} = J \tilde{\mathbf{S}}_i \cdot \tilde{\mathbf{S}}_j + K \tilde{S}_i^z \tilde{S}_j^z + J_{xy} (\tilde{S}_i^x \tilde{S}_j^y + \tilde{S}_i^y \tilde{S}_j^x)$$

+ longer range Heisenberg J_2 and J_3

Katakuri, Nishimoto, Yushankhai, Stoyanova, Kandpal, Choi, Coldea, Rousochatzakis, Hozoi & JvdB, NJP 16, 013056 (2014)

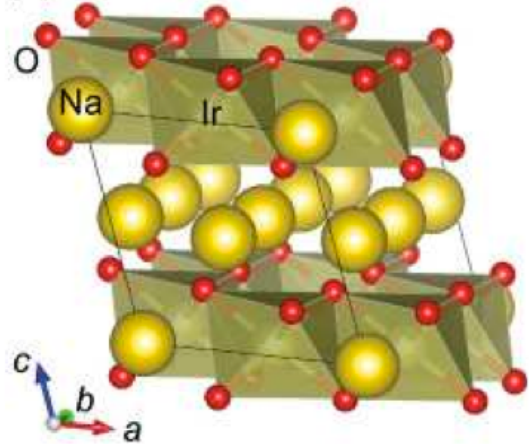


$$\mathcal{H}_{ij}^{\text{D}_{2\text{h}}} = J \tilde{\mathbf{S}}_i \cdot \tilde{\mathbf{S}}_j + K \tilde{S}_i^z \tilde{S}_j^z + J_{xy} (\tilde{S}_i^x \tilde{S}_j^y + \tilde{S}_i^y \tilde{S}_j^x)$$

+ longer range Heisenberg J_2 and J_3

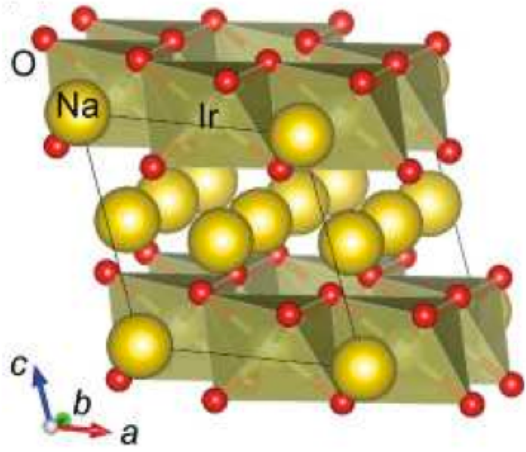
Katakuri, Nishimoto, Yushankhai, Stoyanova, Kandpal, Choi, Coldea, Rousouchatzakis, Hozoi & JvdB, NJP 16, 013056 (2014)

honeycomb Li_2IrO_3



Method	CASSCF+SOC	MRCI+SOC
<i>B1</i> , $\angle(\text{Ir}-\text{O}-\text{Ir})=95.3^\circ$, $d(\text{Ir}-\text{Ir})=2.98 \text{ \AA}$ ($\times 1$) ^a :		
Ψ_2	0.0	0.0
$\Psi_3 = \Phi_3 = (\uparrow\uparrow - \downarrow\downarrow)/\sqrt{2}$	1.6	3.2
Ψ_1	5.4	7.7
$\Psi_S = \Phi_S = (\uparrow\downarrow - \downarrow\uparrow)/\sqrt{2}$	25.5	24.8
$(J, K, \Gamma_{xy}, \Gamma_{zx} = -\Gamma_{yz})^b$		$(-19.2, -6.0, -1.1, -4.8)$
<i>B2</i> , $\angle(\text{Ir}-\text{O}-\text{Ir})=94.7^\circ$, $d(\text{Ir}-\text{Ir})=2.98 \text{ \AA}$ ($\times 2$) ^c :		
$\Psi_3 = \Phi_3 = (\uparrow\uparrow - \downarrow\downarrow)/\sqrt{2}$	0.0	0.0
Ψ_2	2.8	3.7
$\Psi_S = \Phi_S = (\uparrow\downarrow - \downarrow\uparrow)/\sqrt{2}$	5.9	7.1
Ψ_1	5.7	8.4
$(J, K, \Gamma_{xy}, \Gamma_{zx} = -\Gamma_{yz})^d$		$(0.8, -11.6, 4.2, -2.0)$

honeycomb Li_2IrO_3

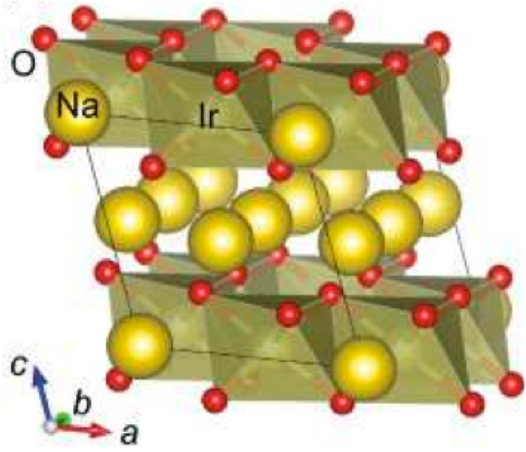


Method	CASSCF+SOC	MRCI+SOC
<i>B1</i> , $\angle(\text{Ir-O-Ir})=95.3^\circ$, $d(\text{Ir-Ir})=2.98 \text{ \AA}$ ($\times 1$) ^a :		
Ψ_2	0.0	0.0
$\Psi_3 = \Phi_3 = (\uparrow\uparrow - \downarrow\downarrow)/\sqrt{2}$	1.6	3.2
Ψ_1	5.4	7.7
$\Psi_S = \Phi_S = (\uparrow\downarrow - \downarrow\uparrow)/\sqrt{2}$	25.5	24.8
$(J, K, \Gamma_{xy}, \Gamma_{zx} = -\Gamma_{yz})^b$		(-19.2, -6.0, -1.1, -4.8)
<i>B2</i> , $\angle(\text{Ir-O-Ir})=94.7^\circ$, $d(\text{Ir-Ir})=2.98 \text{ \AA}$ ($\times 2$) ^c :		
$\Psi_3 = \Phi_3 = (\uparrow\uparrow - \downarrow\downarrow)/\sqrt{2}$	0.0	0.0
Ψ_2	2.8	3.7
$\Psi_S = \Phi_S = (\uparrow\downarrow - \downarrow\uparrow)/\sqrt{2}$	5.9	7.1
Ψ_1	5.7	8.4
$(J, K, \Gamma_{xy}, \Gamma_{zx} = -\Gamma_{yz})^d$		(0.8, -11.6, 4.2, -2.0)

- bond with large FM J

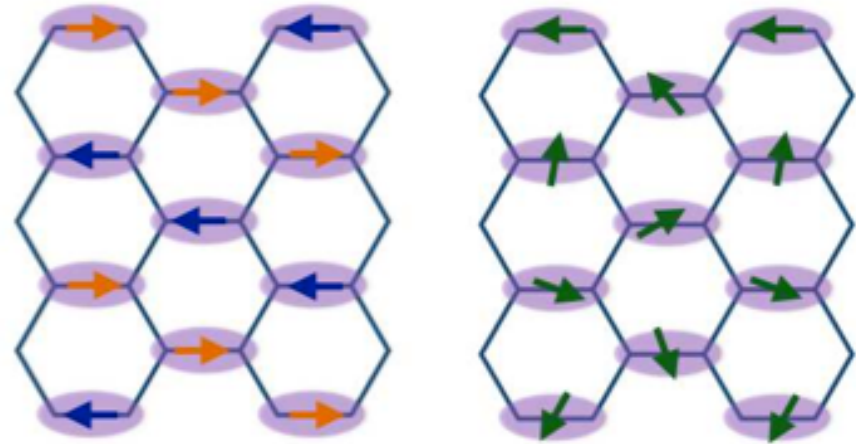
- bond with substantial FM K

honeycomb Li_2IrO_3

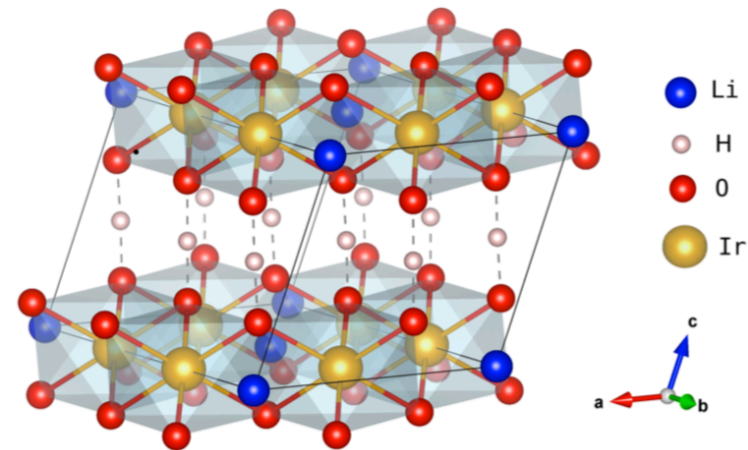


Method	CASSCF+SOC	MRCI+SOC
<i>B1</i> , $\angle(\text{Ir-O-Ir})=95.3^\circ$, $d(\text{Ir-Ir})=2.98 \text{ \AA}$ ($\times 1$) ^a :		
Ψ_2	0.0	0.0
$\Psi_3 = \Phi_3 = (\uparrow\uparrow - \downarrow\downarrow)/\sqrt{2}$	1.6	3.2
Ψ_1	5.4	7.7
$\Psi_S = \Phi_S = (\uparrow\downarrow - \downarrow\uparrow)/\sqrt{2}$	25.5	24.8
$(J, K, \Gamma_{xy}, \Gamma_{zx} = -\Gamma_{yz})^b$		$(-19.2, -6.0, -1.1, -4.8)$
<i>B2</i> , $\angle(\text{Ir-O-Ir})=94.7^\circ$, $d(\text{Ir-Ir})=2.98 \text{ \AA}$ ($\times 2$) ^c :		
$\Psi_3 = \Phi_3 = (\uparrow\uparrow - \downarrow\downarrow)/\sqrt{2}$	0.0	0.0
Ψ_2	2.8	3.7
$\Psi_S = \Phi_S = (\uparrow\downarrow - \downarrow\uparrow)/\sqrt{2}$	5.9	7.1
Ψ_1	5.7	8.4
$(J, K, \Gamma_{xy}, \Gamma_{zx} = -\Gamma_{yz})^d$		$(0.8, -11.6, 4.2, -2.0)$

- bond with large FM J
- bond with substantial FM K
- triplet dimer formation!



honeycomb $H_3LiIr_2O_6$



nature

International journal of science

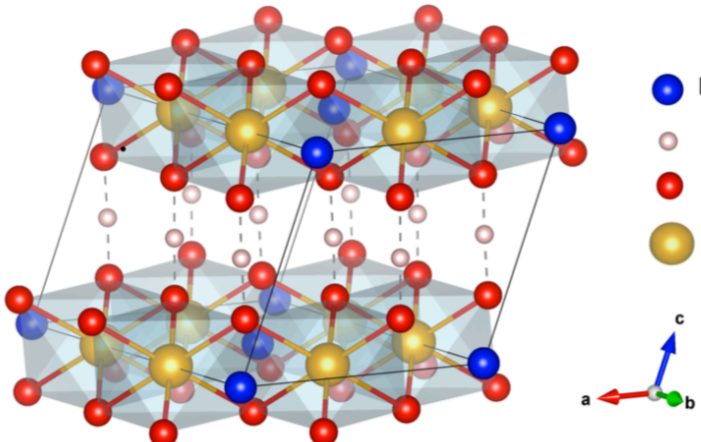
A spin-orbital-entangled quantum liquid on a honeycomb lattice

K. Kitagawa, T. Takayama, Y. Matsumoto, A. Kato, R. Takano, Y. Kishimoto, S. Bette, R. Dinnebier, G. Jackeli & H. Takagi ✉

Nature **554**, 341–345 (15 February 2018)

Received: 18 July 2017

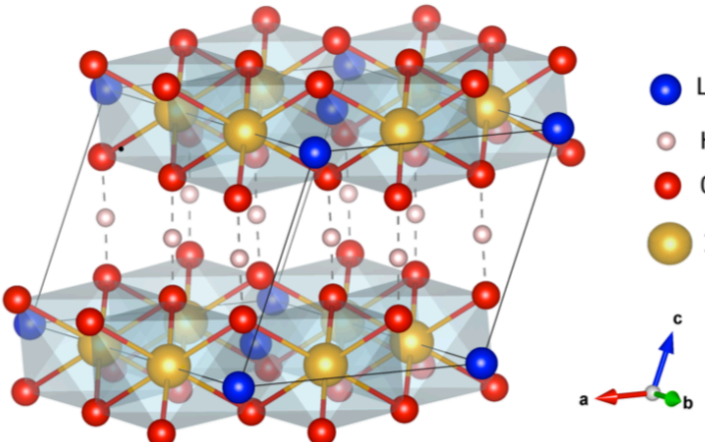
honeycomb $H_3LiIr_2O_6$



Bond	Experimental crystal structure					
	\angle Ir-O-Ir	K	J	Γ_{xy}	$\Gamma_{yz} = -\Gamma_{zx}$	
B2 (3.10 Å)	99.8°	-12.0	1.8	-0.2	-3.2	
B1 (3.05 Å)	99.0°	-12.6	1.5	-1.8	-0.65	

Yadav, Ray, Eldeeb, Nishimoto, Hozoi & JvdB, PRL 121, 197203 (2018)

honeycomb $H_3LiIr_2O_6$

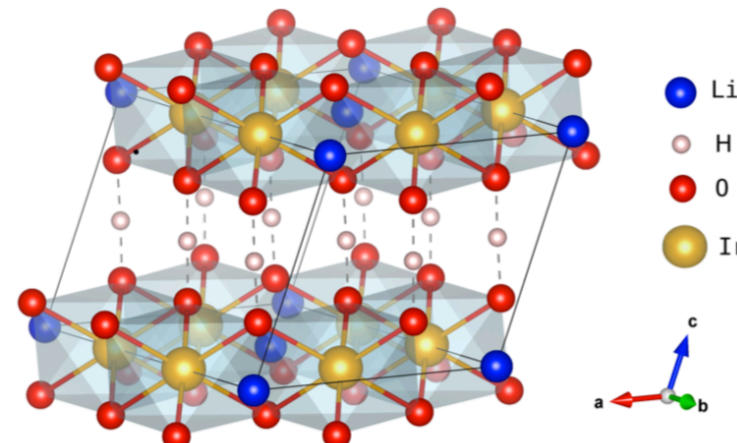


Bond	Experimental crystal structure					
	$\angle \text{Ir-O-Ir}$	K	J	Γ_{xy}	$\Gamma_{yz} = -\Gamma_{zx}$	
B2 (3.10 Å)	99.8°	-12.0	1.8	-0.2	-3.2	
B1 (3.05 Å)	99.0°	-12.6	1.5	-1.8	-0.65	

- $FM K$, weak $AFM J$, large K/J

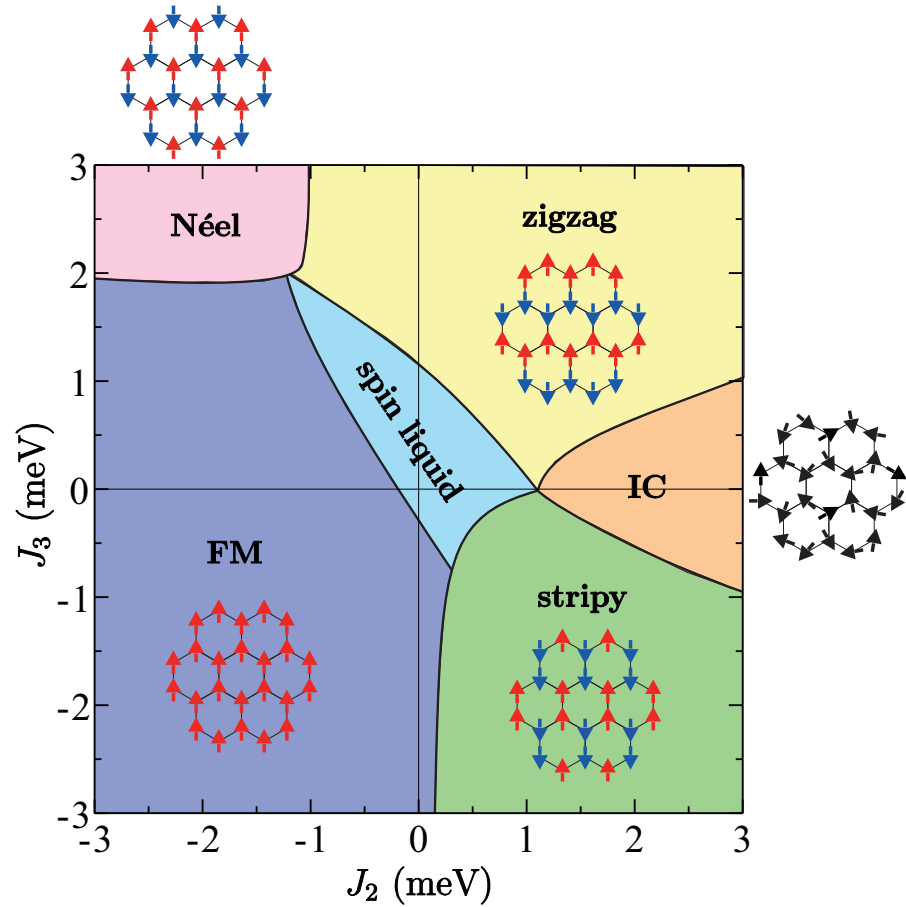
- weak bond anisotropy

honeycomb $H_3LiIr_2O_6$

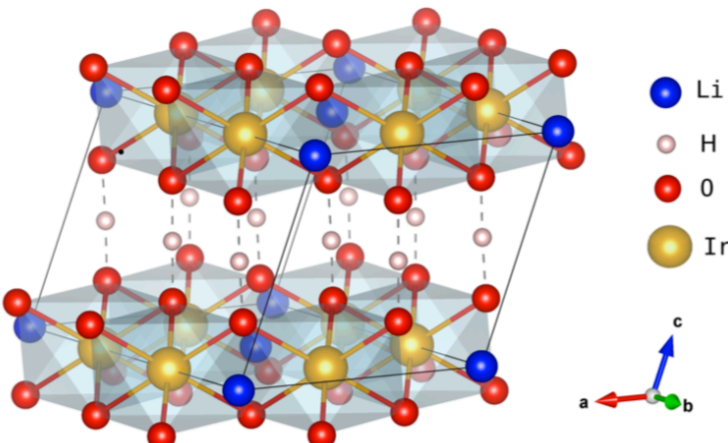


- FM K , weak AFM J , large K/J
- weak bond anisotropy

Bond	Experimental crystal structure					
	\angle Ir-O-Ir	K	J	Γ_{xy}	$\Gamma_{yz} = -\Gamma_{zx}$	
B2 (3.10 Å)	99.8°	-12.0	1.8	-0.2	-3.2	
B1 (3.05 Å)	99.0°	-12.6	1.5	-1.8	-0.65	



honeycomb $H_3LiIr_2O_6$



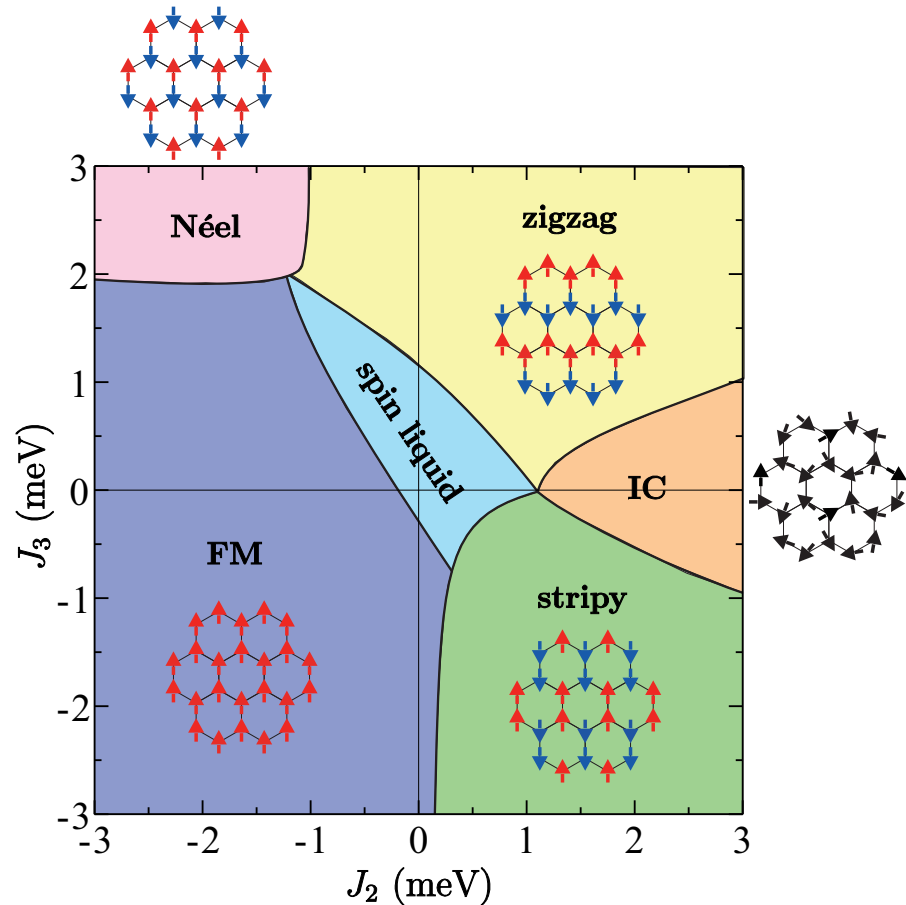
Bond	$\angle \text{Ir-O-Ir}$	K	J	Γ_{xy}	$\Gamma_{yz} = -\Gamma_{zx}$
B2 (3.10 Å)	99.8°	-12.0	1.8	-0.2	-3.2
B1 (3.05 Å)	99.0°	-12.6	1.5	-1.8	-0.65

- FM K , weak AFM J , large K/J

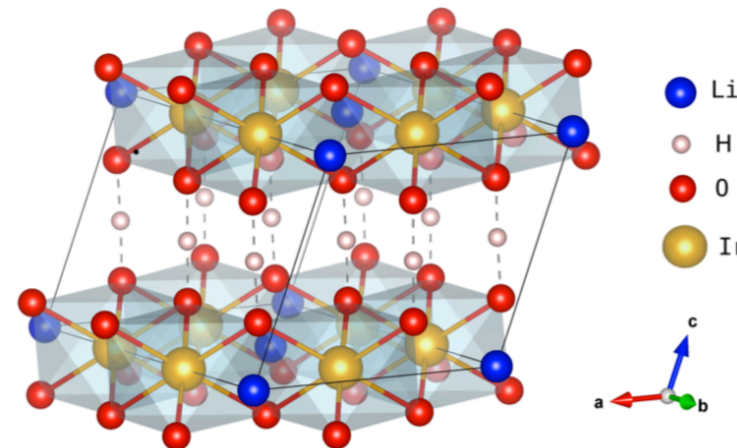
- weak bond anisotropy

- why no LRO by J_2 and J_3 ?

- why K smaller than Na_2IrO_3 ?



honeycomb $H_3LiIr_2O_6$



Bond	Experimental crystal structure					
	\angle Ir-O-Ir	K	J	Γ_{xy}	$\Gamma_{yz} = -\Gamma_{zx}$	
B2 (3.10 Å)	99.8°	-12.0	1.8	-0.2	-3.2	
B1 (3.05 Å)	99.0°	-12.6	1.5	-1.8	-0.65	

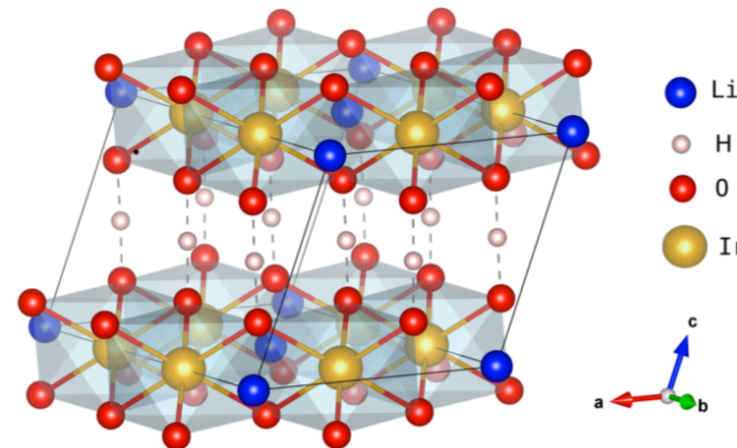
Remove H from Ir-O-Ir links
& smear out the + charge

Bond	K	J	Γ_{xy}	$\Gamma_{yz} = -\Gamma_{zx}$
B2 (3.10 Å)	-38.1	5.9	5.0	-11.1
B1 (3.05 Å)	-40.0	4.6	7.9	-14.0

Yadav, Ray, Eldeeb, Nishimoto, Hozoi
& JvdB, PRL 121, 197203 (2018)

Yadav, Eldeeb, Ray, Aswartham, Sturza, Nishimoto,
JvdB & Hozoi, Chemical Science 10,1866 (2019)

honeycomb $H_3LiIr_2O_6$



Bond	Experimental crystal structure					
	\angle Ir-O-Ir	K	J	Γ_{xy}	$\Gamma_{yz} = -\Gamma_{zx}$	
B2 (3.10 Å)	99.8°	-12.0	1.8	-0.2	-3.2	
B1 (3.05 Å)	99.0°	-12.6	1.5	-1.8	-0.65	

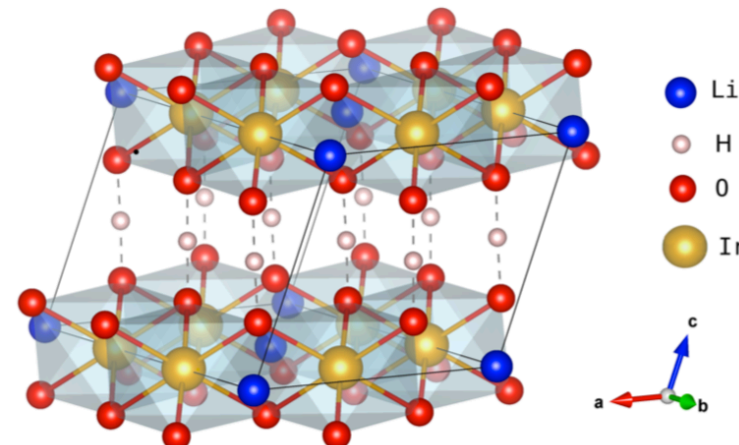
Remove H from Ir-O-Ir links
& smear out the + charge

Bond	K	J	Γ_{xy}	$\Gamma_{yz} = -\Gamma_{zx}$
B2 (3.10 Å)	-38.1	5.9	5.0	-11.1
B1 (3.05 Å)	-40.0	4.6	7.9	-14.0

Yadav, Ray, Eldeeb, Nishimoto, Hozoi
& JvdB, PRL 121, 197203 (2018)

Yadav, Eldeeb, Ray, Aswartham, Sturza, Nishimoto,
JvdB & Hozoi, Chemical Science 10,1866 (2019)

honeycomb $H_3LiIr_2O_6$



Bond	Experimental crystal structure					
	\angle Ir-O-Ir	K	J	Γ_{xy}	$\Gamma_{yz} = -\Gamma_{zx}$	
B2 (3.10 Å)	99.8°	-12.0	1.8	-0.2	-3.2	
B1 (3.05 Å)	99.0°	-12.6	1.5	-1.8	-0.65	

Remove H from Ir-O-Ir links
& smear out the + charge

Bond	K	J	Γ_{xy}	$\Gamma_{yz} = -\Gamma_{zx}$
B2 (3.10 Å)	-38.1	5.9	5.0	-11.1
B1 (3.05 Å)	-40.0	4.6	7.9	-14.0

- *H polarizes oxygen orbital relevant for superexchange*
- *very strong effect of hydrogen disorder - affects QSL?*

Yadav, Ray, Eldeeb, Nishimoto, Hozoi & JvdB, PRL 121, 197203 (2018)

Yadav, Eldeeb, Ray, Aswartham, Sturza, Nishimoto, JvdB & Hozoi, Chemical Science 10,1866 (2019)

honeycomb K_2IrO_3

- C_3 symmetry
- Defect structure $K_xIr_yO_2$
- Magnetic disorder above $2K$

Johnson, Broeders, Mehlawat, Li, Singh,
Valenti, Coldea arXiv:1908.04584 (2019)

Mehlawat & Singh, arXiv:1908.08475 (2019)

honeycomb K_2IrO_3

- C_3 symmetry
- Defect structure $K_xIr_yO_2$
- Magnetic disorder above $2K$

Johnson, Broeders, Mehlawat, Li, Singh,
Valenti, Coldea arXiv:1908.04584 (2019)

Mehlawat & Singh, arXiv:1908.08475 (2019)

A ₂ IrO ₃	∠Ir-O-Ir	K	J	Γ_{xy}	$\Gamma_{yz} = -\Gamma_{zx}$
A = K	95.0°($\times 3$)	-6.3	1.3	5.2	-8.9
A = Na	99.5°($\times 1$) 98.0°($\times 2$)	-20.8 -15.6	5.2 2.2	-0.7 -1.1	-0.8 0.8

honeycomb K_2IrO_3

- C_3 symmetry
- Defect structure $K_xIr_yO_2$
- Magnetic disorder above $2K$

Johnson, Broeders, Mehlawat, Li, Singh, Valenti, Coldea arXiv:1908.04584 (2019)

Mehlawat & Singh, arXiv:1908.08475 (2019)

A_2IrO_3	\angle Ir-O-Ir	K	J	Γ_{xy}	$\Gamma_{yz} = -\Gamma_{zx}$
A = K	95.0°($\times 3$)	-6.3	1.3	5.2	-8.9
A = Na	99.5°($\times 1$) 98.0°($\times 2$)	-20.8 -15.6	5.2 2.2	-0.7 -1.1	-0.8 0.8

honeycomb K_2IrO_3

- C_3 symmetry
- Defect structure $K_xIr_yO_2$
- Magnetic disorder above $2K$

Johnson, Broeders, Mehlawat, Li, Singh, Valenti, Coldea arXiv:1908.04584 (2019)

Mehlawat & Singh, arXiv:1908.08475 (2019)

A_2IrO_3	$\angle \text{Ir-O-Ir}$	K	J	Γ_{xy}	$\Gamma_{yz} = -\Gamma_{zx}$
$A = K$	$95.0^\circ (\times 3)$	-6.3	1.3	5.2	-8.9
$A = Na$	$99.5^\circ (\times 1)$	-20.8	5.2	-0.7	-0.8
	$98.0^\circ (\times 2)$	-15.6	2.2	-1.1	0.8

- MRCI: large off-diagonal magnetic interactions $\rightarrow C_3$

Yadav, Nishimoto, Richter Jvdb, Ray, preprint (2019)

honeycomb K_2IrO_3

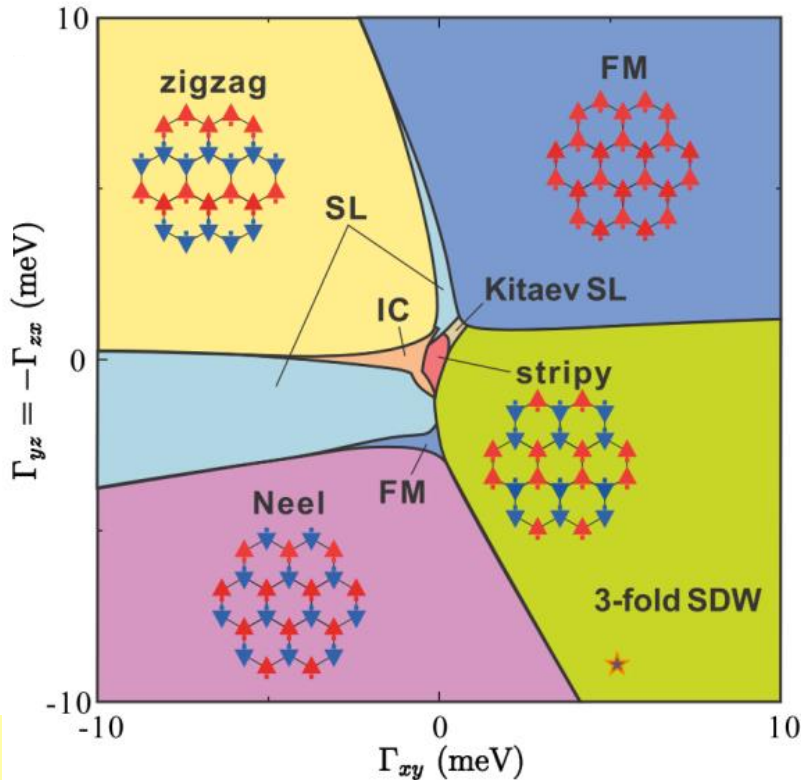
- C_3 symmetry
- Defect structure $K_xIr_yO_2$
- Magnetic disorder above 2K

Johnson, Broeders, Mehlawat, Li, Singh, Valenti, Coldea arXiv:1908.04584 (2019)

Mehlawat & Singh, arXiv:1908.08475 (2019)

A_2IrO_3	$\angle\text{Ir-O-Ir}$	K	J	Γ_{xy}	$\Gamma_{yz} = -\Gamma_{zx}$
$A = K$	$95.0^\circ (\times 3)$	-6.3	1.3	5.2	-8.9
$A = \text{Na}$	$99.5^\circ (\times 1)$ $98.0^\circ (\times 2)$	-20.8 -15.6	5.2 2.2	-0.7 -1.1	-0.8 0.8

- MRCI: large off-diagonal magnetic interactions $\rightarrow C_3$
- Alternative route to stabilize (Kitaev) QSL



Electronic & magnetic structure of α -RuCl₃

Honeycomb RuCl₃

Quantum
chemistry
calculations

$$\mathcal{H}_{i,j} = J \tilde{\mathbf{S}}_i \cdot \tilde{\mathbf{S}}_j + K \tilde{S}_i^z \tilde{S}_j^z + \sum_{\alpha \neq \beta} \Gamma_{\alpha\beta} (\tilde{S}_i^\alpha \tilde{S}_j^\beta + \tilde{S}_i^\beta \tilde{S}_j^\alpha)$$

Structure	\angle Ru-Cl-Ru	K	J	Γ_{xy}	$\Gamma_{zx} = -\Gamma_{yz}$
$C2/m$ [30]	94°	-5.6	1.2	-1.2	-0.7
$C2/m$ [29]					
Link 1 ($\times 2$)	94°	-5.3	1.2	-1.1	-0.7
Link 2 ($\times 1$)	93°	-4.8	-0.3	-1.5	-0.7
$P3_112$ [28]	89°	-1.2	-0.5	-1.0	-0.4

Sears, Songvilay, Plumb, Clancy, Qiu, Zhao, Parshall & Y-J Kim, PRB 91, 144420 (2015)

Yadav, Bogdanov, Katukuri, Nishimoto, JvdB & Hozoi, Sci. Rep. 6, 37508 (2016)

Honeycomb RuCl₃

Quantum chemistry calculations

$$\mathcal{H}_{i,j} = J \tilde{\mathbf{S}}_i \cdot \tilde{\mathbf{S}}_j + K \tilde{S}_i^z \tilde{S}_j^z + \sum_{\alpha \neq \beta} \Gamma_{\alpha\beta} (\tilde{S}_i^\alpha \tilde{S}_j^\beta + \tilde{S}_i^\beta \tilde{S}_j^\alpha)$$

Structure	\angle Ru-Cl-Ru	K	J	Γ_{xy}	$\Gamma_{zx} = -\Gamma_{yz}$
$C2/m$ [30]	94°	-5.6	1.2	-1.2	-0.7
$C2/m$ [29]					
Link 1 ($\times 2$)	94°	-5.3	1.2	-1.1	-0.7
Link 2 ($\times 1$)	93°	-4.8	-0.3	-1.5	-0.7
$P3_112$ [28]	89°	-1.2	-0.5	-1.0	-0.4

K large FM, J small AFM

$|K/J| \sim 5$

Winter, Tsirlin, Daghofer, JvdB, Singh, Gegenwart & Valenti, JPCM 29, 493002 (2017)

Sears, Songvilay, Plumb, Clancy, Qiu, Zhao, Parshall & Y-J Kim, PRB 91, 144420 (2015)

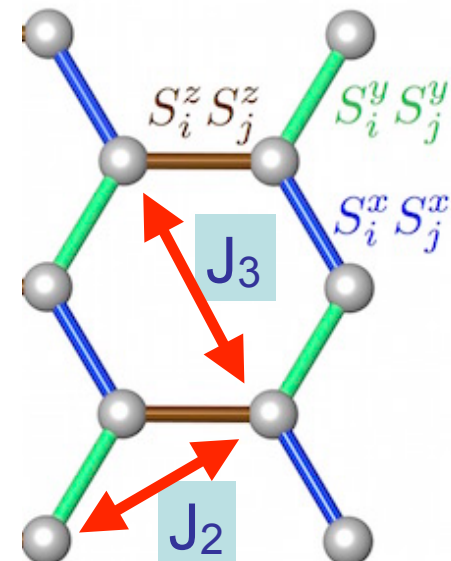
Yadav, Bogdanov, Katukuri, Nishimoto, JvdB & Hozoi, Sci. Rep. 6, 37508 (2016)

Honeycomb RuCl₃

Exact
diagonalization
calculations

$$\mathcal{H}_{i,j} = J \tilde{\mathbf{S}}_i \cdot \tilde{\mathbf{S}}_j + K \tilde{S}_i^z \tilde{S}_j^z + \sum_{\alpha \neq \beta} \Gamma_{\alpha\beta} (\tilde{S}_i^\alpha \tilde{S}_j^\beta + \tilde{S}_i^\beta \tilde{S}_j^\alpha)$$

+ longer range Heisenberg J₂ and J₃

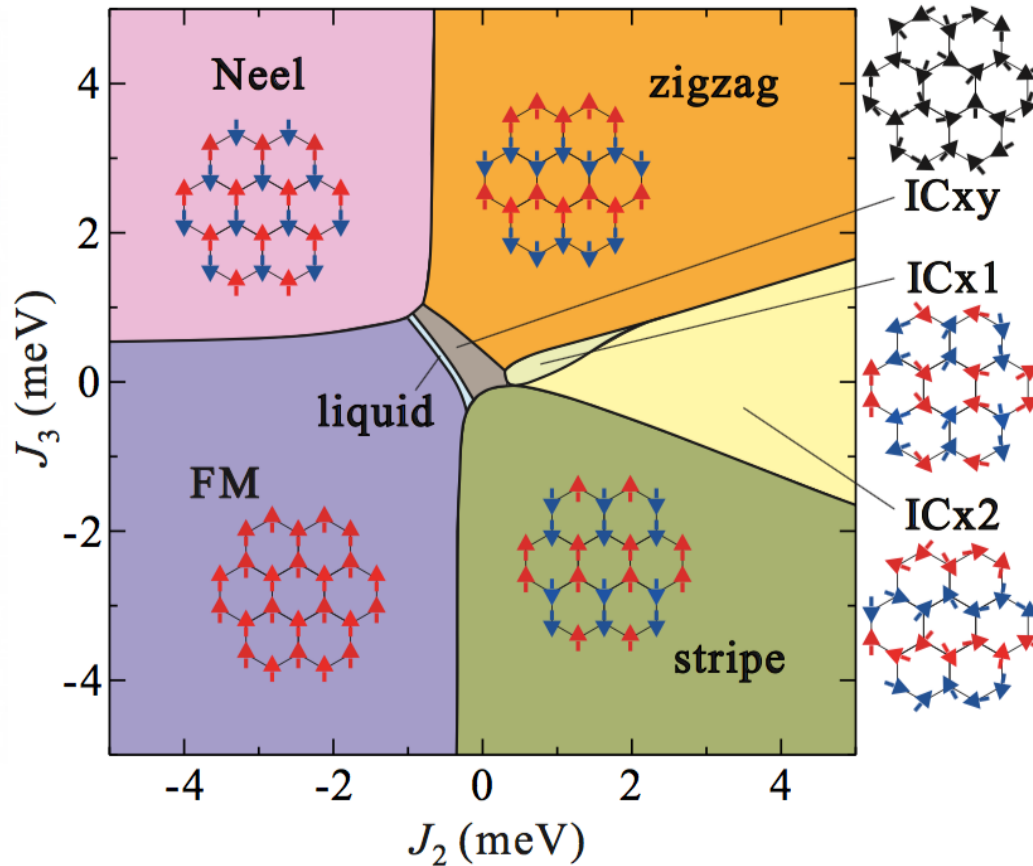
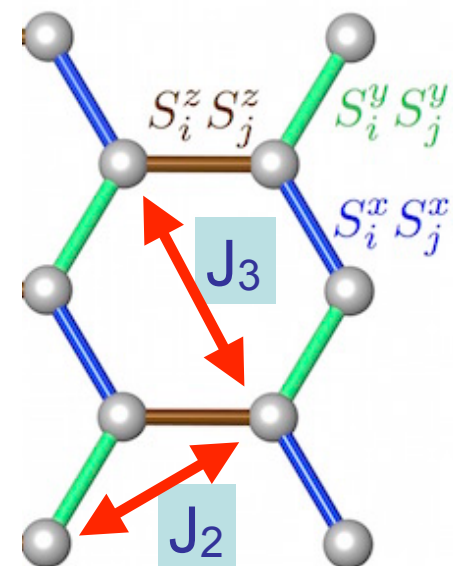


Honeycomb RuCl₃

Exact diagonalization calculations

$$\mathcal{H}_{i,j} = J \tilde{\mathbf{S}}_i \cdot \tilde{\mathbf{S}}_j + K \tilde{S}_i^z \tilde{S}_j^z + \sum_{\alpha \neq \beta} \Gamma_{\alpha\beta} (\tilde{S}_i^\alpha \tilde{S}_j^\beta + \tilde{S}_i^\beta \tilde{S}_j^\alpha)$$

+ longer range Heisenberg J_2 and J_3



zig-zag
order
driven by
 J_2 & J_3

Local electronic structure of α -RuCl₃

Quantum
chemistry
calculations

Ru ³⁺ 4d ⁵ splittings	CASSCF	CASSCF +SOC	MRCI	MRCI +SOC
2T_2 (t_{2g}^5)	0	0	0	0
	0.066	0.193	0.067	0.195
	0.069	0.232	0.071	0.234
4T_1 ($t_{2g}^4 e_g^1$)	1.08	1.25	1.28	1.33
	1.12		1.30	
	1.13	1.37	1.31	1.48
4T_2 ($t_{2g}^4 e_g^1$)	1.76	1.90	1.97	2.09
	1.81		2.01	
	1.83	1.98	2.03	2.17
6A_1 ($t_{2g}^3 e_g^2$)	1.01	1.09 ($\times 6$)	1.51	1.74 ($\times 6$)

$$g_{xx} = g_{yy} = 2.51; g_{zz} = 1.09$$

Local electronic structure of α -RuCl₃

Quantum chemistry calculations

Ru ³⁺ 4d ⁵ splittings	CASSCF CASSCF +SOC	MRCI MRCI +SOC		
2T_2 (t_{2g}^5)	0 0.066 0.069	0 0.193 0.232	0 0.067 0.071	0 0.195 0.234
4T_1 ($t_{2g}^4 e_g^1$)	1.08 1.12 1.13	1.25 1.37	1.28 1.30 1.31	1.33 1.48
4T_2 ($t_{2g}^4 e_g^1$)	1.76 1.81 1.83	1.90 1.98	1.97 2.01 2.03	2.09 2.17
6A_1 ($t_{2g}^3 e_g^2$)	1.01	1.09 ($\times 6$)	1.51	1.74 ($\times 6$)

$$g_{xx} = g_{yy} = 2.51; g_{zz} = 1.09$$

Local electronic structure of α -RuCl₃

Quantum chemistry calculations

Ru ³⁺ 4d ⁵ splittings	CASSCF CASSCF +SOC	MRCI MRCI +SOC
2T_2 (t_{2g}^5)	0 0.066 0.069	0 0.193 0.232
4T_1 ($t_{2g}^4 e_g^1$)	1.08 1.12 1.13	1.25 1.37
4T_2 ($t_{2g}^4 e_g^1$)	1.76 1.81 1.83	1.90 1.98
6A_1 ($t_{2g}^3 e_g^2$)	1.01	1.09 ($\times 6$)
		1.51
		1.74 ($\times 6$)

~0.2 eV splitting j=1/2 to j=3/2

$$g_{xx} = g_{yy} = 2.51; g_{zz} = 1.09$$

Magnetic nearest neighbor interactions in α -RuCl₃

Quantum
chemistry
calculations

$$\mathcal{H}_{i,j} = J \tilde{\mathbf{S}}_i \cdot \tilde{\mathbf{S}}_j + K \tilde{S}_i^z \tilde{S}_j^z + \sum_{\alpha \neq \beta} \Gamma_{\alpha\beta} (\tilde{S}_i^\alpha \tilde{S}_j^\beta + \tilde{S}_i^\beta \tilde{S}_j^\alpha)$$

Sears, Songvilay, Plumb, Clancy, Qiu, Zhao, Parshall & Y-J Kim, PRB 91, 144420 (2015)

Yadav, Bogdanov, Katukuri, Nishimoto, JvdB & Hozoi, Sci. Rep. 6, 37508 (2016)

Magnetic nearest neighbor interactions in α -RuCl₃

Quantum
chemistry
calculations

$$\mathcal{H}_{i,j} = J \tilde{\mathbf{S}}_i \cdot \tilde{\mathbf{S}}_j + K \tilde{S}_i^z \tilde{S}_j^z + \sum_{\alpha \neq \beta} \Gamma_{\alpha\beta} (\tilde{S}_i^\alpha \tilde{S}_j^\beta + \tilde{S}_i^\beta \tilde{S}_j^\alpha)$$

Structure	\angle Ru-Cl-Ru	K	J	Γ_{xy}	$\Gamma_{zx} = -\Gamma_{yz}$
$C2/m$ [30]	94°	-5.6	1.2	-1.2	-0.7
$C2/m$ [29]					
Link 1 ($\times 2$)	94°	-5.3	1.2	-1.1	-0.7
Link 2 ($\times 1$)	93°	-4.8	-0.3	-1.5	-0.7
$P3_112$ [28]	89°	-1.2	-0.5	-1.0	-0.4

Sears, Songvilay, Plumb, Clancy, Qiu, Zhao, Parshall & Y-J Kim, PRB 91, 144420 (2015)

Yadav, Bogdanov, Katukuri, Nishimoto, JvdB & Hozoi, Sci. Rep. 6, 37508 (2016)

Magnetic nearest neighbor interactions in α -RuCl₃

Quantum chemistry calculations

$$\mathcal{H}_{i,j} = J \tilde{\mathbf{S}}_i \cdot \tilde{\mathbf{S}}_j + K \tilde{S}_i^z \tilde{S}_j^z + \sum_{\alpha \neq \beta} \Gamma_{\alpha\beta} (\tilde{S}_i^\alpha \tilde{S}_j^\beta + \tilde{S}_i^\beta \tilde{S}_j^\alpha)$$

Structure	\angle Ru-Cl-Ru	K	J	Γ_{xy}	$\Gamma_{zx} = -\Gamma_{yz}$
$C2/m$ [30]	94°	-5.6	1.2	-1.2	-0.7
$C2/m$ [29]					
Link 1 ($\times 2$)	94°	-5.3	1.2	-1.1	-0.7
Link 2 ($\times 1$)	93°	-4.8	-0.3	-1.5	-0.7
$P3_112$ [28]	89°	-1.2	-0.5	-1.0	-0.4

K large FM, J small AFM

$|K/J| \sim 5$

Winter, Tsirlin, Daghofer, JvdB, Singh,
Gegenwart & Valenti, JPCM (2018)

Sears, Songvilay, Plumb, Clancy, Qiu, Zhao, Parshall & Y-J Kim, PRB 91, 144420 (2015)

Yadav, Bogdanov, Katukuri, Nishimoto, JvdB & Hozoi, Sci. Rep. 6, 37508 (2016)

Magnetic nearest neighbor interactions in α -RuCl₃

Quantum chemistry calculations

$$\mathcal{H}_{i,j} = J \tilde{\mathbf{S}}_i \cdot \tilde{\mathbf{S}}_j + K \tilde{S}_i^z \tilde{S}_j^z + \sum_{\alpha \neq \beta} \Gamma_{\alpha\beta} (\tilde{S}_i^\alpha \tilde{S}_j^\beta + \tilde{S}_i^\beta \tilde{S}_j^\alpha)$$

Structure	\angle Ru-Cl-Ru	K	J	Γ_{xy}	$\Gamma_{zx} = -\Gamma_{yz}$
$C2/m$ [30]	94°	-5.6	1.2	-1.2	-0.7
$C2/m$ [29]					
Link 1 ($\times 2$)	94°	-5.3	1.2	-1.1	-0.7
Link 2 ($\times 1$)	93°	-4.8	-0.3	-1.5	-0.7
$P3_112$ [28]	89°	-1.2	-0.5	-1.0	-0.4

K large FM, J small AFM

$|K/J| \sim 5$

However INS: K AFM

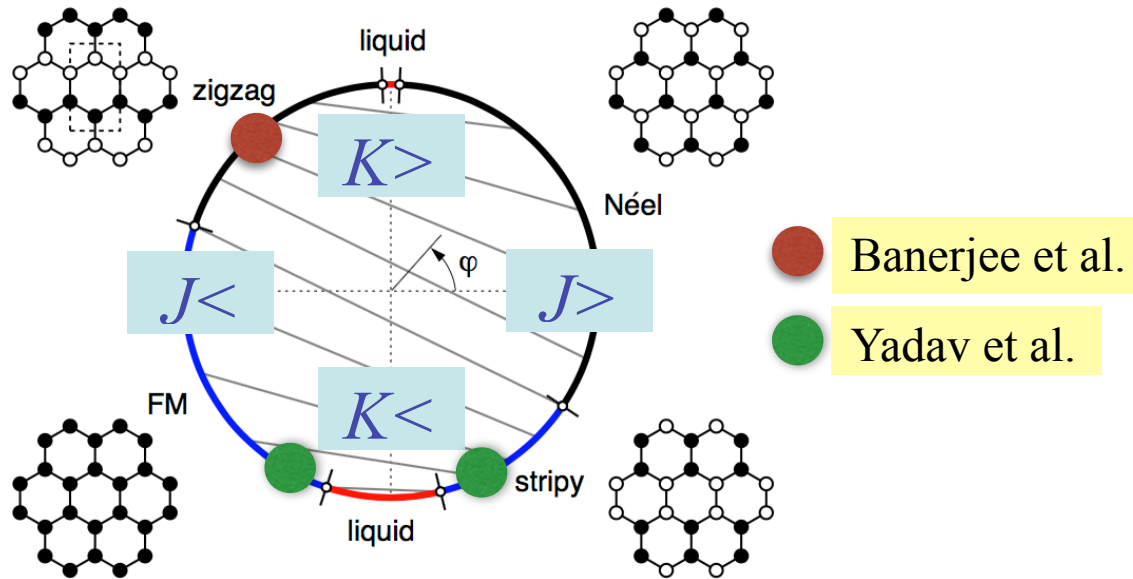
Banerjee et al., Nat. Mater. 4604 (2016)

Winter, Tsirlin, Daghofer, JvdB, Singh,
Gegenwart & Valenti, JPCM (2018)

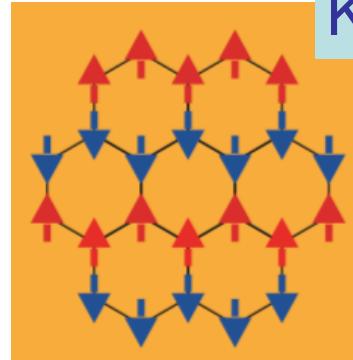
Sears, Songvilay, Plumb, Clancy, Qiu, Zhao, Parshall & Y-J Kim, PRB 91, 144420 (2015)

Yadav, Bogdanov, Katukuri, Nishimoto, JvdB & Hozoi, Sci. Rep. 6, 37508 (2016)

Magnetic nearest neighbor interactions in α -RuCl₃



Experimentally: zig-zag order below ~ 8 K



K large FM, J small AFM

$|K/J| \sim 5$

However INS: K AFM

Banerjee et al., Nat. Mater. 4604 (2016)

Sears, Songvilay, Plumb, Clancy, Qiu, Zhao, Parshall & Y-J Kim, PRB 91, 144420 (2015)

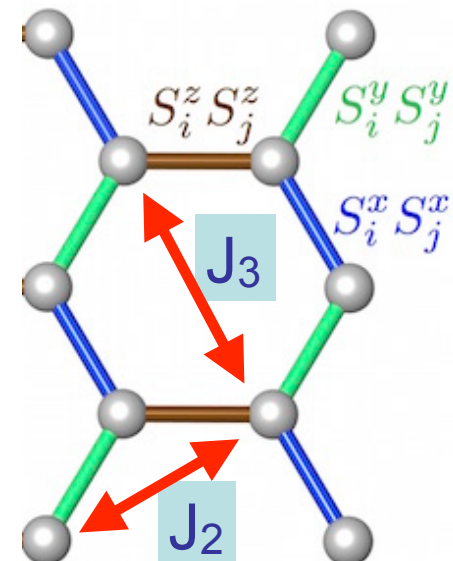
Yadav, Bogdanov, Katukuri, Nishimoto, JvdB & Hozoi, Sci. Rep. 6, 37508 (2016)

Magnetic nearest neighbor interactions in α -RuCl₃

Exact
diagonalization
calculations

$$\mathcal{H}_{i,j} = J \tilde{\mathbf{S}}_i \cdot \tilde{\mathbf{S}}_j + K \tilde{S}_i^z \tilde{S}_j^z + \sum_{\alpha \neq \beta} \Gamma_{\alpha\beta} (\tilde{S}_i^\alpha \tilde{S}_j^\beta + \tilde{S}_i^\beta \tilde{S}_j^\alpha)$$

+ longer range Heisenberg J₂ and J₃

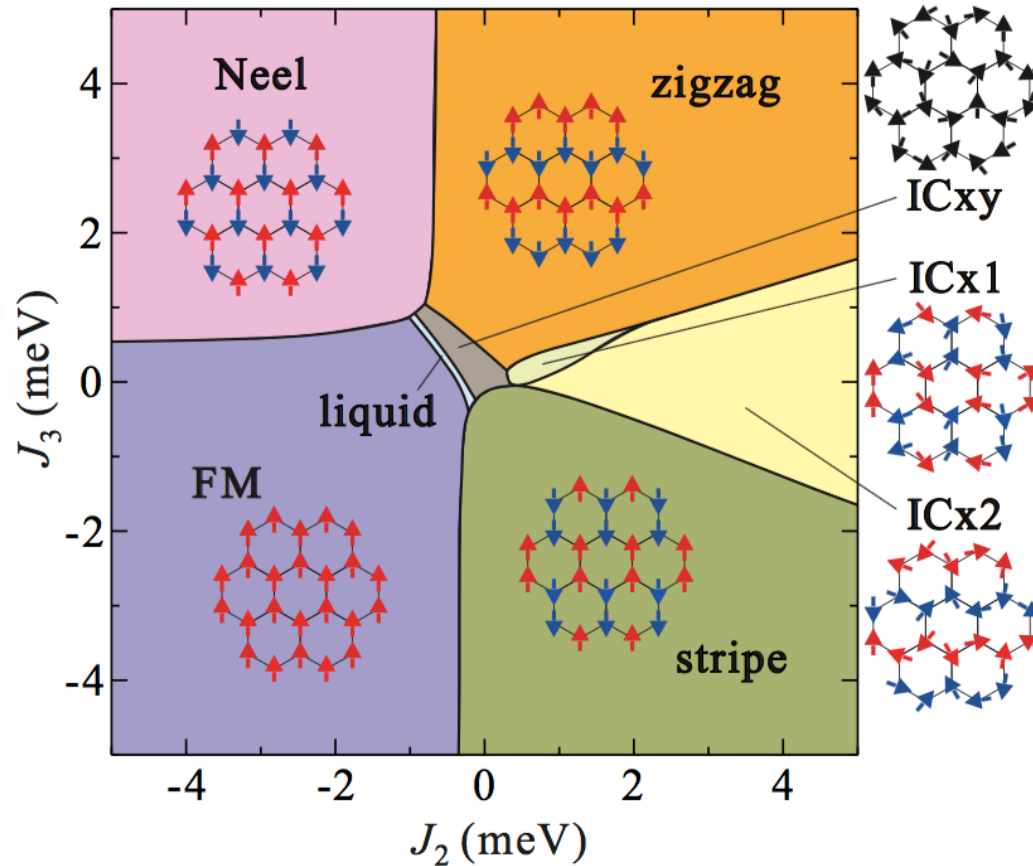
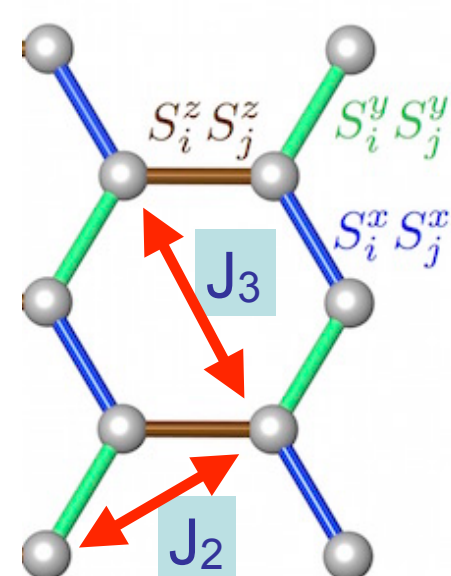


Magnetic nearest neighbor interactions in α -RuCl₃

Exact
diagonalization
calculations

$$\mathcal{H}_{i,j} = J \tilde{\mathbf{S}}_i \cdot \tilde{\mathbf{S}}_j + K \tilde{S}_i^z \tilde{S}_j^z + \sum_{\alpha \neq \beta} \Gamma_{\alpha\beta} (\tilde{S}_i^\alpha \tilde{S}_j^\beta + \tilde{S}_i^\beta \tilde{S}_j^\alpha)$$

+ longer range Heisenberg J_2 and J_3



zig-zag
order
driven by
 J_2 & J_3

Magnetic nearest neighbor interactions in α -RuCl₃

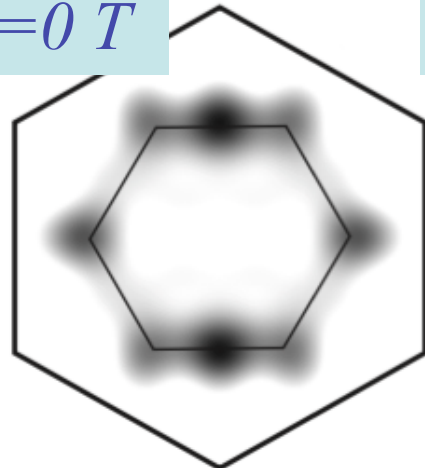
Exact
diagonalization
calculations

$$\mathcal{H}_{i,j} = J \tilde{\mathbf{S}}_i \cdot \tilde{\mathbf{S}}_j + K \tilde{S}_i^z \tilde{S}_j^z + \sum_{\alpha \neq \beta} \Gamma_{\alpha\beta} (\tilde{S}_i^\alpha \tilde{S}_j^\beta + \tilde{S}_i^\beta \tilde{S}_j^\alpha)$$

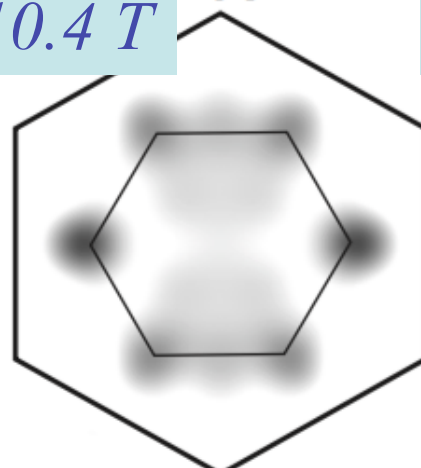
+ longer range Heisenberg J₂ and J₃

Static spin structure factor S(Q) from ED

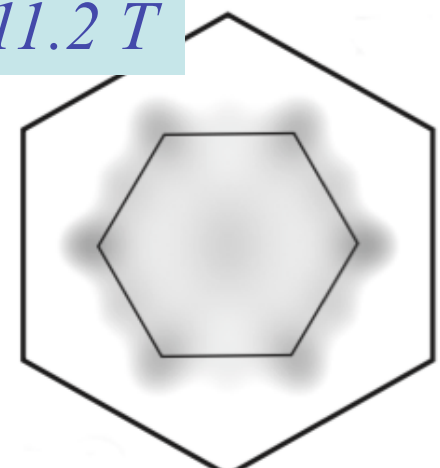
B=0 T



B=10.4 T



B=11.2 T



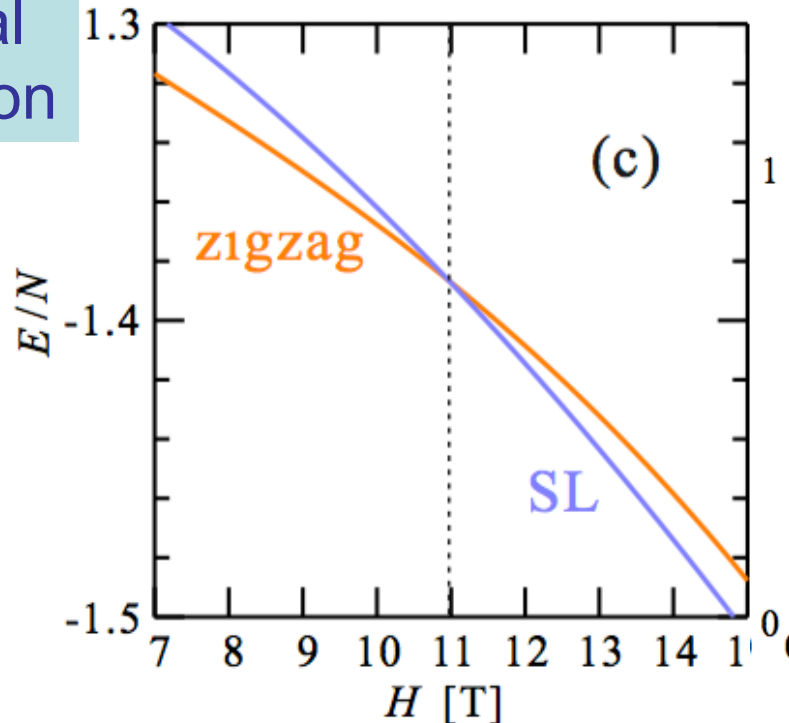
Magnetic nearest neighbor interactions in α -RuCl₃

Exact
diagonalization
calculations

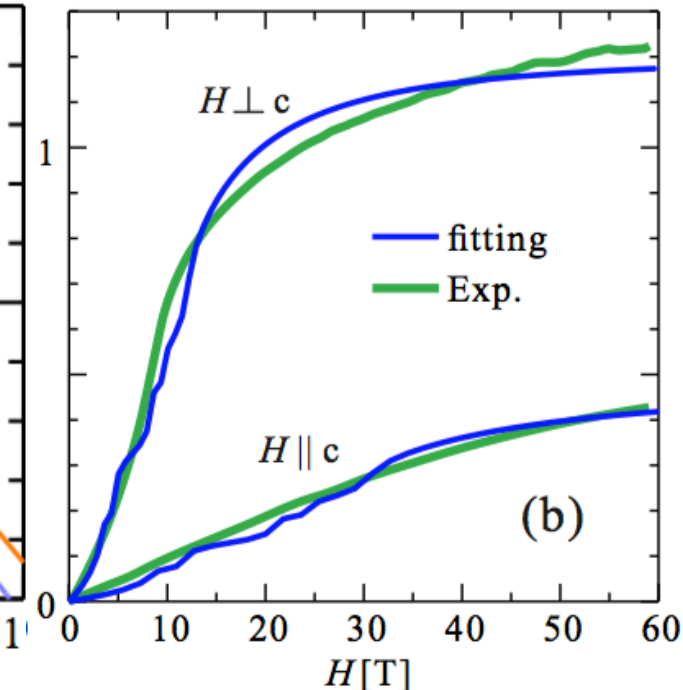
$$\mathcal{H}_{i,j} = J \tilde{\mathbf{S}}_i \cdot \tilde{\mathbf{S}}_j + K \tilde{S}_i^z \tilde{S}_j^z + \sum_{\alpha \neq \beta} \Gamma_{\alpha\beta} (\tilde{S}_i^\alpha \tilde{S}_j^\beta + \tilde{S}_i^\beta \tilde{S}_j^\alpha)$$

+ longer range Heisenberg J₂ and J₃

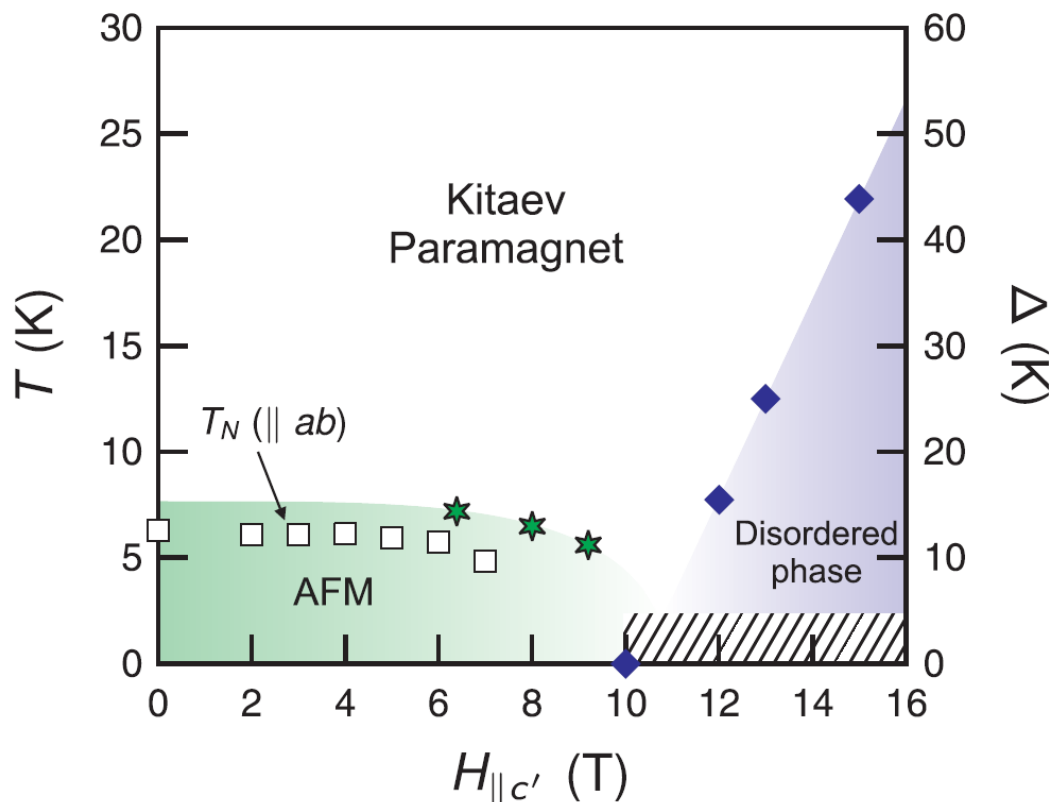
Compare to
experimental
magnetization



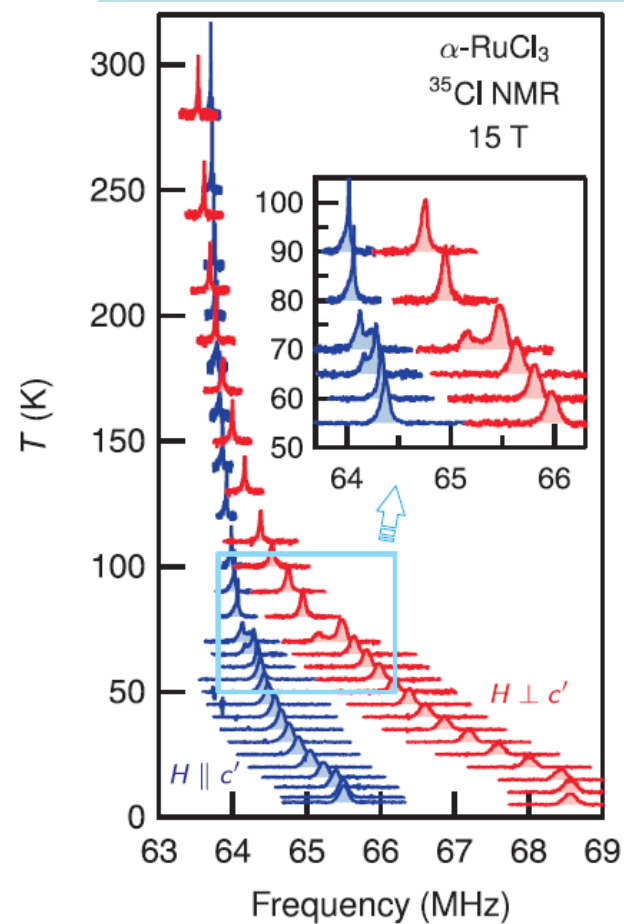
Fit g-factors



Observation of B-induced spin liquid in RuCl₃

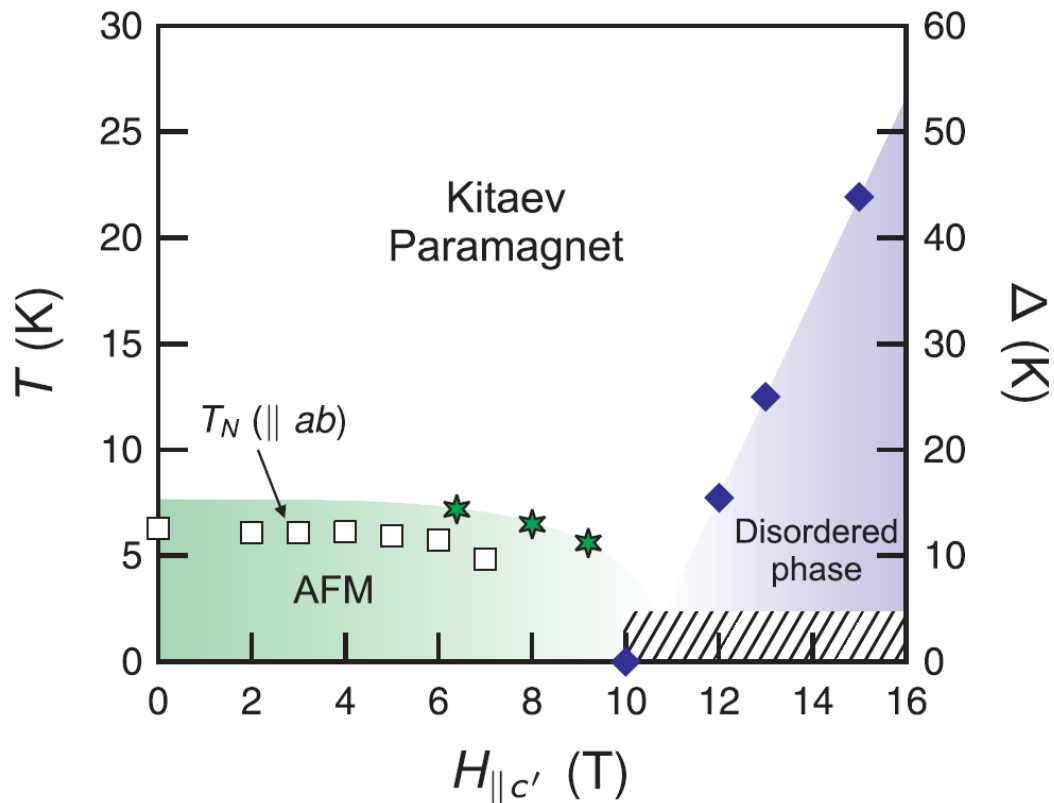


gapped spin liquid

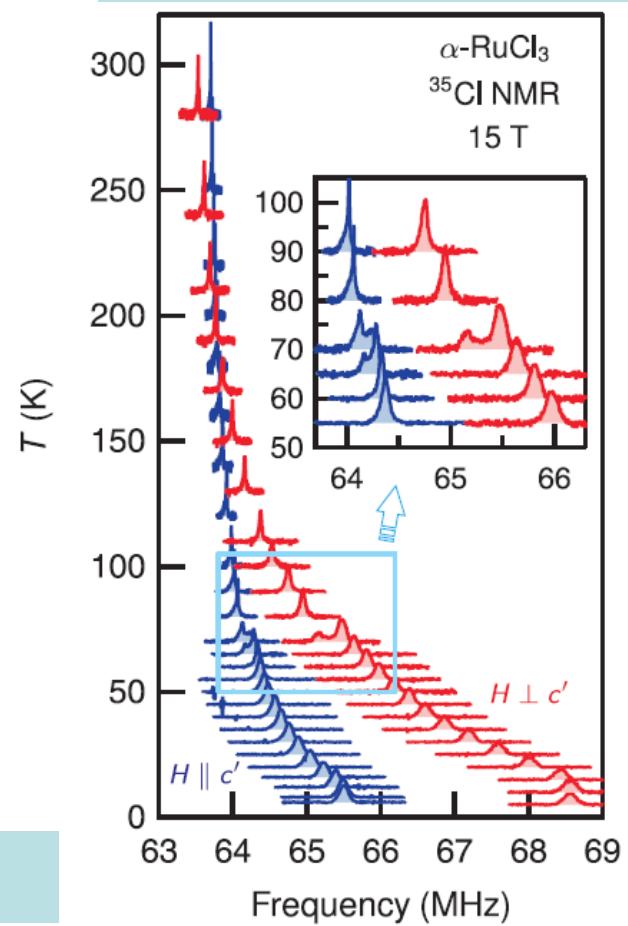


Baek, Do, Choi, Kwon, Wolter, Nishimoto, JvdB
& Büchner, PRL 119, 037201 (2017)

Observation of B-induced spin liquid in RuCl₃



gapped spin liquid



now also reported by neutron scattering

Banerjee et al., Quantum Mat. 3, 8 (2018)

Baek, Do, Choi, Kwon, Wolter, Nishimoto, JvdB & Büchner, PRL 119, 037201 (2017)

Conclusions

Based on quantum chemistry & cluster ED:

Conclusions

Based on quantum chemistry & cluster ED:

213 honeycomb iridates: $K \sim -15 \text{ meV}$ (ballpark)

interactions beyond Kitaev

strong bond anisotropies

Conclusions

Based on quantum chemistry & cluster ED:

213 honeycomb iridates: $K \sim -15 \text{ meV}$ (ballpark)

interactions beyond Kitaev

strong bond anisotropies

honeycomb $\text{H}_3\text{LiIr}_2\text{O}_6$ $K \sim -12 \text{ meV}$, $|K/J| > 6$

very strong effect of H disorder on magnetism

Conclusions

Based on quantum chemistry & cluster ED:

213 honeycomb iridates: $K \sim -15 \text{ meV}$ (ballpark)

interactions beyond Kitaev

strong bond anisotropies

honeycomb $\text{H}_3\text{LiIr}_2\text{O}_6$ $K \sim -12 \text{ meV}$, $|K/J| > 6$

very strong effect of H disorder on magnetism

honeycomb K_2IrO_3 $K \sim -6 \text{ meV}$, $|K/J| \sim 5$, $|K| \sim |\Gamma|$

Conclusions

Based on quantum chemistry & cluster ED:

213 honeycomb iridates: $K \sim -15 \text{ meV}$ (ballpark)

interactions beyond Kitaev

strong bond anisotropies

honeycomb $\text{H}_3\text{LiIr}_2\text{O}_6$ $K \sim -12 \text{ meV}$, $|K/J| > 6$

very strong effect of H disorder on magnetism

honeycomb K_2IrO_3 $K \sim -6 \text{ meV}$, $|K/J| \sim 5$, $|K| \sim |\Gamma|$

ruthenium trichloride: $K \sim -5 \text{ meV}$, $|K/J| \sim 5$

residual interactions weak, anisotropy weak

in-plane field above $B = \sim 8 \text{ T}$: gapped spin liquid